Annual Report FY 2006

平成 18 年度活動報告

Institute for Geothermal Sciences

Graduate School of Science

Kyoto University

京都大学

大学院理学研究科

附属地球熱学研究施設

Institute for Geothermal Sciences
Graduate School of Science, Kyoto University

京都大学大学院理学研究科 附属地球熱学研究施設

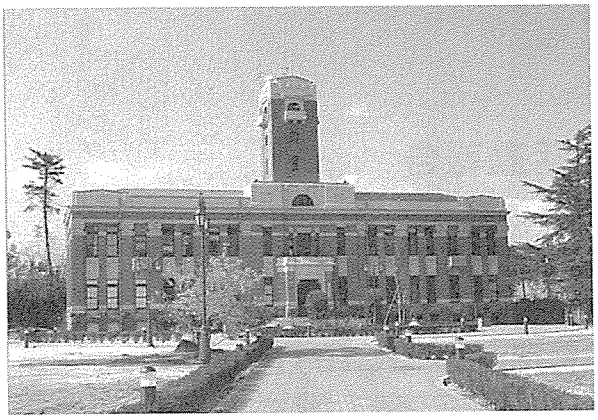

Beppu Geothermal Research Laboratory
Noguchibaru, Beppu, Oita 874-0903
Japan
Telephone: +81-977-22-0713
Facsimile: +81-977-22-0965

別府
〒874-0903 大分県別府市野口原
電話: 0977-22-0713
ファックス: 0977-22-0965
Homepage: http://www.vgs.kyoto-u.ac.jp

Aso Volcanological Laboratory
Minamiaso, Kumamoto 869-1404, Japan
Telephone: +81-9676-7-0022
Facsimile: +81-9676-7-2153

阿蘇（火山研究センター）
〒896-1404 熊本県阿蘇郡南阿蘇村河陽
5280
電話: 0967-67-0022
ファックス: 0967-67-2153
Homepage:
http://www.aso.vgs.kyoto-u.ac.jp/

Front Cover Image:
A strombolian explosion in the 1st crater of Mt. Nakadake, Aso volcano in October 1979.
(Photo by M. Sako)
表紙の写真
1979 年 10 月の阿蘇中岳第一火口のストロンボリ噴火の様子（迫幹夫撮影）

Chinetu-chan designed by Miho Saito
Editional compilation by T. Kawamoto, Printed by Primedia

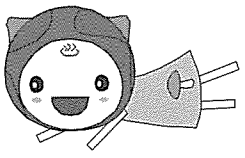

序

平成９年に火山研究施設（阿蘇）と地球物理学研究施設（別府）が現地球熱学研究施設に統合された改組以来10年の歳月が経過した．地球上で最大規模の火山・地熱温泉活動域のひとつである中部九州地域を巨大な実験装置とみなして，野外観測や室内実験などを中心に，造構運動・火山活動・地熱温泉活動など地球の熱的活動に関する地球熱学の学問体系の構築をめざしている．この基本理念に立脚して，専門分野の異なる研究者が弾力的に協力できるよう，大部門制を採り，以下の５つの研究分野が置かれている．地熱流体論研究分野，地熱テクトニクス研究分野，火山構造論研究分野，火山活動論研究分野，地球熱学情報研究分野（外国人客員）である．平成16年度には京都大学が法人化され，研究教育の効率化さらには定員削減を余儀なくされる状況にある．法人化３年目にはいり，施設運営のためには財政的に運営交付金に加えて競争的資金の確保が重要になっている．

他方，平成16年度設置された施設運営協議会が６回開催され，理学研究科との連携が実質化されてきているが，遠隔地の課題をみすえながら，阿蘇と別府の有機的な連携を強化する努力がより一層必要となっている．このような中で，学内での地球熱学研究施設の研究教育面での位置付けをより明確にすることが必要であり，平成19年４月からは，懸案であった京都勤務が，理学研究科附属施設の京都分室の形で認められ，院生・学生の教育や研究科内での役割分担の課題に取り組みはじめた．

人事面では長年施設の研究・教育で尽力された田中良和・須藤靖明両先生が平成19年３月31日をもって退職され，京都大学から離れられた．９月末に外国人客員のインドネシアバンドン工科大学の Wahyu Srigutomo 氏が離任し，エジプト・ミニア大学の Helmy Hassan 氏が別府に着任した．網田和宏氏が平成18年５月31日付けで機関研究員を退職し，秋田大学工学資源学研究科助手として移動し，山田国見氏が機関研究員として平成18年６月16日に着任し，平成18年８月31日をもって退職し，原子力機構へ転任した．栗谷豪氏が平成19年１月31日付けで機関研究員を退職し，東北大学大学院理学研究科地学専攻助手へ転任した．後任の機関研究員として浜田盛久氏が平成18年10月16日付けで，石橋秀巳氏が平成19年４月１日付けで別府に着任した．

21世紀 COE も４年目になり，研究施設の研究テーマが関係する重点課題 J2b で成果をあげ，J3b での京都キャンパス・インドネシア ITB との共同研究（鍾乳洞プロジェクト）が展開された．別府・阿蘇をフィールドとした多目的観測サイトの活動も数多く実施され，その内容が COEKAGI２１のホームページに随時掲載された．昨年度設置された TV 会議システムはセミナーや特別講演を中心に活用され，遠隔地からの情報発信に大きな役割をになっている．

平成19年６月

平成18年度地球熱学研究施設長 竹村恵二

Preface

Ten years has passed since the reorganization of our Institute for Geothermal Sciences from Beppu Geophysical Research Laboratory and Aso Volcanological Laboratory in 1997. We regard central Kyushu, one of the most active volcanic and geothermal fields in the world, as a natural experimental facility. Our Institute has aimed for a comprehensive understanding the thermal structure and the dynamics of the Earth' interior based on volcanism, geothermics and tectonics by use of field work, laboratory experiments, and theoretical approaches. A variety of research fields can mix together under this interdisciplinary system. We have the following five research units: geothermal fluids, geothermal tectonics, volcanic structure, volcano-dynamics and geothermal intelligence section (a visiting research scholar from abroad). In 2004 fiscal year, Kyoto University was reformed to juridical personalization of national universities. This puts us under pressure to do efficient education and research with limited human and financial resources suppurted by the goverment. Total revenue decreased, forcing us to get other competitive fundings.

The meetings of our steering committee, which was first organized in 2004, were held six times in Kyoto campus, and the cooperative relationship between our institute and Division of earth and Plananetary Sciences was intensified. We are physically remote from main campus, and also we need to make efforts to intensify cooperative work between Aso and Beppu. In 2007 fiscal year, the Kyoto Branch of our institute was established in Kyoto campus for a task for intensive teaching duty and for taking a responsibility in the management for the Division of Earth and Planetary Sciences.

Professors Yoshikazu TANAKA and Yasuaki SUDO, who have been members of our institute for about 40 years, retired in March 2007. Dr. Wahyu SRIGUTOMO as a visiting faculty left from Aso, and Dr. Hassan HELMY arrived at Beppu. A postdoctoral associate, Dr. Kazuhiro AMITA left to Akita University and Dr. Kunimi YAMADA arrived at Beppu, and left to Japan Atomic Energy Agency in September 2006. Dr. Takeshi KURITANI arrived at Beppu in April and left to Tohoku University in February 2007, and Dr. Morihisa HAMADA arrived at Beppu in October 2006 and Dr. Hidemi ISHIBASHI arrived at Beppu in April 2007.

KAGI 21 (the 21st Century Centers of Excellent program) has been supported by JSPS for these four years, and our institute made a great contribution to water and material circulation at the active geosphere, stalagmite project and as a field station of the multi-purpose field sites for education and research activity. TV meeting systems connecting among Kyoto, Uji, Aso and Beppu has been used constantly for seminars and occasionally for special lectures to have better exchange of information among us.

Beppu, June 2007
Keiji TAKEMURA, Professor/Director

目次　Contents

構 成 員 Members

教授 ***Professors***

鍵山恒臣 Tsuneomi Kagiyama

竹村惠二 (施設長) Keiji Takemura (Director)

田中良和 Yoshikazu Tanaka

2007年3月退職

助教授 ***Associate Professors***

大倉敬宏 Takahiro Ohkura

大沢信二 Shinji Ohsawa

須藤靖明 Yasuaki Sudo

2007年3月退職

古川善紹 Yoshitsugu Furukawa

助手 ***Assistant Professors***

宇津木充 Mitsuru Utsugi

川本竜彦 Tatsuhiko Kawamoto

柴田知之 Tomoyuki Shibata

山本順司 Junji Yamamoto

外国人客員 ***Visiting Faculty***

ワヒュー スリグトモ Wahyu Srigutomo

2006年9月帰国

ハッサン ヘルミー Hassan M. Helmy

2006年10月着任

技術職員 ***Technical Professionals***

井上寛之 Hiroyuki Inoue

馬渡秀夫 Hideo Mawatari

吉川慎 Shin Yoshikawa

教務補佐員 ***Research Assistant***

芳川雅子 Masako Yoshikawa

研究機関研究員 ***Research Associates***

網田和宏 Kazuhiro Amita

2006年5月辞職、秋田大学へ

栗谷豪 Takeshi Kuritani

2006年4月着任 2007年1月辞職、東北大学へ

杉本健 Takeshi Sugimoto

寺田暁彦 Akihiko Terada

2006年4月着任

浜田盛久 Morihisa Hamada

2006年10月着任

山田国見 Kunimi Yamada

2006年6月着任 2006年8月辞職、原研開発機構へ

研修員 ***Research Fellow***

なし

研究生 ***Research Student***

なし

JSPS研究員 ***JSPS Postdoctoral Fellow***

齋藤武士 Takeshi Saito

COE研究員 ***Research Associate (COE)***

西村光史 Koshi Nishimura

大学院生 ***Graduate Student***

岡本響 Kyo Okamoto

小森省吾 Shogo Komori

三根崇彦 Takahiko Mine

事務補佐員 ***Secretaries***

今村町子 Matiko Imamura

東端歩 Ayumi Higashibata

宮崎奈美 Nami Miyazaki

臨時用務員 ***Supply Janitor***

山崎咲代 Sakiyo Yamasaki

研究活動　Research Activities

機関内共同研究　Institution Colaboration

Seismicity within the Philippine Sea Slab in the Central and Southern Kyushu, Japan

T. Ohkura, K. Okamoto, T. Seno(Univ. of Tokyo)

In order to determine where the intraslab earthquakes occur, within the oceanic crust or slab mantle, or both of them, in the central and southern Kyushu, Japan, we analyzed the waveform data and examined existence of seismic waves guided by the oceanic crust of the subducting Philippine Sea plate. And with a view to locate hypocenters of the intraslab earthquakes with a high accuracy, we relocated them using the double-difference hypocenter determination method and obtained a three dimensional seismic velocity structure using the double-difference tomography method.

The results are as follows: (1) From waveform analysis and hypocenter determination, we found that many intraslab earthquakes occurred within the oceanic crust, which shows low Vp and Vs, in the northern part of the study area, where no low frequency tremor is observed. (2) The results of hypocenter determination and the three-dimensional tomography show that intraslab earthquakes occurred within the oceanic mantle in the study area.

However, it is still unclear whether earthquakes occurred within the oceanic crust in the southern part of the study area.

Semiautomatic Chemical Separation System for radiogenic isotope analyses

T. Shibata, M. Yoshikawa, T. Sugimoto

INTRODUCTION

In the last few decades, the isotopic compositions of Sr, Nd and Pb were used to solve many scientific problems in earth sciences. Although applying this approach has proved great success, a shortage in the isotopic data base for many regions does exist. This might be due to the fact that measuring the Sr, Nd and Pb isotope ratios is time consuming and requires very clean environment during sample preparation. Great advances have been made to enhance the quality of isotope ratios measurements during the last few years by introducing the automated thermal ionization mass spectrometers (TIMS). Measuring the isotopic ratios by this instrument are relatively simple and fast, however, the rate of data production still faces the problem of long-time needed for sample preparation. As the difficulties arise from sample

preparation, it will be very helpful to find a simple, practical and efficient technique of element separation without need for special costly installments.

Recently, automatic procedure separating Sr from river water and carbonate rocks by dynamic ion-exchange high-performance liquid chromatography (HPLC) has been developed (Meynadier et al., 2006). Important technical problem of this method is that large amount of organic materials, which prevent the ionization in TIMS, come from the closed column of HPLC (Stray, 1992). The HPLC technique is, moreover, expensive and is not still applied to silicate rocks. Therefore, new analysis methods applying the automated HPLC system have be established individually by each laboratory. Indeed, these difficulties have limited the use of this technique.

In many laboratories, which are carrying isotopic analysis, are using open column for chemical separation. If we can find an automated method of chemical separation employing open column, no modification to the chemical procedures is required. Thus, it will contribute to the improvement not only of geochemical study of igneous rocks but also of wide-range of earth sciences.

When we design the automation, the procedures of chemical separation by open column can be divided into three steps: 1) changing the solution (sample solution and eluants) to be loaded on to column bed, 2) sending the solution, and 3) collection of the fraction containing the element of interest. In this paper, we have focused on the 2); and applied to Sr and Nd isotope analyses. It is expected that the semiautomatic chemical separation system reduce the time for analyst at isotope analyses. Such a new semiautomatic technique will allow all laboratories to use this approach including those using the multi-collector inductive coupled plasma mass spectrometry instruments.

EXPERIMENT

The analytical methods for Sr and Nd isotope analyses are essentially the same as those of Yoshikawa and Nakamura (1993), Yoshikawa et al. (2001) and Shibata and Yoshikawa (2004).

Semi Automated System

The procedure of sample and eluant loading onto the column is illustrated in Figure 1. The constitution of the system is summarized in Table 1. The automated system is composed of a solution rack, peristaltic pump, tube fixing stand and open columns. The height of the stand is adjusted in according to the type of the open column. Sample solution and eluants are stored in cleaned test tubes and put on the solution rack, and are sucked up by the peristaltic

Fig. 1. Schematic description of the semiautomatic system of chemical separation by open column. The solutions (sample solution and eluant) are injected from the test tubes to the open column by peristaltic pump automatically. Changing the test tube and starting the collection of eluate are done manually. procedure.

pump with PVC tube, which is connected to Tefron® tube at each end. The sucked solutions are then loaded onto the columns. The flow rate of the pump depends up on size and resin of each column (Table 1). Important is to empty reservoir of column before a next drop of the solution fall onto the resin bed. When the solution in a test tube has been empty, then the tube is moved to the next test tube manually. Because the collecting vessel is also manually changed, the numbers of test tube and amount of eluant in it are designed to be empty during vessel change (Fig. 1). The used pump is able to deal with eight tube lines so that simultaneous chemical separation of eight samples is possible.

Table 1. Semiautomatic system for chemical separation

		Specification
Solution sending system	Peristaltic Pump	Galison 312 / MINIPULS 3
	Tube	ϕ0.25 mm, PVC
		Rpm
Flow rate	First column	6.00
	Second column for Sr	5.00
	Second column for Nd	0.50

Table 2. The results of Sr and Nd isotope ratios of standard rock samples

	$^{87}Sr/^{86}Sr$		$^{143}Nd/^{144}Nd$	
JB-2	0.703671	±0.000016	0.513081	±0.000013
JA-3	0.704134	±0.000010	0.512940	±0.000012

The isotope ratios were analyzed by TIMS (ThermoFishers MAT 262) with staic multi-collector mode following Yoshikawa et al (2001). Normalizing factors to correct for fractionation of Sr and Nd are $^{86}Sr/^{88}Sr$=0.1194 and $^{146}Nd/^{144}Nd$=0.7219, respectively. Measured ratios for standard materials were $^{87}Sr/^{86}Sr$=0.710279±0.000028 (2σ) for NIST SRM987 (n=5), $^{143}Nd/^{144}Nd$=0.511851±0.000013 (2σ) for La Jolla (n=9).

Chemical Separation of Rb–Sr and Sm–Nd by first column

The elution sequences of chemical separations for Sr and Nd are summarized in Figure 2. The decomposed sample dissolved in 1.0 ml 2.5 mol l-1 HCl is stored in a test tube (S1). Using the peristaltic pump, sample solution is sucked up from the test tube and loaded onto the column packed with 1.0 ml of AG 50W X8, which is conditioned by 2.5 mol l-1 HCl. When the test tube becomes empty, the inlet of peristaltic pump is switched manually to next test tube storing 2.0 ml of 2.5 mol l-1 HCl (F1). All of the 2.5 mol l-1 HCl is loaded onto the column and pass through it, PFA vial is set below the column. The peristaltic pump system is switched manually to the test tube storing 5.0 ml of 2.5 mol l-1 HCl (F2), and then collecting Rb and Sr fraction starts. Collection of the fraction of Sm and Nd starts with switching the pump system to the 5.5 ml of 6 mol l-1 HCl (F3). The collected fractions are dried on hotplate at 100 C°.

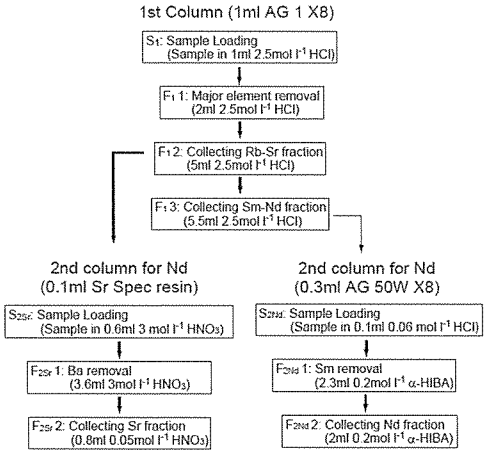

Fig. 2. Elution sequences for separating Sr and Nd from rock samples by semiautomatic system. The procedures are basically followed Yoshikawa et al. (2001), Shibata et al. (2003) and Pin and Bassin (1992). α-HIBA is α-hydroxy iso-butyric acid.

Isolation of Sr and Nd by second column

The dried Rb-Sr and Sm-Nd fractions are dissolved by 0.6 ml of 3.0 mol l-1 HNO3 and 0.1 ml of 0.06 mol l-1 HCl, respectively. Similar to the procedure used for the first column, Sr is purified with 3.0 mol l-1 HNO3, 0.5 mol l-1 HNO3, and Nd is purified with 0.2 mol l-1 α-HIBA using 0.3 ml cation-exchange chromatography (AG 50W X8) in ammonium form (Fig. 2).

RESULTS AND DISCUSSIONS

The semiautomatic chemical separation system was applied to the Sr and Nd isotope analyses of JB-2 and JA-3 (standard igneous rock samples provided by Geological Survey of Japan). The results of the analyses are listed in Table 2, and show good agreement with previously published data of the same standards (Shibata et al., 2003). During the measurements of Sr and Nd isotope ratios by TIMS, interfering ion beams, such as those of Rb and Sm are not observed. This means that the semiautomatic system is suitable for chemical separation of Sr and Nd from igneous rock samples. The total time for the measurement is similar to that of the conventional method, however, the time of chemical separations is reduced about one third of the time consumed in the manual method.

Vital problems which limit the productivity of Rb, Sr and Pb isotopes are the time-consuming sample preparation and critical clean conditions needed. The traditional manual technique faces the problem of long-time procedure and the possibility of error during handling. The full-automated system (HPLC) of Meynadier et al. (2006) enhances the quality of isotopic data but faces the problem of usability to certain materials (water and carbonates), high costs and time needed for element separation. Relative to the HPLC method, the proposed system is cheaper, time-saver and applicable to wide-range of geological materials. Furthermore, using our suggested system will not requires any changes in the analysis method, which the analyst used to use, unlike in the HPLC method. Applying our semiautomatic system will not require any change in elution sequences, just adding the semiautomatic system, which consists of peristaltic pump, for chemical separation. Therefore, when the semiautomatic separation system is to be installed in any laboratory, no modification is necessary for all procedure and previously used apparatus. The low cost and easy installation of our semiautomatic system is useful for laboratories performing isotope analyses by the classical chemical separation using open column chemistry. This means that our semiautomatic system can be applied to all kind of samples, which are commonly analyzed in a laboratory. Furthermore, it is possible to install the semiautomatic system in a small clean space, such as clean bench so that the expensive clean room is not always necessary. By the combining auto sampler and fraction collector to our semiautomatic system, the procedure of chemical separation can be full automated. If personal mistake in handling the suggested system are avoided, almost no disadvantages appear.

CONCLUDING REMARKS

A semiautomatic technique for chemical separation of Sr and Nd isotope analyses is established. The technique comprises automatic sample loading and collection of the element fractions. The measured Sr and Nd isotope ratios of rock standards (JB-2 and JA-3) prepared using by the semiautomatic system show good agreement with published values. This technique reduces the sample preparation time to two-thirds of the time consumed in classic manual technique and should highly reduce the errors that might result due to analyst sensitivity. It could be installed at any isotope laboratory and used at low cost to prepare any type of geological materials. This system could be easily upgraded to full automatic by combining an automatic sampler and fraction collector. Applying this new semiautomatic technique will increase the rate of production and quality of isotopic data.

References

Meynadier, L. Gorge, C. Birck, J-L. and Allègre, C. J. (2006) Automated separation of Sr from natural water samples or carbonate rocks by high performance ion chromatography, Chemical Geology, 227, 26– 36.

Pin, C. and Bassin, C. (1992) Evaluation of a strontium-specific extraction chromatographic method for isotopic analysis in geological materials, Analytica Chimica Acta, 269, 249-255.

Shibata, T. and Yoshikawa, M. (2004) Precise Isotope Determination of Trace Amounts of Nd in Magnesium-rich Samples, Journal of the Mass Spectrometry Society of Japan, 52, 317-324.

Shibata, T. Yoshikawa, M. and Tatsumi, Y. (2003) An analytical method for determining precise Sr and Nd isotopic compositions and results for thirteen rock standard materials: Frontier Research on Earth Evolution 1, IFREE Report for 2001–2002, pp. 363–367, Institute for Frontier Resarch on Earth Evolution, Japan Marine Science and Technology Center, Yokosuka, Japan.

Stray, H. (1992) Improved HPLC method for the separation of Rb and Sr in connection with Rb-Sr dating, Chemical Geology, 102, 129-135.

Yoshikawa, M. and Nakamura, E. (1993) Precise isotopic determination of trace amounts of Sr in magnesium-rich samples, Journal of Mineralogy, Petrology and Economic Geology, 88, 548-561.

Yoshikawa, M. Shibata, T. and Tatsumi, Y. (2001) The Sr, Nd and Pb isotopic ratios of GSJ standard rocks: Annual Report. of Institute for Geothermal Sciences, Kyoto Univ., 2000 FY, pp30.

(submitted to JMPS)

Some problems with the latest lava flows at Tsurumi Volcano, East Kyushu, Japan

K. Takemura, T. Saito, T. Sugimoto, H. Mawatari

Tsurumi volcano is one of the active volcanoes emplaced within the Beppu-Shimabara graben, Kyushu, Japan. It started its activity more than 60, 000 years ago and recent activity was studied by Fujisawa et al. (2002). They concluded that the latest lava flows were effused between 7.3 and 10.5 cal ka BP by using tephrochronology and radiocarbon dating. However, recent study of our group revealed that there are some problems with the tephrochronology of the latest lava (TS lava) at Tsurumi volcano. We conducted the field survey, Lithofacies and bulk rock chemistry of lava flows of Mt. Tsurumi-dake.

1. Occurrence of soil sequence and tephra covering latest lava flows

Around Tsurumi volcano, K-Ah ash layer, erupted at 7, 300 cal BP, is intercalated in black volcanic ash soils. It is a stratified fine-grained volcanic ash with bright orange color. According to Fujisawa et al. (2002), K-Ah ash was identified from the soils which covered TS lava flows in one outcrop. They concluded that the eruption age of TS lava is older than the K-Ah eruption (7, 300 cal BP) from this observation only. In order to reexamine the stratigraphy and identification of volcanic ash layers, we surveyed an outcrop, where Fujisawa et al. (2002) was studied, and collected ash samples from characteristic layers (Fig. 1).

T-Ts ash layer, erupted at 1, 800 cal BP, and YA1 ash layer, erupted at 2, 200 cal BP, were identified at the outcrop (Fig. 2). However, K-Ah did not show clear stratification. We guessed that K-Ah ash is included in volcanic soil under YA1 because the soil is light brown in color. We collected soil samples. Volcanic glasses and minerals were extracted from the samples and refractive indices of glasses were measured by using thermal immersion method (Danhara et al., 1992). We also analyzed T-Ts ash for comparison.

As a result, there was little amount of bubble-wall-type glass, which is the main feature of K-Ah volcanic ash, from both samples (Fig. 3). Most glasses were aggregated with minerals of plagioclase, hornblende and FeTi oxides. Refractive indices of glasses showed a bimodal distribution. Bubble-wall-type glass showed higher index about 1.510, which is in the range of K-Ah ash (1.508-1.516, Machida and Arai, 1992), while aggregated glass showed lower index under 1.5 (Fig. 4). Bubble-wall-type glasses were also identified in T-Ts ash, suggesting accidental contamination after the deposition of K-Ah ash. Although the existence of bubble-wall-type glass with higher index indicates that the soil was formed after the deposition of K-Ah ash, we cannot say the soil was formed at about 7, 300 years ago, which is the eruption age of K-Ah volcanic ash. This means that we cannot say the eruption age of TS lava is older than the K-Ah eruption (7, 300 cal BP).

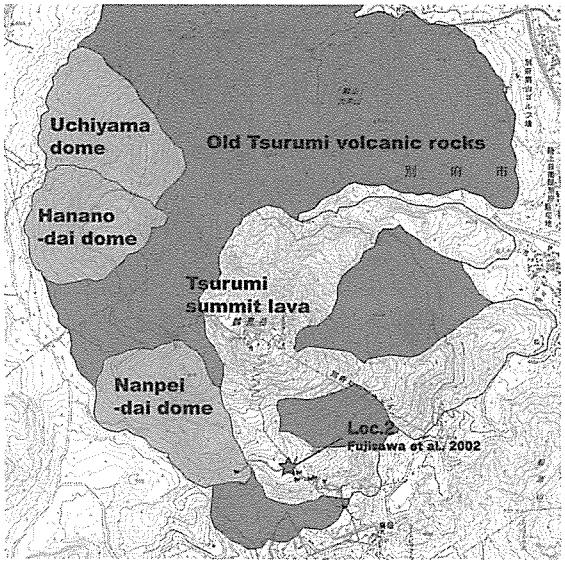

Fig. 1 Geological map of Tsurumi volcano and TS lava flows. A star indicates a sampling locality.

Fig. 2 A photograph and a columnar section of the sampling locality.

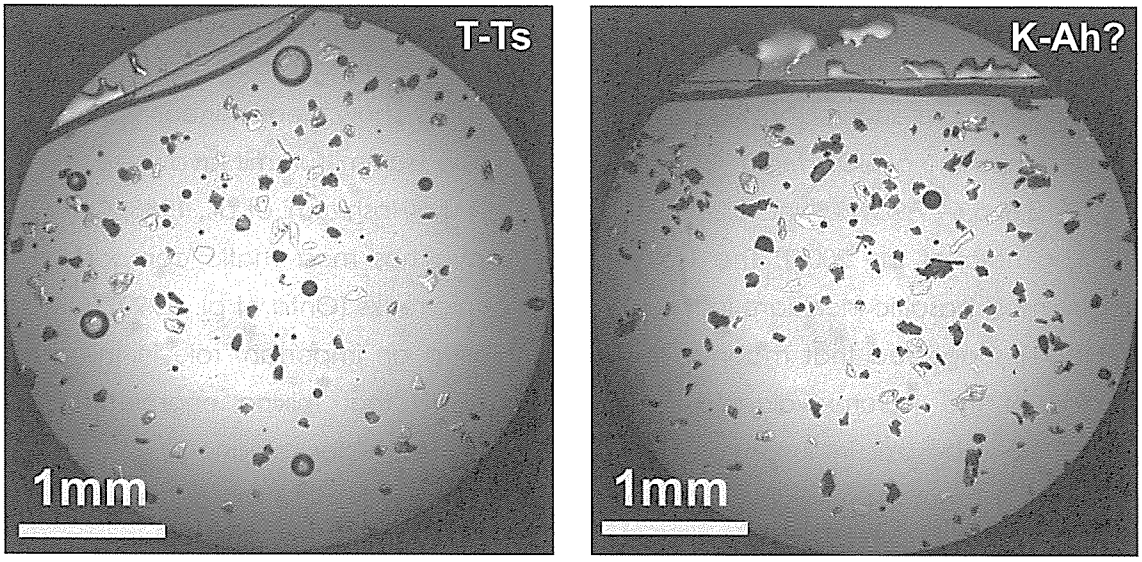

Fig. 3 Photomicrographs of constituent grain minerals of T-Ts ash (left) and the volcanic soil samples (right).

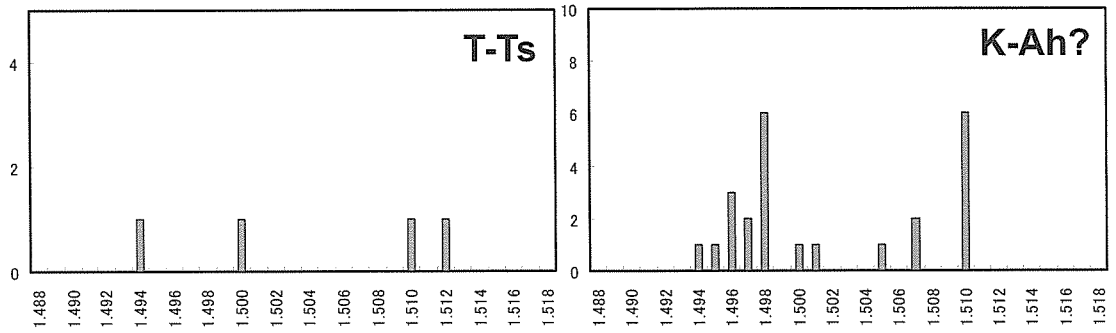

Fig. 4 Histograms of refractive indices of volcanic glass in T-Ts ash (left) and the volcanic soil samples (right).

2. Lithofacies and bulk rock chemistry of the Tsurumi summit lava

The Tsurumi-summit lava which filled up the summit crater and formed a summit lava dome flowed down southward and eastward (Kobayashi, 1984). A detailed distribution of the Tsurumi-summit lava is different depending on previous researchers (e.g. Kobayashi, 1984; Hoshizumi et al., 1988; Ohta et al., 1990; Fujisawa et al., 2002). We collected nine samples in the vicinities of the distribution boundary of the Tsurumi-summit lava that previous researchers had reported, in the purpose to investigate accurate boundary of it.

Phenocryst assemblage of the Tsurumi-summit lava is plagioclase, hornblende, clinopyroxene, orthopyroxene, biotite, quartz, opaques, and olivine. This is similar to lavas from the older units of the Tsurumi-dake volcano as the Old Tsurumi volcanic rocks and Garan-dake, Uchi-yama, Hanano-dai, Nanpei-dai lava domes. The groundmass of the Tsurumi-summit lava is hyalopilitic and composed of plagioclase, pyroxenes, hydrous minerals, magnetite and glass. This is similar to the Old Tsurumi volcanic rocks. On the other hand, lavas from Garan-dake, Uchi-yama, Hanano-dai, Nanpei-dai lava domes show intergranular texture.

The previously reported whole rock major elements compositions of the Tsurumi volcanic rocks are showed in Fig. 5. All volcanic rocks show nearly linear variation. The composition range of SiO2, MgO, CaO, and K2O for the Tsurumi-summit lava were 56.7– 59.6 wt%, 2.6- 3.8, 5.6– 7.9 wt%, and 1.2–1.9 wt%, respectively (Hoshizumi et al., 1988; Ohta et al., 1990, Sugimoto et al., 2006). The Tsurumi-summit lava has most mafic composition and contains most basaltic inclusions in the Tsurumi volcanic rocks (Ohta et al., 1990). Ohta and Aoki (1991) suggested that magma mixing has played an important role in the magma evolution of the Tsurumi volcanic rocks. They argued that mixing endmembers were represented by basaltic inclusions and dacite from adjacent older volcanoes.

The Tsurumi-summit lava is almost clearly distinguished from other Tsurumi volcanic rocks by bulk-rocks chemistry. It is possible to give the constraint to distribution area in the Tsurumi-summit lava by detailed and systematic analysis of lava samples.

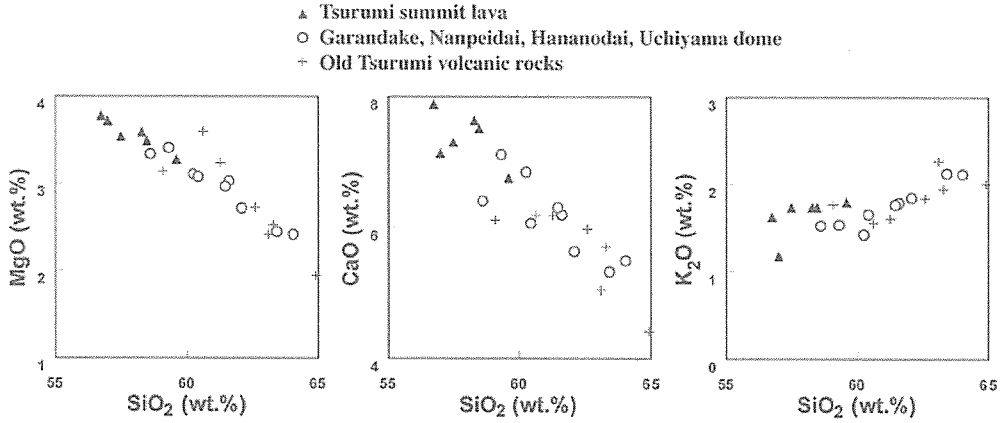

Fig. 5. Harker's diagrams for the Tsurumi volcanic rocks

A report on stable-isotopic and geochemical analyses of drip water samples from Buniayu limestone caves, in Indonesia

M. Yamada (Okayama Univ. Sci.), *S. Ohsawa*, K. Kitaoka (Okayama Univ. Sci.), Y. Watanabe, H. Matsuoka (Kyoto Univ.), B. Brahmantyo, K. A. Maryunani (ITB), T. Tagami (Kyoto Univ.), *K. Takemura*, S. Yoden (Kyoto Univ.)

1. Introduction

We carried out stable-isotopic and geochemical analyses of drip waters (4 drip water samples from Cipicung and Ciawitali caves and 3 cold spring water samples around the cave) collected from Buniayu limestone caves in Sukabumi, West Java, Indonesia (Fig. 1). Aims of the analyses are understanding of formation process of the cave drip water and chemical reactions related to the formation of speleothem. In this report, we will show results of data analyses of major chemical compositions, water isotope compositions (δD and $\delta^{18}O$), stable carbon isotope ratios ($\delta^{13}C$) of dissolved inorganic carbon (DIC).

Fig. 1 Location map showing Sukabumi

2. Results and discussions

Origins of drip water, calcium and bicarbonate ions in drip water

The drip waters are shown to be mostly originated from local meteoric water (rain) by their δD and $\delta^{18}O$ (Fig. 1). Calcium ion and HCO_3^-, which occupy the greater part of the dissolved constituents in the drip waters, are in chemically equivalent (Ca^{2+} : HCO_3^- = 1 : 2). This relation shows that Ca^{2+} and HCO_3^- of the drip waters are derived from the chemical reaction between the limestone bedrock and the infiltrating rain water absorbing a CO_2 ($CaCO_3 + H_2O+CO_2 = Ca^{2+} + 2\ HCO_3^-$). The $\delta^{13}C$ values of DIC of the drip waters are not between the $\delta^{13}C$ of DIC equilibrated with atmospheric CO_2 and that of the limestone, but are nearly in the middle of $\delta^{13}C$ values of DIC equilibrated with soil-CO_2 and the limestone (Fig. 3), therefore the CO_2 absorbed in the infiltrating rain water is expressed to be CO_2 originated in the soil layer over the limestone bedrock.

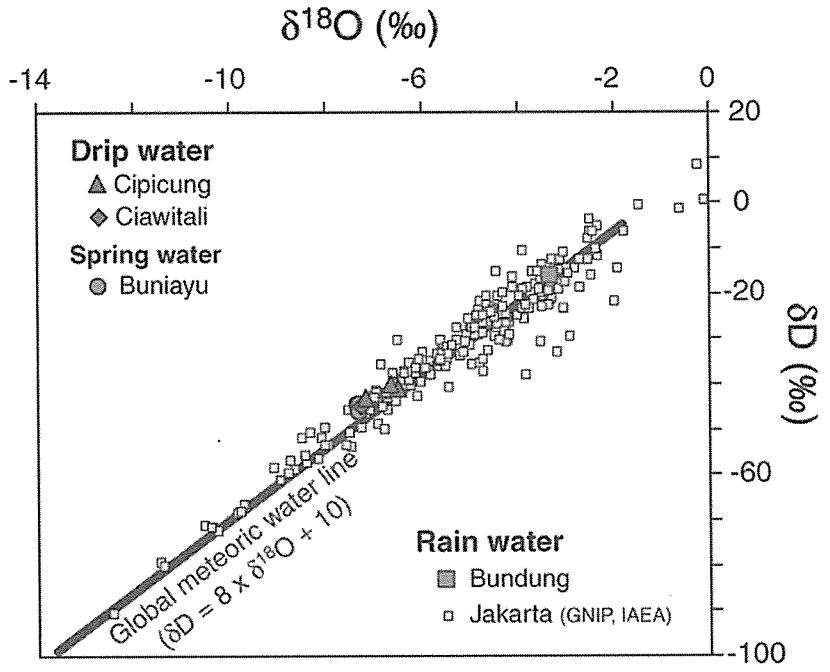

Fig.2 Stable hydrogen and oxygen isotope compositions of Buniayu cave drip waters and spring waters in Sukabumi area, and of rain waters in Bundung and Jakarta.

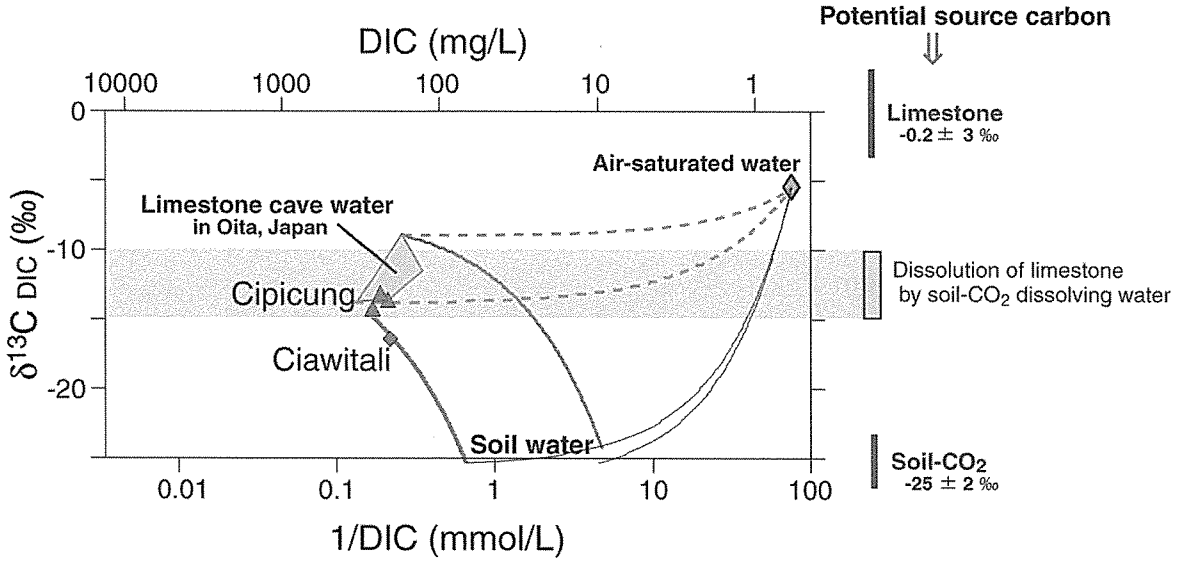

Fig.3 Relationship between stable carbon isotope ratio and concentration of DIC (dissolved inorganic carbon) in cave drip waters of Buniayu limestone caves

Trace elements in melt inclusions analyzed by laser ablation inductively coupled plasma mass spectrometry (LA-ICP-MS)

J. Yamamoto, K. Nishimura

At the present day, earth scientists await for an appropriate technique for rapid and precise in situ determination of trace element composition of minute region in geological materials. LA-ICP-MS analysis allows us to elucidate chemical composition of solid material with high spatial resolution (< 50 micrometer). Its advance should be closely linked with progress in the earth sciences. We are now able to discuss incompatible element compositions of grain-boundary component, fluid inclusion and melt inclusion using LA-ICP-MS. Furthermore, it is possible to determine trace element compositions of insoluble minerals for acid treatment such as chromian-spinel. Here we report the measuring ability of a LA-ICP-MS installed at the institute for Geothermal Sciences, Kyoto University.

1. Introduction

Laser ablation is a powerful tool for in situ sampling of solid materials. Trace elements being incompatible with ambient minerals are distributed into interstitial part within rocks. For example, in the lithospheric mantle, large ion lithophile elements (LILE: e.g., K, Rb, Cs and Ba) and high-field-strength elements (HFSE: Ti, Nb, Ta, Zr and Hf) are concentrated in grain-boundary components or accessory minerals such as feldspar, amphibole, phlogopite, apatite and titanites. Combination with the laser-ablation sample introduction method (LA-ICP-MS) enables us to make in-situ trace element analysis of such materials with high

special resolution. The method is effective to elucidate the origin of the grain-boundary components, fluid inclusions and small accessory minerals by comparing the trace element patterns of whole rock. Furthermore, we are able to investigate trace element compositions of hardly soluble minerals in acid such as chromian-spinel. In this manuscript, we report the advance of the analysis method for solid materials using the laser-ablation technique.

2. Our laser ablation system

The analysis was performed by a quadrupole ICP-MS (PQ3, Thermo Elemental, U.K.) at the Institute for Geothermal Sciences, Kyoto University equipped with a laser-ablation microprobe (CETAC LSX 500, Cetac Technologies, Omaha, NE, USA). For the analyses, a UV (266 nm) laser beam is focused onto the surface of a solid sample. The laser used for this study is a Q-switched Nd-YAG laser operated at 7 mJ per pulse. Peak and background regions were selected from the time-resolved spectra of each sample, and the selected replicates averaged to determine the net count rate for each mass. We describe basic characteristics of our laser ablation system as follows.

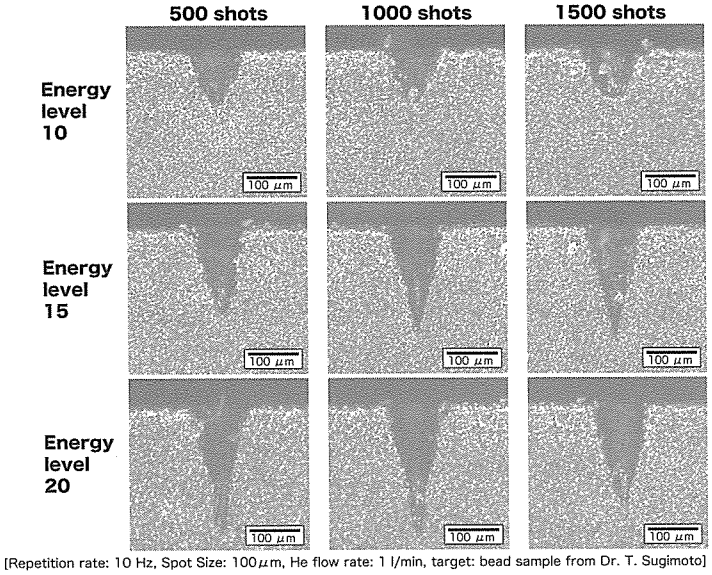

[Repetition rate: 10 Hz, Spot Size: 100μm, He flow rate: 1 l/min, target: bead sample from Dr. T. Sugimoto]

Figure 1. Cross-sections of the laser ablation holes on a bead sample.

2.1. Laser ablation hole

The shape of laser ablation hole was examined in detail on a glass bead supported from Dr. T. Sugimoto. Figure 1 shows the cross sections of the laser ablation hole as a function of pulses of laser shot (10Hz and beam of 100 micrometer across) with different energies of 6.4 J/cm2 (Energy Level 10), 8.9 J/cm2 (Energy Level 15) and 10.2 J/cm2 (Energy Level 20). The holes were cut vertically

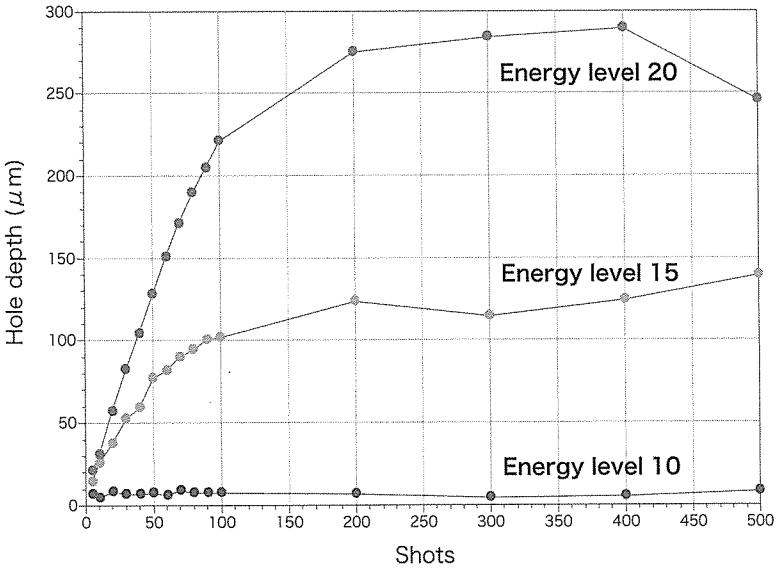

[Repetation rate: 10 Hz, Spot size: 100 μm, He flow rate: 1 l/min]

Figure 2. Relationship between hole depth by laser shot and the number of laser pulse depending on the energy of laser.

through the center and observed under the microscope. The holes are formed of a conical shape reflecting fusiform-shaped high-energy region. The depth of holes increases with increasing laser power, but it appears there is no linkage with laser pulse at the condition.

2.2. Hole depth and drilling rate

The relationship between the depth of holes and the number of laser pulse is shown in Fig. 2. Linear relationship can be obtained until the number of shot is less than 100. There is not much point in accumulating laser pulse of more than a few hundred, suggesting that the present laser ablation system has a limitation in the depth of hole.

Figure 3 shows a relationship between the depth of hole and size of laser spot. Roughly linear correlation is observed, indicating uniform aspect ratio of focus region of laser energy.

The effect of pulse rate on the depth of hole has been evaluated (Fig. 4). Laser ablation at 4 Hz works with the highest efficiency.

2.3. Outline of our analytical condition using laser ablation

We can make sufficient sampling from minerals on thick section using laser with energy of more than 8.9 J/cm2 and 4 Hz in the present system. We adopted helium gas as a carrier of sample for LA-ICP-MS analysis. In experiments using argon gas as a carrier, some amount of powdery materials was deposited around the laser hole, which is well documented by Ishida et al. (2004). Furthermore, using helium gas enhanced sensitivity. Relative element sensitivities were calibrated against the NIST 612 glass, with values cross-checked against other well-characterized natural material including mantle-derived pyroxenes. Detection limits ranged from several tens of ppb for a variety of elements including rare earth elements, Th and U. Replicate analyses of the NIST 610 glass indicate an analytical precision of less than 10 %.

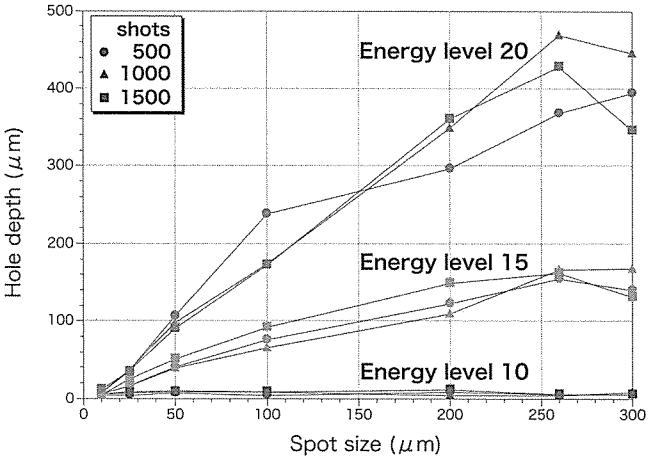

[Repetation rate: 10 Hz, He flow rate: 1 l/min]

Figure 3. Relationship between hole depth and size of laser spot.

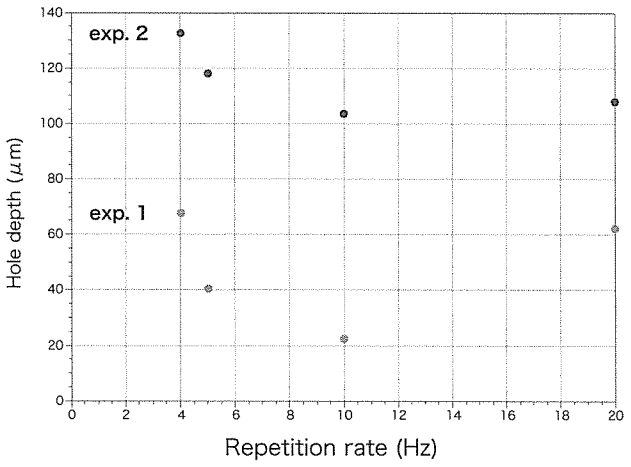

[Energy level: 15, Spot size: 100 μm, 1000 shots, He flow rate: 1 l/min]

Figure 4. Relationship between hole depth and repetition rate of laser pulse.

2.4. Uncertainty of data obtained by the present laser ablation system

2.4.1. Accuracy

We evaluate the accuracy of data obtained by our laser ablation system by comparison with the reported value. Figure 5 shows Leedy-normalized REE patterns of a petit-spot basalt. Inter-element fractionation for the present REE contents was corrected by normalization using ^{44}Ca. Hirano et al. (2001) reported extremely high LREE compositions. Such downward-sloping line is well represented in our data. Note that slight negative anomaly in Ce was detected in the present data.

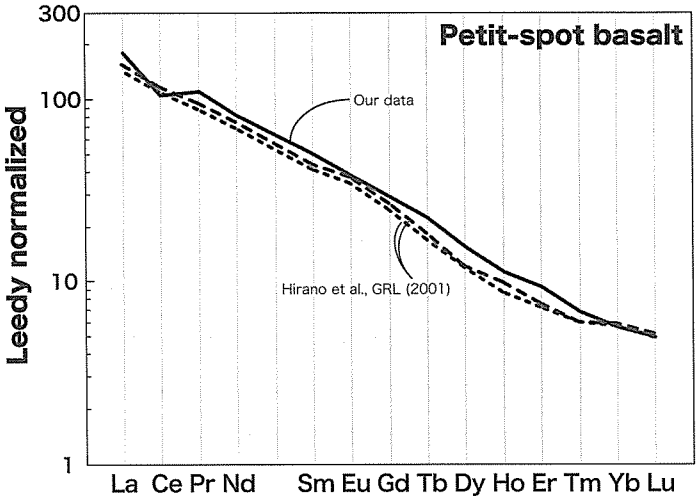

Figure 5. Leedy-normalized REE pattern of a petit spot basalt.

2.4.2. Precision

In LA-ICP-MS analysis, it is difficult to estimate precision of data. We evaluate the precision using multiple data obtained from a mineral. Dashed lines in Fig. 6 represent trace element patterns of a clinopyroxene, which are obtained by multiple analyses of the clinopyroxene. Reproducibility of the elements, whose compatibility is higher than La, is fairly good. Furthermore, such elements show good agreement with those obtained by a solution analysis.

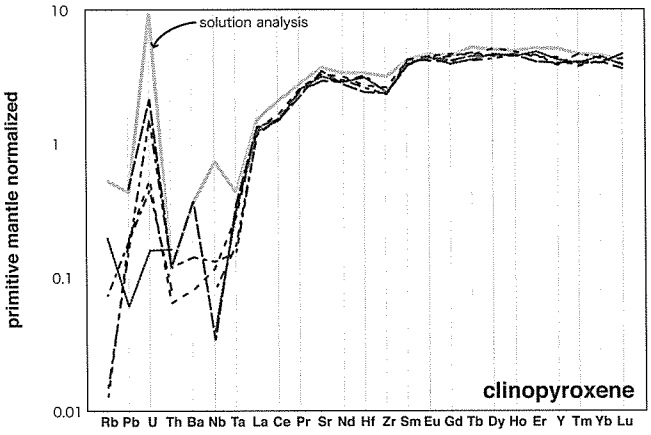

Figure 6. Normalized trace element patterns for a clinopyroxene in a mantle xenolith sampled from Far Eastern Russia. Analyses were repeated five times. Data of solution analysis is from Yamamoto (2001).

Dispersion of highly incompatible trace elements results from their low concentration. Detection limit for the present system is several tens of ppb for many trace elements. In case trace elements fall below one hundred of ppb, the uncertainty of the data increases substantially (> 100%).

2.5. Laser ablation analysis of chromian-spinel

In a solution experiment, mineral samples are decomposed by an acid treatment. During the decomposition, chromian-spinel and Ti-oxide remained, which may be HFSE host minerals (Bodinier et al., 1996; Kalfoun et al., 2002). The lacks of chromian-spinel or Ti-oxide on measurement of the whole rock cause a possible negative anomaly in HFSE in the pattern of the whole rock. Chromian-spinel can be ablated by 266 nm laser light. We analyzed trace elements of chromian-spinel from a lherzolite xenolith by a LA-ICP-MS. Inter-element

fractionation was corrected by normalization using ^{53}Cr. As the result no trace element exceeds the detection limits. That is, the present chromian-spinel is negligible for the trace element budget of the peridotite. LA-ICP-MS analysis enables us to discuss accurately HFSE contents in a mantle rock.

3. Laser ablation analysis of melt inclusion and grain-boundary component

Conceptually, the analysis of a melt inclusion using LA-ICP-MS is simple. Materials in the melt inclusions are sampled in-situ by laser beam as usual mode of procedure. Correction of inter-element fractionation is possible if major element composition of the melt inclusion is determined by EPMA before the LA-ICP-MS analysis. In the case of small melt inclusions (< 50 micrometer), surrounding host mineral would be ablated and mixed with the melt inclusion. In such case, we can discuss the characteristics of the melt inclusion by comparison with the trace element composition of the host mineral using elemental ratio. Here we introduce a striking example of a study examining the origin of a melt inclusion.

3.1. Multiple fluid in the mantle wedge

At an active margin of a continent or an island arc, several kinds of fluids infiltrate into the mantle wedge. For example, aqueous fluids released from the descending oceanic lithosphere trigger partial melting of the mantle wedge. Then, the melt ascends through the mantle wedge leading to the subduction-related volcanism. In that case, part of the melt would remain in the mantle wedge as a grain-boundary component or as a melt inclusion.

Many trace elements are incompatible in mantle rocks. For example, in the lithospheric mantle, large ion lithophile elements (LILE: e.g., K, Rb, Cs and Ba) and high-field-strength elements (HFSE: Ti, Nb, Ta, Zr and Hf) are concentrated in accessory minerals. Fluid inclusions trapped in mantle minerals differ compositionally from whole rocks and the grain-boundary component. This study is intended to elucidate the origin of the melt inclusion and grain-boundary components by combination of LA-ICP-MS analyses and solution ICP-MS analyses.

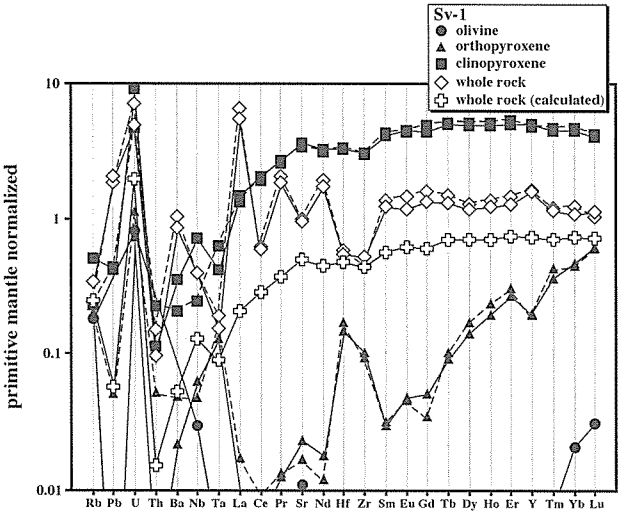

Figure 7. Normalized trace element patterns for constituent minerals and the whole rock of a mantle xenolith (Sv-1, Far Eastern Russia). Analyses were duplicated separately for orthopyroxene, clinopyroxene and whole rock. The trace element pattern for the whole rock calculated by modal proportion and trace element compositions of the constituent minerals is also plotted.

3.2. Cryptic host phase for trace elements in a mantle rock

Figure 7 shows normalized trace element patterns for constituent minerals of a mantle-derived xenolith and the whole rock. Since incompatible trace elements tend to occur mostly in clinopyroxene in spinel peridotites

(e.g., Bedini & Bodinier, 1999), the primitive mantle-normalized trace element pattern of clinopyroxene from spinel peridotites usually mimic that of the whole rock, especially for less incompatible elements. The trace element pattern of the whole rock is not correlated with those of the constituent minerals, especially for more incompatible elements. Particularly, the whole-rock pattern shows clear negative anomalies in Rb, Th, Ce, Sr and HFSE. It is noteworthy that such anomalies are not detected in the constituent minerals. The depletions in Rb, Th, Ce, Sr and HFSE are probably ascribable to the occurrence of the other host phase for incompatible elements in the xenolith, such as grain-boundary component that are poor in Ce, Hf and Zr.

Here is figure 8, which shows comparison of trace element compositions between the analyzed whole rock and the calculated whole rock. It is helpful to show trace element composition of the cryptic host phase for the trace elements. The contents of highly incompatible elements of the analyzed whole rock tend to be higher than those of the calculated whole rocks. Hiraga et al. (2004) predicted that elements of their ionic radius (or incompatibility) larger than Sr will mainly stay at grain boundaries and this seems to appear in Fig. 8. Enrichment of incompatible elements at the grain boundaries relative to the grain matrices does not, however, occur parallel to the incompatibility of the elements. Particularly, the analyzed whole rock of the sample shows spikes of Pb, Ba and La, and depletions in Rb, U, Ce, Sr and HFSE. This indicates that, though the grain-boundary component had been in the process establishing approximate equilibrium in trace element partition with grain matrices, the anomalies reflect an initial property of the grain-boundary component.

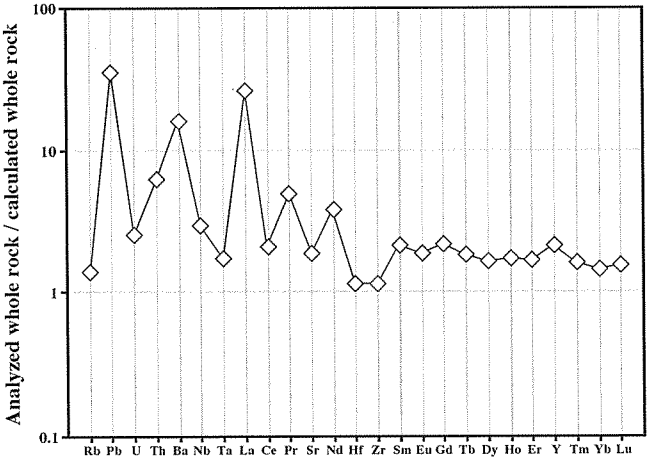

Figure 8. Trace element patterns for the analyzed whole rock normalized by the calculated whole rocks.

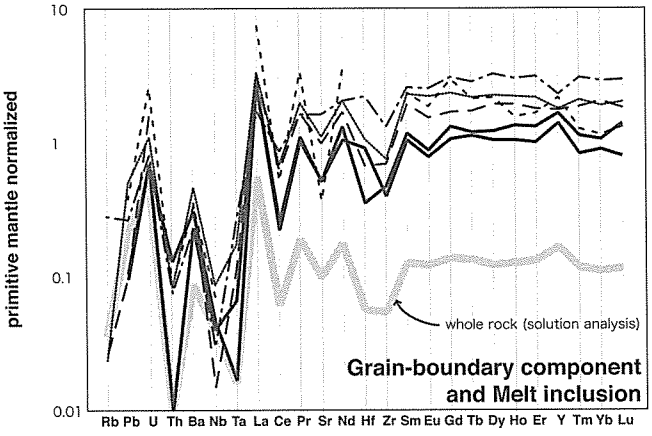

Figure 9. Primitive mantle-normalized trace element patterns for grain-boundary component (dashed lines) and melt inclusion (solid lines) analyzed by LA-ICP-MS accompanied by the analyzed whole rock.

3.3. Trace element compositions of grain-boundary component and melt inclusion

In order to distinguish distribution of the cryptic material, we analyzed trace element compositions of the grain-boundary components and melt inclusion using LA-ICP-MS. Figure 9

shows trace element patterns for the grain-boundary components and melt inclusions accompanied by the pattern for the analyzed whole rock. Both the grain-boundary components and the melt inclusions apparently show negative anomalies in Rb, Th, Ce, Sr and HFSE. Figure 10 shows a result of a line scanning analysis of the trace elements in the mantle xenolith. It is quite obvious that the grain-boundary component is a causative agent for the anomalies.

Both the grain-boundary component and melt inclusion show abrupt peaks in U (Fig. 9). Possible depletion in U in the components was estimated from Fig. 8. The above discrepancy can be explained by the slight contamination of the grain-boundary components during an acid decomposition of constituent minerals. That is, incomplete acid leaching for U before the acid decomposition procedure results in high U content of the calculated whole rock (Fig. 8). Trace element analysis using LA-ICP-MS is potentially capable to relieve such confusion.

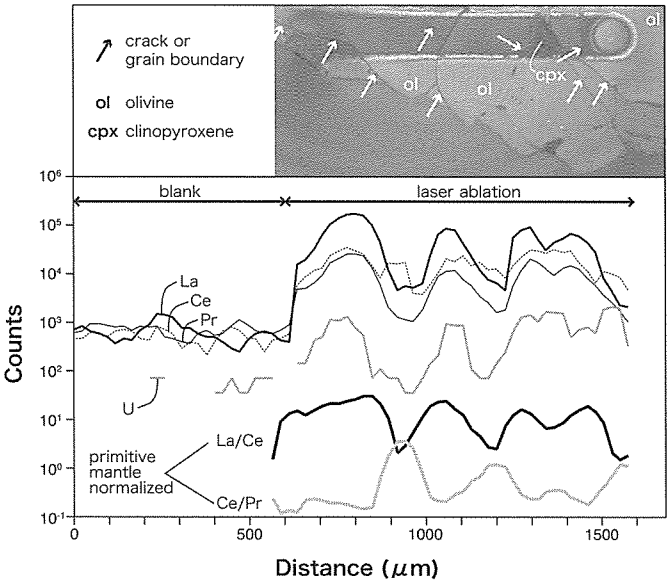

Figure 10. The result of line analysis of the mantle xenolith. Laser beam traverse across a lot of grain-boundary and cracks in the mantle xenolith. Note that the material derived from the grain-boundary and cracks shows high U content and apparent negative anomaly in Ce.

4. Summary

We examined the ability of a LA-ICP-MS to measure trace element compositions of geological materials. The LA-ICP-MS can be used for the rapid and precise determination of trace element compositions in a variety of samples with high special resolution. Furthermore, the method enables us to examine trace element compositions of insoluble minerals for acid treatment. LA-ICP-MS promises to make significant contributions to geological science.

5. Acknowledgements

We thank K. Amita, S. Fukuda, H. Ishibashi, Y. Ishida, T. Kawamoto, Y. Maeda, Y. Nishio, S. Ohsawa, Y.V. Sahoo, T. Shibata, T. Sugimoto, K. Takemura, R. Tatsuta, S. Tokunaga and Y. Watanabe for their support and assistance in analyses of trace elements by ICP-MS.

6. References

Bedini R.M. and Bodinier J.-L. (1999) Distribution of incompatible trace elements between the constituents of spinel peridotite xenoliths: ICP-MS data from the East African Rift. Geochimica et Cosmochimica Acta 63, 3883-3900.

Bodinier J.-L., Merlet C., Bedini R.M., Simien F., Remaidi M. and Garrido C.J. (1996) Distribution of niobium, tantalum and other highly incompatible trace elements in the lithospheric mantle: The spinel paradox. Geochim. Cosmochim. Acta 60, 545-550.

Hiraga T., Anderson I.M. and Kohlstedt D.L. (2004) Grain boundaries as reservoirs of incompatible elements in the Earth's mantle. Nature 427, 699-703.

Hirano N., Kawamura K., Hattori M., Saito K. and Ogawa Y. (2001) A new type of intra-plate volcanism; young alkali-basalts discovered from the subducting Pacific Plate, northern Japan Trench. Geophys. Res. Lett. 28, 2719-2722.

Ishida Y., Morishita T., Arai S. and Shirasaka M. (2004) Simultaneous in-situ multi-element analysis of minerals on thin section using LA-ICP-MS. The Science Reports of Kanazawa University 48, 31-42.

Kalfoun F., Ionov D. and Merlet C. (2002) HFSE residence and Nb/Ta ratios in metasomatised, rutile-bearing mantle peridotites. Earth Planet. Sci. Lett. 199, 49-65.

Yamamoto J. (2001) Investigation of the subcontinental mantle based on noble gas isotopes, petrological and spectroscopic studies of Siberian mantle xenoliths. PhD Thesis University of Tokyo, pp.132.

P-T conditions, Nd-Sr isotopic compositions and the timing of metasomatizm recorded in peridotite xenoliths of French Massif Central.

M.Yoshikawa, T. Kawamoto, J. Yamamoto

Cenozoic volcanoes in French Central Massif brought many peridotite xenoliths and extensive studies were carried out with those peridotite samples by the use of petrography, trace element chemistry and isotopic compositions. We examined the P-T conditions of 10 peridotite xenoliths in scoria deposits from Puy Beaunit and Mont Briancon, and in lava flow from Ray Pic (Bruzet), and describe textural and chemical features of the partial melt texture of phlogopite vein in a Puy Beaunit xenolith and discuss the timing of the metasomatism forming the phlogopite using the Rb-Sr systematics of clinopyroxene and phlogopite.

PT conditions

We determined the equilibrium temperatures based on the two-pyroxene geothermometer using chemical compositions of Ca-rich and Ca-poor pyroxenes (Wells, 1977 CMP). The density, and therefore the pressure, of CO_2 fluid inclusions in host minerals can be estimated from the Fermi diad splitting of Raman spectra of CO_2. If the pressure of CO_2 fluid inclusions was determined, the depth where the CO_2 inclusions were entrained can be obtained (Yamamoto and Kagi, 2006 ChemLet). The estimated ranges of equilibrium temperatures and pressures are 860-940℃ and 0.47-0.68 GPa for Puy Beaunit, 920-1000℃ and 0.95-1.1 GPa for Mont Briancon and 960-990℃ and 0.91-1.1 GPa for Ray Pic (Bruzet), respectively. Puy Beaunit

xenoliths were derived from obviously shallower depths (around 25 km) than the other localities (around 32-42 km). We conclude that the peridotite xenoliths of Puy Beaunit were brought up from the present Moho depth (around 25km, Zanga et al., 1997). The xenoliths from the Puy Beaunit are characterized by the followings: (1) recrystallization texture, (2) existence of hydrous minerals and interstitial glasses, and (3) enriched Sr-Nd isotopic compositions (Mercier and Nicolas, 1975; Downes and Dupuy, 1987). On the basis of isotopic and textural signature, it has been inferred that Beaunit xenoliths were from the depth for the Moho discontinuity (Mercier and Nicolas, 1975; Downes and Dupuy, 1987; Femenias et al., 2005). Furthermore, mixing relationship of major element compositions between interstitial glasses and Cenozoic alkaline basalts has been suggested (Wilson and Downes, 1991).

Vesiculated glass through partial melting of phlogopite veins

One peridotite xenolith in Puy Beaunit has rounded shape phlogopite surrounded by vesiculated glass. Chemical compositions of glasses have high K_2O, Al_2O_3 and CaO contents and enriched isotopic compositions of Sr and Nd than previously reported (Wilson and Downes, 1991; Downes and Dupuy, 1987). Sr and Nd compositions of the Cenozoic alkaline basalts are plotted between primitive basalt and glasses or clinopyroxenes in this sample. This suggest that metasomatism forming phlogopite vein plays a role in basaltic genesis in this region. The chemical compositions of the glasses and the crystalline phases allow us to carry out mass balance calculations among them. The glass chemistry can be formed by the following reaction in nine components of SiO_2-TiO_2-Al_2O_3-Cr_2O_3-MgO-FeO-CaO-Na_2O-K_2O system:

1.1 opx + 0.25 cpx +0.79 phl = 1.0 ol + 1.0 gl + 0.01 sp

opx = enstatite, cpx = diopside, phl = phlogopite, sp = Cr-spinel, ol = forsterite, gl = glass. From these observations, we suggest that a partial melting of phlogopite and pyroxenes formed the glass and olivine + spinel crystallization.

Timing of metasomatism, the formation of phlogopite vein

The Rb-Sr isotopic systematics of phlogopite and clinopyroxene give a reference age of around 60 Ma. This age is younger compared than previous obtained melt extraction age of the Massif Central xenoliths (ca. 360Ma; Witting et al., 2005) and metasomatized age during Variscan orogeny inferred from model ages (e.g. Dunai and Baur, 1995). We propose that this age represent the metasomatism beneath the French Massive Central.

研究報告　Scientific Reports

Measuring lava eruption temperatures with a digital camcorder at Kilauea volcano, Hawaii, USA

G. Carling, *T. Saito*, A. Dangerfield, J. Radebaugh, D. Tingey, J. Keith, J. South (Brigham Young University)

The rise in capability of consumer-grade equipment has yielded a new level of remote sensing of active volcanism. We report measurements of temperatures of skylights and lava flows at the active Kilauea basaltic lava flow field that were obtained using a consumer Sony Handycam with a digital CCD and spectral range from the visible through the near-infrared. This camera was calibrated to produce images that were processed using the Thermoshot software, developed by Saito et al. (2005, EPS 57, e5-e8), which converts a grayscale bitmap image into a thermal image. In this manner, the Sony camcorder can be used as a radiation thermometer.

A skylight and a surface flow at Kilauea were photographed at a range of 5-10 m with our Sony HDR-HC1 camcorder. We simultaneously measured lava temperatures by thermocouple and close-range surface temperatures by optical pyrometer. The Sony digital images were imported to Thermoshot, which produced individual pixel brightness temperatures of 600-1200°C for the skylight, and 500-900°C for the surface flow. The temperatures correlated with actual surface temperatures of individual flow features as measured by thermocouple and pyrometer to within +/- 50°C.

The thermal images created in Thermoshot are useful for obtaining information on the temperature distribution of flow features. Remarkable details of the internal thermal structure of skylights and the surface morphology of lava flows can be seen. Cooler soda straws and flow bands are visible in the skylight, and evidence of inflation can be seen in the flow in a uniformly hotter base to flow lobes. The ease of obtaining thermal data at short wavelengths is of great value in providing another level of close-range remote sensing monitoring of active, basaltic, volcanic features. (EGU general assembly 2007)

Magmatic unmixing in spinel from Late Precambrian Concentrically-Zoned Mafic-Ultramafic Intrusions, Eastern Desert, Egypt

A. Ahmed (Helwan Univ Egypt), *H. Helmy, S. Arai (Kanazawa Univ), M. Yoshikawa*

Spinel is widespread in the ultramafic core rocks of zoned late Precambrian mafic-ultramafic

complexes from the Eastern Desert of Egypt. These complexes are not metamorphosed although weakly altered. Silicate mineralogy and chemistry suggest formation by crystal fractionation from a hydrous magma. Relatively high Cr_2O_3 contents are recorded in pyroxenes and amphiboles from the three plutons. The chrome spinel crystallized at different stages of melt evolution; as early cumulus inclusions in olivine, inclusions in pyroxenes and amphiboles and late-magmatic intercumulus phase. The intercumulus chrome spinel is completely mixed and show narrow-range of chemical composition, mainly Fe^{3+}-rich spinel. Spinel inclusions in clinopyroxene and amphibole reveal a wide range of Al and Mg contents and are commonly zoned. The different chemistries of those spinels reflect various stages of melt evolution and re-equilibration with the host minerals. The early cumulus chrome spinel reveals a complex unmixing structures and compositions. Three types of unmixed spinels are recognized; crystallographically oriented, irregular and complete separation. Unmixing products are Al-rich and Fe^{3+}-rich spinels with an extensive solid solution between the two end members. The compositions of the different types of exsolutions define a miscibility gap with respect to Cr-Al-Fe^{3+}, extending from the Fe^{3+}-Al join towards the Cr corner. Spinel unmixing occurs in response to cooling and increase in the oxidation state. The chemistry and grain size of the initial spinel and the cooling rate control the type of unmixing and the chemistry of the final products. Causes of spinel unmixing during late-magmatic stage are analogous to those in metamorphosed complexes. The chemistry of the unmixed spinels are completely different from the initial spinel composition and are not useful in petrogenetic interpretations. Spinels from oxidized magmas are likely to re-equilibrate during cooling and are not good tools for genetic considerations.

Magmatic Exsolution and Unmixing in Spinel from Late Precambrian Concentrically-Zoned Mafic-Ultramafic Intrusions, Eastern Desert, Egypt

A. Ahmed (Helwan University, Egypt), *H. Helmy*, S. Arai (Kanazawa University), *M. Yoshikawa*

Textural and compositional variations of spinel from mafic-ultramafic complexes from Egypt indicate strong reequilibration and unmixing during late magmatic stage. Extensive sub-solidus re-equilibration processes during protracted cooling from magmatic temperatures down to the temperature of the local geotherm has taken place. Spinel unmixing are caused due to slow cooling, prolonged drop in pressure and increase in oxygen activity in a process analogous to metamorphic processes. The hydrous nature of the mgamas and the dynamic environments in which they were crystallized, explain the chrome spinel textural and compositional variations. The chemistry of unmixed spinel can give misleading petrogenetic interpretations.

Effect of pressure on the crystallization differentiation of hydrous undifferentiated island arc basalt

***M. Hamada*, T. Fujii (Univ Tokyo)**

Dissolution of H_2O characterizes the island arc magmatism and plays a major role in producing diversity in magma compositions, phase relations and differentiation trends. The crustal pressure at which crystallization takes place is another major intensive variable which affects the phase relations and/or phase proportions of island arc basalts. We investigated phase relations of undifferentiated (Mg#~60) hydrous island arc basalt experimentally to clarify the effect of crustal pressure (2 to 7 kb) on the crystallization differentiation in the island arc. The obtained degree of crystallization was as much as ~50 wt.%. Composition of the starting material is enriched in normative orthopyroxene content compared with previous experiments. Experiments were originally designed to conduct under NNO buffer, but experiments under QFM (~NNO-1) buffer were also performed to discuss the effect of f_{O2} on phase relations.

With H_2O less than 1 (±1) wt.% in primary magma, a suite of melt compositions forms tholeiitic differentiation trends, although they differs according to pressure. At 2 kb, crystallization differentiation is controlled by olivine + plagioclase. Increasing pressure ≥ 4 kb induces early crystallization of orthopyroxene instead of olivine. As a result, enrichment of SiO_2 content in residual melt becomes suppressed.

With H_2O more than 3(±1) wt.% in primary magma, calc-alkaline differentiation trends were inevitably obtained due to early crystallization of magnetite and/or clinopyroxene, proportion of which were sensitive to H_2O content in melt and f_{O2}. At 2 kb, crystallization differentiation is controlled by olivine + plagioclase + magnetite. At pressure ≥ 4 kb, crystallization differentiation is controlled by olivine + clinopyroxene ± plagioclase ± orthopyroxene ± magnetite. Contribution of clinopyroxene instead of orthopyroxene became significant as near liquidus phase, resulting in the enrichment of SiO_2 and depletion of FeO*.

Our experimental results are useful to understand crystallization differentiation trends of island arc basalts. For example, the contrasting differentiation trends between Izu-Oshima volcano and Fuji volcano, both of which are tholeiitic volcanoes located in the northern Izu arc, could be explained by crystallization differentiation with primary H_2O less than ~1 wt.% under different pressure. Tholeiitic differentiation trend commonly observed at the volcanic front such as Izu-Oshima volcano is interpreted as a result of crystallization at pressure less than ~2 kb. Basalt-dominated crystallization trend at Fuji volcano would be produced by crystallization at deeper level (more than 3-4 kb), which would resulted in the greater contribution of pyroxenes and suppressing enrichment of SiO_2 in the residual melt.

Petrology of the Genina Gharbia mafic-ultramafic intrusion, Eastern Desert, Egypt: insight to deep levels of late-Precambrian island arcs

H. Helmy, M. Yoshikawa, T. Shibata, **S. Arai (Kanazawa University),**
H. Kagami (Niigata University)

The Arabian-Nubian shield represents one of the most important sites of juvenile crustal growth during the late Proterozoic. The Pan-African grew more than 2 million square kilometers during the period 800-600 Ma. A large percentage of this growth is derived from the mantle by subduction accretion and arc collision. The Genina Gharbia (GG) intrusion, located in the Eastern Desert of Egypt along one of the deep fracture zones trending ENE, is interpreted be the remains of a magma chamber that crystallized at the base of a mature interoceanic island arc. It is one of a number of isolated masses of zoned peridotite-gabbro complexes that recur along the major fracture zones. These masses, the roots of late Precambrian island arc, were uplifted during the Pan-African Orogeny. In this contribution we present petrographic, chemical and mineralogical characteristics of the (GG) mafic-ultramafic plutonic rocks as insights to deep levels of Precambrian island arcs for the purpose of constraining the evolution and compositions of their parental melts. The GG mafic-ultramafic intrusion is located about 140 km southeast of Aswan. It covers an area of 9 km long and 3.5 km wide and comprises olivine diorite (in the margin), gabbros, pyroxenites, hornblende pyroxenites, and hornblende-bearing peridotite (in the core). The contacts between different lithologies within the intrusion are either gradational or tectonic. This association intruded Precambrian metasedimentary and island arc volcanic rocks. The intrusion is non-metamorphosed and show cumulate textures. Massive and disseminated Cu-Ni sulfide ores are found in hornblende gabbro and hornblende-bearing peridotite. Both mafic and ultramafic rock units are characterized by high modal content of hornblende and abundant biotite and apatite indicating hydrous nature of the parent magma. Mafic minerals in the peridotite core are more magnesian than those in the margin rocks (Mg# Ol 85-73, Opx 83-68, Cpx 87-79, Hbl 87-73). Two types of spinel are identified; Al-rich and Fe-rich spinel, with extensive solid solution between them reflecting extensive sub-solidus equilibration. Orthopyroxene is enstatite with high Al_2O_3 (1.93) and Cr_2O_3 (0.6 wt.%) contents. Amphiboles of the ultramafic cores have constantly high Cr_2O_3 contents (1.1 wt.%). Reaction between olivine and plagioclase to form hornblende is common. The variations in modal abundance and mineral chemistry throughout the intrusion are consistent with fractional crystallization and accumulation. The compositions of olivine, spinel and pyroxenes are used to constrain the evolution of the parental magma and to estimate the temperature and oxygen activity in the melt. The major and trace elements whole rock chemistry is consistent with evolution by fractional crystallization from a mantle-derived arc magma where the Mg-number decrease and REE and HFSE increase with differentiation. The different lithologies at GG have high

$^{147}Sm/^{144}Nd$ (0.132 – 0.186) and high initial $^{143}Nd/^{144}Nd$ ratios (0.5125 – 0.5128). The rocks exhibit positive εNd values (+4.8 to +6.7) very similar to other zoned and island arc complexes from the Eastern Desert. Based on textural relationships and chemical trends it is concluded that the GG rocks originated by igneous accumulation from a hydrous magma at the base (ca. 30 km depth) of a mature island-arc before being emplaced along the fault zones during the Pan-African Orogeny. The parental magma has been derived from a mantle source that was previously contaminated by subduction of Mozambique oceanic crust.

Second Critical Endpoint Between Aqueous Fluids And High-Magnesian Andesite/ Oceanic Sediment

***T. Kawamoto*, M. Kanzaki (Misasa, Okayama University), K. Mibe (ERI University of Tokyo), K. N. Matsukage (Mito, Ibaraki University), S. Ono (IFREE, JAMSTEC)**

Aqueous fluids dissolve significant amounts of silicates under high-temperature and high-pressure condition. Silicate components dissolved in aqueous fluids coexisting with mantle peridotite change their major element chemistry from andesitic at 1-2 GPa to peridotitic at 3 GPa and higher pressures (Ayers et al., 1997; Stalder et al., 2001; Mibe et al., 2002; Kawamoto et al., 2004). In the present study, we show direct observations of unmixing and mixing between aqueous fluid and a high-magnesian andesite (Tatsumi, 1981) and between aqueous fluid and an oceanic sediment (Ono, 1998) by use of synchrotron X-ray radiography with multi-anvil type high-T and high-P apparatus at SPring-8 (Mibe et al., 2004). We observed aqueous fluid and a high-Mg andesitic (HMA) melt coexisting in pressures lower than 2.7 GPa. While above 2.8 GPa, we observed only one fluid phase, suggesting that the HMA and aqueous fluids are completely mixing and become supercritical. Because subducting oceanic lithosphere has oceanic sediments on its surface, such oceanic sediments should inevitably be flushed with aqueous fluids liberated from dehydration reactions of hydrous minerals in basaltic and peridotitic layers underneath the sediment layer. In addition to the HMA, we determined a critical endpoint between an oceanic sediment and aqueous fluid, which is located at around 2.6 GPa.

Mibe et al. (2007, and in preparation) found a second critical endpoint between aqueous fluids and a peridotitic/ a MORB melt at 3.8/ 3.0 GPa, respectively. Based on these available data, we suggest that slab-derived fluids should be under supercritical conditions at the downgoing slabs beneath the volcanic arcs (3 - 6 GPa, Tatsumi and Eggins, 1995). This means a continuous change from aqueous fluids to hydrous melts at the base of mantle wedge. Whether the slab-derived fluids have chemical characteristics like a partial melt or an aqueous fluid depends on the temperature; slab derived-supercritical fluids in relatively warm

regions can dissolve more silicate components than slab derived-supercritical fluids in relatively cold regions.

The melt-like supercritical fluid formed at the base of the warm mantle wedge will separate into a melt phase and a fluid phase when the supercritical fluid meets its critical curve during its ascent (Bureau and Keppler, 1999). The formation of such two phases in mantle wedge may result in double-magmatism, for example, coexisting of adakite rocks and common island-arc rocks (Defant and Drummond, 1990), or HMA and basalt (Tatsumi, 1981). The adakite and HMA magmas are supposed to be formed by partial melting of subducting lithosphere (Defant and Drummond, 1990; Tatsumi, 2006). We think that they can be generated by reaction with the melts or aqueous fluids separated from the supercritical fluids. In order to produce such a dense supercritical fluid, high-temperature conditions are required, which is similar to the partial-melting theory for adakite and HMA (Defant and Drummond, 1990; Tatsumi, 2006). Yet our hypothesis can make account for the coexistence of those silica-rich magmas (adakite and HMA) and the other magmas.

References

Ayers, J.C., Dittmer, S.K., Layne, G.D. (1997) Partitioning of elements between peridotite and H_2O at 2.0-3.0 GPa and 900-1100 °C, and application to models of subduction zone processes. Earth and Planetary Science Letters, 150, 381－398.

Bureau, H., Keppler, H. (1999) Complete miscibility between silicate melts and hydrous fluids in the upper mantle; experimental evidence and geochemical implications. Earth and Planetary Science Letters, 165, 187-196.

Defant, M.J., Drummond, M.S. (1990) Derivation of some modern arc magmas by melting of young subducted lithosphere. Nature, 347(6294), 662-665.

Kawamoto, T., Matsukage, K.N., Mibe, K., Isshiki, M., Nishimura, K., Ishimatsu, N., Ono, S. (2004) Mg/Si ratios of aqueous fluids coexisting with forsterite and enstatite based on the phase relations in the Mg_2SiO_4-SiO_2-H_2O system. American Mineralogist, 89, 1433-1437.

Mibe, K., Fujii, T., Yasuda, A. (2002) Composition of aqueous fluid coexisting with mantle minerals at high pressure and its bearing on the differentiation of the Earth's mantle. Geochimica et Cosmochimica Acta, 66, 2273-2285.

Mibe, K., Kanzaki, M., Kawamoto, T., Matsukage, K.N., Fei, Y., Ono, S. (2004) Determination of the second critical endpoint in silicate-H_2O systems using high-pressure and high-temperature X-ray radiography. Geochimica et Cosmochimica Acta, 68, 5189-5195

Mibe, K., Kanzaki, M., Kawamoto, T., Matsukage, K.N., Fei, Y., Ono, S. (2007) Second Critical Endpoint in Peridotite-H_2O System. Journal of Geophysical Research, in press.

Ono, S. (1998) Stability limits of hydrous minerals in sediment and mid-ocean ridge basalt compositions: implications for water transport in subduction zones. Journal of Geophysical Research, 103, 18253-18267.

Stalder, R., Ulmer, P., Thompson, A.B., Günther, D. (2001) High pressure fluids in the system $MgO-SiO_2-H_2O$ under upper mantle conditions. Contributions to Mineralogy and Petrology, 140, 607-618.

Tatsumi, Y. (1981) Melting experiments on a high-magnesian andesite. Earth and Planetary Science Letters, 54, 357-365

Tatsumi, Y., Eggins, S. (1995) Subduction zone magmatism. Blackwell.

Tatsumi, Y. (2006) High-Mg Andesites in the Setouchi Volcanic Belt, Southwestern Japan: Analogy to Archean Magmatism and Continental Crust Formation? Annual Review of Earth and Planetary Sciences, 34, 467-499.

Difference of hydrogen bondings in pure water and alkali chloride solutions based on Raman spectroscopy and MD calculation

Y.Kumagai (Geophysics major, Faculty of Science, Kyoto University),
M.Kanzaki (Misasa, Okayama University), *T.Kawamoto*

We have conducted two series of experiments in order to understand chemical features of aqueous fluids and sea water in the earths interior: (1) Raman scattering spectra of alkali chloride solutions under high pressure conditions at room temperature, and (2) molecular dynamics calculations of pure water and NaCl solutions. Base on these data, we will discuss structural difference be t ween pure H_2O and alkali chloride solutions.

1 Introduction H_2O is the most abundant volatile species in the earths interior. H_2O have effects on almost all phenomena in the earths interior. Kawamoto and the others (2004) suggested a possible structural change from low-pressure water to high-pressure water based on Raman spectroscopy of pure H_2O (Kawamoto, Ochiai, Kagi, Changes in the structure of water deduced from the pressure dependence of the Raman OH frequency. Journal of Chemical Physics 120, 5867-5870, 2004). Sea water can be the aqueous fluid which is introduced into the earths mantle through subduction. Therefore, it is important to know the structural features of alkali chloride solutions under high-pressure conditions. In the present study, we obtained Raman spectra of $XCl12H_2O$ and $XCl72H_2O$ where X is Li, Na, and K under room temperature and high-pressure conditions up to 2 GPa. In addition to this, we carried out molecular dynamics calculations in the systems of pure H_2O and NaCl solutions.

2.1 High-pressure spectroscopy We put alkali chloride solutions inside of a hole in a rhenium plate located in the middle of a diamond anvil cell with a ruby chip as a pressure marker. High pressure can be attained by approaching two diamonds. Sample can be observed visually under a microscope. At each pressure, Raman spectrum was sampled with Raman

microscope (Kaiser Hololab 5000) in the institute of Geothermal Sciences, Kyoto University.

2.2 Molecular dynamics calculation By the use of the MD program developed by Dr. Katsuyuki Kawamura of the Tokyo Institute of Technology (MXDORTO, version 2006), we carried out a series of calculations of pure H_2O (512 H_2O) and NaCl solutions (8 NaCl in 512 H_2O, 16 NaCl in 512 H_2O). So far now, the calculations were done at room temperature and room pressure. An effect of pressure will be investigated in the near future.

3 Results The Raman data show an increase of Raman frequency with increasing concentration of alkali chloride. This can suggest that the length of hydrogen bonding of H_2O increases in the solutions (Nakamoto, K., Margoshes. M., and Rundle, R.E. Stretching frequencies as a function of distances in hydrogen bonds. Journal of the American Chemical Society, 77, 6480-6486 1955). Alternatively, it can be interpreted as a result of decreasing strength of hydrogen bonding. As a function of pressure, the Raman frequencies decrease, suggesting shortening length of hydrogen bonding or strengthening hydrogen bonding. The pressure dependence of Raman frequency seems constant in the XCl12H_2O solutions, while it has a kink at 0.4 GPa in XCl72H_2O solutions, especially NaCl72H_2O. Therefore, it is likely to mention that sea water may have a possible structural change as suggested for pure H_2O.

MD calculations gave us the lengths of hydrogen bonding, the numbers of hydrogen bonding, and the vibration spectra of pure H_2O and the two NaCl solutions. We learned the followings: (1) Increasing NaCl decreases the number of hydrogen bonding between H_2O molecules. (2) Increasing NaCl decreases the lengths of hydrogen bonding. This feature was not expected, because the Raman spectroscopy suggested an opposite possibility. (3) Vibration frequency increase with increasing NaCl. This is consistent with our Raman experimental observation.

4 Conclusion The present MD calculation and the Raman spectroscopy suggest that the number of hydrogen bonding between H_2O molecules decrease in NaCl solutions, and this results in decreasing the strength of hydrogen bonding between H_2O molecules. The weaker hydrogen-bonding feature can be seen in the higher Raman frequencies in solutions than in pure water. The existence of a kink in a pressure dependence of the Raman frequencies in NaCl 72H_2O solution suggests that seawater may have a structural change as observed in pure H_2O under high PT conditions.

Water and Magma

T. Kuritani

Water has been continuously degassed from the Earth's interior by magmatism throughout evolution, and can significantly affect dynamic processes of its carrier, i.e., magmas, during their transport from the mantle to the Earth's surface. This paper summarizes the effects of water on the physical and thermodynamic properties of magmas, and their roles in magmatic processes. Magmas commonly contain at least ~0.2 wt.% of water, and some magmas can have up to 6 wt.%. Despite the fact that water is a minor component in silicate liquids, the effects of dissolved water on the properties of silicate melt are significant, because it has a much lower molecular weight at ~18.0 than those of the other components (SiO_2: ~60.1, for example). Dissolved water greatly affects the density and the viscosity of silicate melts, thereby controlling rates of dynamic processes of magmas, such as segregation of primary melts in the mantle, transport of magmas from the mantle to the crust, convections and crystal-melt separation in crustal magma chambers, and ascent of magmas in volcanic conduits. Water also influences solid-melt thermodynamic equilibrium relationships, and this affects the chemical differentiation paths of magmas, in addition to the amount of melt production in the mantle by changing solidus temperatures. The eruptive behavior of volcanoes is driven by the exsolution of magmatic water, and as such depends on the water solubility of magmas mainly as a function of pressure. Water has also played important roles in the evolution of the Earth. Magma generation has been induced by water in the Earth's interior, and magmas have carried materials and energy from the interior to the surface of the Earth. In particular, water transport beneath island arcs is important in the global water cycle, and has greatly affected the environment of the Earth's surface.

(Journal of Geography, Vol. 116, 2007)

Rates of Thermal and Chemical Evolution of Magmas in a Cooling Magma Chamber: a Chronological and Theoretical Study on Basaltic and Andesitic Lavas from Rishiri Volcano, Japan

***T. Kuritani* (ISEI, IGS), T. Yokoyama (ISEI), E. Nakamura (ISEI)**

Rates of magmatic processes in a cooling magma chamber were investigated for alkali basalt and trachytic andesite lavas erupted sequentially from Rishiri Volcano, northern Japan, by dating of these lavas using ^{238}U-^{230}Th radioactive disequilibrium and ^{14}C dating methods, in

combination with theoretical analyses. We obtained the eruption age of the basaltic lavas to be 29.3 ± 0.6 ka by ^{14}C dating of charcoals. The eruption age of the andesitic lavas was estimated to be 20.2 ± 3.1 ka, utilizing a whole rock isochron formed by U-Th fractionation as a result of degassing after lava emplacement. Because these two lavas represent a series of magmas produced by assimilation and fractional crystallization in the same magma chamber, the difference of the ages (i.e. ~9 kyr) is a timescale of magmatic evolution. The thermal and chemical evolution of the Rishiri magma chamber was modeled using mass and energy balance constraints, as well as quantitative information obtained from petrological and geochemical observations on the lavas. Using the timescale of ~9 kyr, the thickness of the magma chamber is estimated to have been about 1.7 km. The model calculations show that, in the early stage of the evolution, the magma cooled at a relatively high rate (>0.1°C/year), and the cooling rate decreased with time. Convective heat flux from the main magma body exceeded 2 W/m^2 when the magma was basaltic, and the intensity diminished exponentially with magmatic evolution. Volume flux of crustal materials to the magma chamber and rate of convective melt exchange (compositional convection) between the main magma and mush melt also decreased with time, from ~0.1 m/year to ~10^{-3} m/year, and from ~1 m/year to ~10^{-2} m/year, respectively, as the magmas evolved from basaltic to andesitic compositions. Although the mechanism of the cooling (i.e. thermal convection and/or compositional convection) of the main magma could not be constrained uniquely by the model, it is suggested that compositional convection was not effective in cooling the main magma, and the magma chamber is considered to have been cooled by thermal convection, in addition to heat conduction.

(Journal of Petrology, Vol. 48, 2007)

Dunite channels in the Horoman peridotites, Japan: Textural and geochemical constraints on melt/fluid transport through the lithosphere

K.Niida (Hokkaido Univ), D.H.Green (ANU), *M.Yoshikawa*, S.M.Eggins (ANU)

Dunite channels generated in the lithospheric mantle have been inferred as pathways of basaltic magmas [1]. Besides the porous flow models, a fracture-controlled melt transport has also been proposed for formation of ophiolitic dunite-chromitite channels [2] [3].

Field observations, mineralogical and geochemical data from the Horoman peridotites suggest the following sequence of dunite formation:

1. Initiation of melt migration channels

Fluid-induced fracturing occurs in the layered peridotites during deformation, followed by high temperature melt migration.

2. High T melt flow along the open fracture

A narrow (cm-wide) segregation of dunite-chromitite cumulate formed along the fracture. Opx-dissolution and pargasite crystallization occurs along the reaction front. The channeling melt may become fluid-saturated.

3. Dunite growth

Reaction front becomes more active, producing 10 to 100 cm-wide replacive dunite by a porous flow of fluid-saturated melt with opx-dissolution melt dominant within the channel.

4. Crystallization of olivine megacrysts

Prior to closure of the open fracture, stagnant melt traps within dunite channel. Porous flow of fluid accelerates crystallization of olivine.

5. Fluid+melt channel closed

Opx+cpx+spinel crystallized from segregation melt along active fracture surfaces within the dunite channels, and often cross-cutting the olivine megacrysts. Fluid inclusions trapped.

References

[1] Kelemen P.B. et al. (1995) *Nature* **375,** 747-753.

[2] Lago B.L. et al. (1982) *JPetrol* **23,** 103-125.

[3] Suhr G. (1999) *JPetrol* **40,** 575-599.

(Abstract of Goldschmidt Conference Geochim. Cosmochim. Acta, 70, 445, 2006)

Trapping P-T conditions of fluid inclusions in quartz veins from the Sanbagawa metamorphic belt, SW Japan

K. Nishimura,* K. Amita (Akita Univ), *S. Ohsawa,
T. Kobayashi (Kyoto Univ), T. Hirajima (Kyoto Univ)

Microthermometry experiments and chemical analyses were conducted for fluid inclusions within quartz veins in a pelitic schist of the Sanbagawa metamorphic belt, Saganoseki, Kyushu, Japan, by using Heating and Cooling stage and micro Raman spectrometer. The quartz veins are developed parallel to the main foliation of the pelitic schist, and are abundant in H_2O -NaCl-CH_4 fluid inclusions (Fig. 1). The trapping P-T conditions of fluid inclusions are determined as 3.7–6.5 kb and 320-450 °C, by combining microthermometry and the pressure dependence of CH_4 Raman shift. Estimated P-T range is consistent with the metamorphic condition of the host rock (6-8 kb, 300-400 °C), suggests that the fluid inclusions are primary ones trapped at the relevant depth and they give a concrete evidence on the fluid composition derived from metamorphic reactions at 10-20km depths.

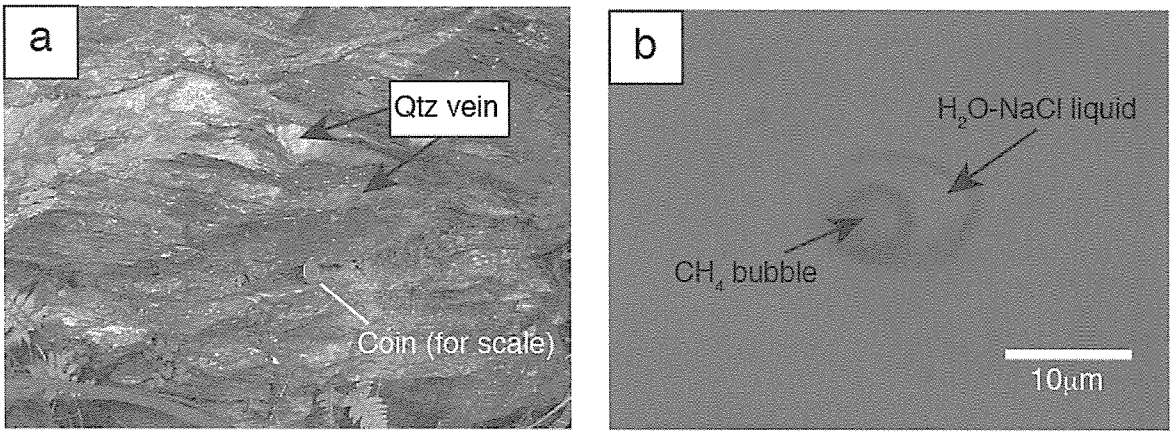

Figure 1. a: Fluid inclusion-bearing quartz vein(s) developed parallel to the main foliation of pelitic schist in the chlorite zone of the Sanbagawa belt, Saganoseki, SW Japan. b: Close up view of a fluid inclusion consisting of H_2O-NaCl liquid and CH_4 bubble, trapped in the quartz vein.

(Submitted to Journal of Mineralogical and Petrological Sciences)

Geochemical features of dehydrated fluid from subducting hydrous oceanic plate inferred from chemical and isotopic signatures of mineralized waters emerging in fore-arc regions of convergent plate boundaries

S. Ohsawa **, K. Amita (Akita Univ.),** ***K. Nishimura*** **, K. Kazahaya (AIST)**

1. Introduction

Nowadays, lots of geophysicists and geologists believe that water is volatilized from subducting hydrous oceanic plate, which is geologically equivalent to high-pressure metamorphic water #(footnote), and it should be the occasion for seismicity and magmatism (etc.) in convergent plate boundaries. However, nobody should have seen such water directly yet.

Recently, "direct" observations of the water volatilized from subducting hydrous oceanic plates, which we call dehydrated fluid from slab, have been started: e.g., geochemical analysis of sea-floor spring accompanied with serpentinite seamount, fluid inclusion study of metamorphic rock, etc. On the other hand, we also suggested that it should be possible to extract information of dehydrated fluid from slab using highly mineralized water discharged from "hot spring" well in the 1000m class in fore-arc region [Amita et al., 2005].

The reason why we aim at fore-arc regions that original features of dehydrated fluid from slab under volcanic arc regions are considerably altered by magma generation on its way to ascend, whereas dehydrated fluid from slab originated beneath fore-arc regions can be expected to ascend directly without such alteration. Of course, it cannot entirely avoid

alterations, for example mantle metasomatism might occur a little, so whether our study succeeds or not depends on whether we find out or not good geochemical indicators of dehydrated fluid from slab.

Purpose of our study is to gather some geochemical evidences that mineralized waters discharged from "hot spring" wells and emerging as warm and cold springs in fore-arc regions of convergent plate boundaries are mostly and/or partially derived from dehydrated fluid from slab, and to understand how chemistry of the dehydrated fluid originated from subducting hydrous oceanic plate changes as it (subduction) becomes deeper.

2. Strongly mineralized waters in fore-arc region of South-West Japan

It has been known that there are unidentified highly mineralized waters emerging along the major tectonic lines. e.g. the Median Tectonic Line (MTL). Range of total dissolved substance (TDS) of the waters extends from 7.8g/L to 51g/L (mean value=22g/L), which ranks as one of the densest hot and mineral spring waters in Japan.

Water isotope compositions (δD and $\delta^{18}O$) of the particularly strongly mineralized waters sampled from Kyushu and Kii, which are denser than modern seawater, are fallen in or close to the range of those of tectono-metamorphic fluid inclusions [Hurai et al., 1997], and the other sampled waters except for dense waters sampled from a gas-field in Kyushu are explained to be formed by mixing of such strongly mineralized waters with shallow groundwater of meteoric origin. This water isotope signature implies that the mineralized waters are mostly and/or partially originated from dehydrated fluids from the hydrous oceanic plate (Philippine-Sea plate) subducting through the Nankai Trough. On the other hand, water isotope compositions of the gas-field brines in Kyushu are fallen within the range of pore waters of marine sediments [Mora, 2005], therefore the gas-field brines are thought to be a squeezed pore water from marine sediments.

The strongly mineralized waters show considerably low Br/Cl(*bromide/chloride*) ratios in comparison with modern seawater and/or the gas-field brines, and are rich in B(*boron*), Li(*lithium*) and Cs(*cesium*) called "typical" fluid-mobile trace elements relative to the gas-field brines. Furthermore, He(*helium*) isotope ratios ($^3He/^4He$) of accompanied gases with the strongly mineralized waters clearly show over $^3He/^4He$ ratio of air and get closer to that of the mantle-derived He. These data reinforce to the above implication that the strongly mineralized waters found in this studied area would be derived from dehydrated fluids from slab.

Depths to the top of the subducting Philippine-Sea plate beneath the sampling locations of the strongly mineralized waters in SW-Japan are about 70km.

3. Mineralized waters in fore-arc region of the North-Island, New Zealand

The North-Island of New Zealand is located in a similar tectonic setting to SW-Japan where oceanic plate is subducting obliquely by several cm/yr and right-lateral faults are formed in

the fore-arc region. It had already found that mantle-derived He bearing mineralized waters, whose oxygen isotope ratios ($\delta^{18}O$) are similar to those of the strongly mineralized waters of SW-Japan but hydrogen isotope ratios (δD) are somewhat higher than them, exist there [Giggenbach et al., 1993]. It was also implied that these mineralized waters in New Zealand could be derived from the subducting hydrous oceanic plate (Pacific plate) through the Hikrangi Trough, and the most likely dehydration process was suggested to be the conversion of smectites to illite.

Depths to the top of the subducting Pacific plate beneath the sampling locations of the focused mineralized waters in the North-Island of New Zealand are about 20km and they are much shallower than those in SW-Japan (ca. 70km). Br/Cl, B/Cl and Li/Cl ratios of the New Zealand waters are all shifted from those of the strongly mineralized waters in SW-Japan to those of the gas-field brines recognized to be a kind of squeezed sediment pore water. Therefore, the mineralized waters in the fore-arc region of the North-Island, New Zealand might be derived from dehydrated fluid in a transition stage of diagenic and metamorphic dehydrations during plate subduction.

4. Comparison between SW-Japan and New Zealand, and conclusive remark

Through the examinations of the highly mineralized waters in the fore-arc region of SW-Japan in contradistinction to the mineralized waters in the North-Island fore-arc of New Zealand and the gas-field brines in the Kyushu fore-arc area of SW-Japan, we could make a model on how geochemical natures of dehydrated fluids from slab change as subduction becomes deeper. Slab dehydration is started as squeeze of sediment pore water at first, and then changes to diagenic dehydration and finally transforms to metamorphic dehydration. In conjunction with such transition of dehydration mode, fluids released from the down-going slab would become poor in D(*deuterium*) and Br, and enriched in B and Li by degree relative to modern seawater. This geochemical change on a series of the slab dehydration is, as it were, a sort of chemical evolution of seawater carried into the Earth's interior.

Hydrous oceanic plate is formed by seawater hydration of oceanic lithosphere stratigraphically constituted of marine sediments, oceanic crust and lithospheric mantle, thus several hydrous minerals, e.g., smectite, chlorite, serpentine, are formed in the oceanic plate before subduction. Dehydrated fluid generating from such subducting hydrous oceanic plate called slab results from high-pressure metamorphic reactions of the hydrous minerals included in the slab.

Magnetic petrology and its implication for magma mixing of the 1991-1995 dacite at Unzen volcano, Japan

T. Saito, N. Ishikawa (IHS, Kyoto)

Magnetic petrologic analyses were carried out on lava samples from the lava dome of the 1991-1995 eruption of Unzen volcano, Japan. As a result, three kinds of titanomagnetites with different Curie temperatures were identified and the difference between the samples from the lava dome which grew exogenously and endogenously were revealed. Titanomagnetites with Tc of 460-500°C and 380-400°C are the predominant magnetic minerals. In addition, a titanomagnetite with Tc of ~540°C, but in low concentration, is also present. The exogenous lava samples contain more titanomagnetite with Tc of 380-400°C and less microphenocrysts of titanomagnetites than the endogenous samples. The equilibrium temperature of 900-920°C, 780-820°C and 720°C is estimated from titanomagnetite with Tc of 380-400°C, 460-500°C and 540°C, respectively. We suggest that these titanomagnetites are probably formed by magma mixing and eruption processes. Titanomagnetite with Tc of 460-500°C was derived from felsic magma (780-820°C) in a shallow chamber. Titanomagnetite with Tc of 380-400°C was produced from the mixed magma (900-920°C). After being squeezed out from the reservoir, a small amount of titanomagnetite with Tc of ~540°C was crystallized. (Earth Planets Space. 2007. in press)

Magnetic petrology and its implications for eruption process of the 1884-1885 andesite lava of Suwanosejima volcano, Japan

T. Saito, M. Iguchi (DPRI, Kyoto), N. Ishikawa (IHS, Kyoto),
M. Torii (Okayama Univ. Sci.), *T. Sugimoto*, *T. Ohkura*

Suwanosejima volcano in Tokara Islands, southwest Japan, is one of the most active volcanoes in Japan. Strombolian eruptions have repeatedly occurred. During the last fatal eruption in 1884-1885, andesite lava flows were effused from the summit crater and covered the eastern flank of the volcano. The lava flow deposits show smooth and ropy surface, like Pahoehoe lava. Lava tubes are also observed in some places. These occurrences indicate that the viscosity of the erupted andesite lava was as low as basaltic lava. In order to clarify the eruption process of the 1884-1885 activity, we carried out magnetic petrological analyses on the 1884-1885 lava samples.

As a result, we found interesting magnetic petrologic characteristics that seemed to be derived from the eruption process of 1884-1885 eruption. Petrological analyses revealed that the lava is two-pyroxene andesite (SiO_2 56.9-57.2 wt.%), containing phenocrysts of plagioclase, clinopyroxene and orthopyroxene. Fe-Ti oxide phenocrysts are absent. Small

microphenocrysts of Fe-Ti oxides are crystallized in the samples from the central part of the flow units. This feature was consistent with magnetic results. Samples from the flow surface showed very high MDF of 100mT, though samples from the inner part showed moderate MDF below 25mT. It suggests that magnetic minerals in the samples from flow surface are very fine titanomagnetites and the samples from inner part contain larger titanomagnetite. Crystallization conditions were estimated by using MELTS program (Ghiorso and Sack, 1995; ver 5.0.0). As a result, an initial water content below 0.5wt.% and high eruption temperature about 1100 degrees C were estimated. It suggests that such dry magma, which lacks Fe-Ti oxide phenocrysts, effused at high temperature about 1100 degrees C and the lava showed high fluidity, resulting in the textures like Pahoehoe lava flow. (H18 annual meeting, DPRI, Kyoto Univ.)

Water, heat and chloride budgets of the crater lake at Naka-dake, Aso volcano, Japan

T. Saito, S. Ohsawa,* T. Hashimoto (Hokkaido), *A. Terada, S. Yoshikawa, T. Ohkura

A volcanic lake is not a simple pool of meteoric water but an unstable hydrothermal reservoir, which is controlled by the balance of volcanic and nonvolcanic heat, water and chemical fluxes into and out of the lake. By studying volcanic lakes, therefore, we can estimate the hydrothermal activity under the lake and detect some signals preceding an eruption. Naka-dake, one of the central cones in Aso caldera, Japan, is an active volcano whose crater is now occupied with light-green-colored hot water. The lake water shows high temperature above 50°C, high acidity below PH 1 and high concentration of chloride anion, suggesting high flux of volcanic input. However, little is known about the crater lake system at Naka-dake. In order to evaluate volcanic input into the crater, box models about water, heat and chloride were constructed and calculations were made by using the data collected between 2000 and 2003. During this period, the water level was gently decreased by more than 10 meters. The results showed that the lake water is mainly supplied by volcanic input (3500-5800 m^3/day) and is dissipated by evaporation from the lake surface (3900-5900 m^3/day) and seepage from the lake bottom (800-2100 m^3/day). Meteoric water flux (460-2900 m^3/day) is not so important. Positive correlation between the chloride concentration of volcanic input and volcanic water flux was suggested. Thermal energy of volcanic input was estimated to be about 110-200 MW, which is the dominant influx. Most heat loss occurred at the lake surface through evaporation (100-150 MW). The enthalpy of volcanic input was estimated to be about 2600-4600 kJ/kg, which corresponds to the enthalpy of steam at several hundred degrees C. (2006 fall meeting, the Volcanological Society of Japan)

Improvement of a radiation thermometry system using a consumer digital camcorder

T. Saito, G. Carling (Brigham Young University), I. Iizawa (Horikawa Senior High School)

A radiation thermometry system using a consumer digital camcorder was developed. Basic idea and system were already reported by Saito et al. (2005). The initial system was calibrated for use by Sony's digital camcorder, DCR-PC120. Recently, camcorders that can record high-definition video are widely available and our system had been asked to use another model. We improved our software to use any camcorders and adjusted a system for a high-definition camcorder, HDR-HC1.

Thermoshot is a software, which converts a grayscale bitmap image into a thermal image. We improved the software to input given coefficients of third degree equation, which relates a pixel brightness with its temperature (Fig. 1). We can obtain a thermal image from any camcorders by using this revised Thermoshot if the coefficients of third degree equation for the camcorder are provided.

We carried out calibration experiments for a high-definition camcorder, HDR-HC1. This is the first model of consumer camcorder, which can record high-definition video, produced by Sony Corporation. The experimental method was followed by Saito et al. (2005). As a result, we got a following relation of brightness and temperature for Nightshot camera mode;

$T = 0.1472I^3 - 2.3059I^2 + 27.529I + 177.23$

T: temperature (degrees C)

I: corrected brightness.

This relation was obtained between 350 and 600 degrees C. Incidentally, the relation for visible camera mode of HDR-HC1 did not differ from that of DCR-PC120. Our work enabled anybody to use HDR-HC1 as a radiation thermometer (Carling et al., 2007).

Thermoshot is posted on the following website.

http://www.gaia.h.kyoto-u.ac.jp.~thermoshot/index_e.htm

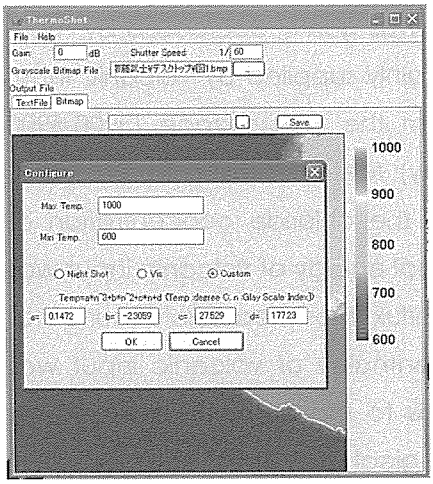

Fig. 1 User interface of Thermoshot. Coefficients can be given from the configuration window.

3-D modeling of resistivity structure of Unzen Volcano, Japan, using TDEM data

W. Srigutomo, T. Kagiyama,* W. Kanda(Kyoto Univ), H. Munekane(Geographycal Survey Institute), T. Hashimoto(Hokkaido Univ), *Y. Tanaka,* H. Utada(Tokyo Univ), *M. Utsugi

High quality transient magnetic data were collected at 50 sites during TDEM campaigns conducted in 1995, 2001 and 2002 in Shimabara Peninsula, Kyushu, Japan, allowing us to investigate possible models of magma supply system below Unzen using a 3-D forward modeling analysis (Fig.1). In the modeling scheme, first, a background 1-D model which explains roughly the data measured at all sites was constructed based on resistivity structure obtained from smoothness-constrained 1-D inversion. Conductive prisms were added to the 1-D background structure to calculate the 3-D response using a staggered grid finite-difference method. A weighted misfit between the data and the 3-D response was compared with the misfit between the data and the 1-D background, by which a degree of improvement to judge the fitness between the calculated response and the observed data can be obtained. To constrain the dimensions and location of the magma supply system, response from several models whose dimension and location were changed systematically was calculated.

The results indicate that a WE-trending elongated conductive body of 1 Ωm traversing Unzen located at 6.2 km deep with 6.1 km thick, 8.8 km NS width and 14.5 WE length is sufficient to explain the observed data as long as concerning a deeper structure below the peninsula. This dyke-like structure is almost perpendicular to the tensile axis of the regional stress field, which suggests the dyke intrusion of hot material from the deeper part below Unzen. Further improvement between the calculated 3D response and the observed data was obtained by adding other high conductive structure in the moderately conductive background of 10 Ωm (water-saturated layer) and in the 100 Ωm layer in the area west of the summit, and in the 10 Ωm layer in the western part of the peninsula (Fig.2). In both shallow structures, conductivity enhancement is interpreted as due to supply of magmatic gas from the deeper source.

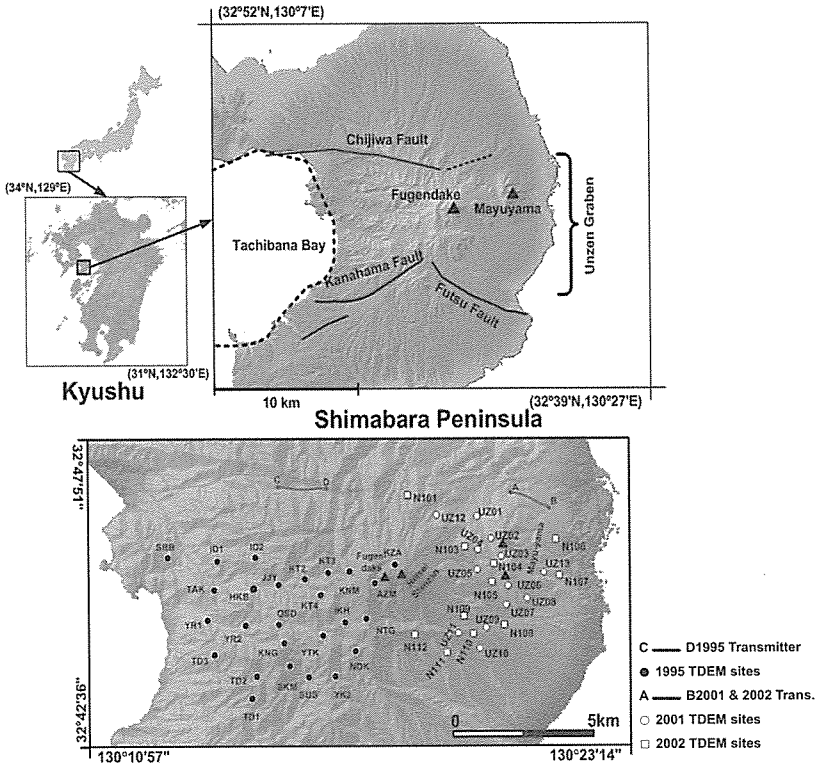

Fig. 1 Map showing Shimabara Peninsula in Kyushu Island, Japan and locations of TDEM survey around Unzen Volcano.

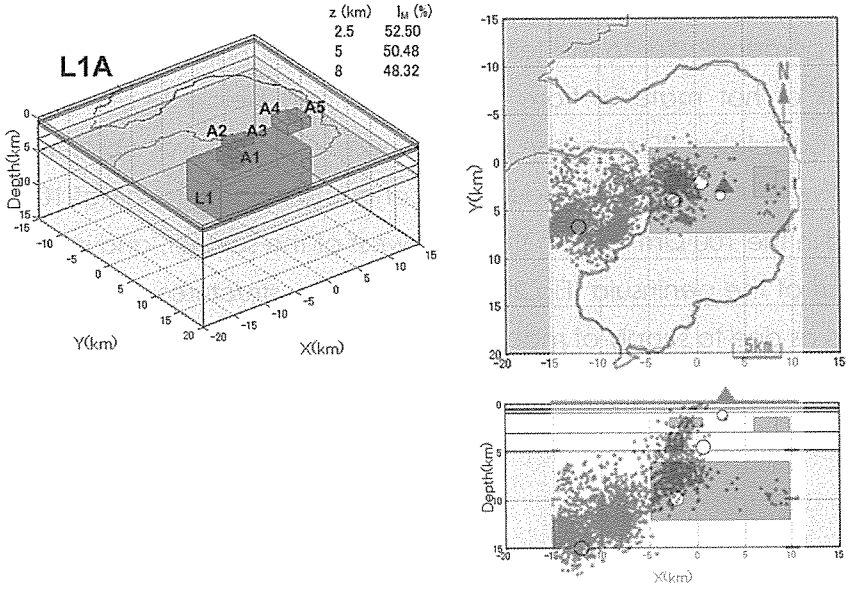

Fig. 2 3-D resistivity model. Upper and lower-right: horizontal and vertical view of the model superimposed by the hypocenter distribution of volcano-tectonic earthquakes occurred in 1985 – 1991 (taken from Umakoshi et al., 2001). Open circles denote locations of magma chambers proposed by Ishihara (1993), Nishi et al. (2001) and Ohta (1973).

Procedure of making a fused glass bead for whole rock major elements analyses by X-ray fluorescence spectrometer RIGAKU SYSTEM3270

T. Sugimoto, T. Shibata, M. Yoshikawa

We described about sample preparation for routine major elements analyses by X-ray fluorescence (XRF) spectrometer RIGAKU SYSTEM3270® at Institute for Geothermal Sciences, Kyoto University. Suitable samples prepared for XRF analyses are pressed powder pellets and fused glass beads (e.g. Nakada et al., 1985; Nakada, 1987; Tsuchiya et al., 1989; Timothy, 1989). The pressed powder pellets are often used in trace elements analyses because they yield higher X-ray intensity and S/N ratio than fused glass beads so that smaller lower-limit of detection and better precision were realized (e.g. Nakada, 1987; Shibata et al., 2004). In major element analyses, however, fused glass beads are principally used because of eliminating the particle-size and mineralogical effect concerning characteristic X-ray, easy treatment and good preservation (e.g. Tsuchiya et al., 1989; Timothy, 1989). In recent, XRF analytical methods aiming at not only silicate rocks but also sedimentary rocks or carbonaceous rocks using glass beads have been developed (e.g. Goto et al., 2002). However, several procedures for making glass beads are necessary in order to analyze wide compositional samples; such as mixed glass beads, additive glass beads and synthetic glass beads. We established a unified procedure of making glass beads of many kinds of unalloyed rock samples by fusing ignited sample with flux ($Li_2B_4O_7$) using a high frequency funace. This makes it possible to analyze wide compositional samples by single set of calibration lines, and reduce costs and time in XRF analyses and maintenance.

Required reagents and apparatuses

Ethanol (ethyl alcohol 99.5%; Wako pure chemical Industries, Co., Ltd.): Used for soaking rocks samples and cleaning apparatuses.

Lithium tetraborate ($Li_2B_4O_7$ anhydrous-HG; Wako pure chemical Industries, Co., Ltd.): Used as flux which was dried at 600 C° for 6 hours in a muffle furnace before its use.

Lithium iodide (LiI anhydrous, 99.9%; Wako pure chemical Industries, Co., Ltd.): Used for exfoliating agent as 10 % LiI solution.

Vibrating sample mill, TI-100 (manufactured by Heiko Seisakusho, Co., Ltd.): Used for pulverising rock samples. A tungsten carbide container used because of contamination-free for major elements. To minimised alkaline, grease and dust contamination from the analyst's hand, the crushing container were handled with plastic gloves.

Porcelain crucible, CW-B00 (manufactured by Tokyo Glass Kikai, Co., Ltd.): Used as ignition vessel which was dried at 600 C° for 2 hours in a muffle furnace to reach a constant weight before its use.

Automatic high-frequency furnace, NT-2000 (manufactured by Tokyo Kagaku, Co., Ltd.): Used for melting mixture of powdered sample and flux with a platinum melting pot *(type CS-2; Tokyo Kagaku, Co., Ltd.)*. The used platinum melting pot was soaked with 6N HCl into a teflon bottle for cleaning.

Sample preparation

The sample preparation procedure is as follows. The rock sample was crushed into small chips (< 5 mm in diameter), employing a jaw crusher. Then fresh pieces are hand picked from crushed chips to avoid secondary alteration effect. This aliquot was soaked with deionized water into a polystyrene bottle with ultrasonic treatment during 5 minutes. A similar washing was continuously done by using the ethanol. The washed aliquot was rinsed in deionized water and dried overnight in an airbath at 110 C°. The dried aliquot was pulverized to a powder with a vibrating sample mill, at least fine enough to the grain degree at the flour level (< 100 mesh). An aliquot less than 10 g was set into ethanol-cleaned tungsten carbide container at a time and pulverized for five minutes. To minimised contamination from the previously pulverized sample, two aliquot of each sample were run separately, and the first aliquot was discarded. The pulverized sample was collected with polystyrene balance tray and kept in a cleaned polystyrene bottle to guard against contamination.

Glass bead preparation

The preparation procedure of fusion glass beads used for the XRF analysis is as follows. First, about 1.5 to 2.5 g of powdered sample was weighed out in a porcelain crucible. It was put into an airbath and dried overnight at 110 C°, and the removed adsorptive water is measured. Then it was ignited at 900 C° for 6 hours in a muffle furnace, and the loss on ignition is measured. Note that carbonate rocks contain high $CaCO_3$ (>80 % for JDo-1 and JLs-1, issued from GSJ), CO_2 (>40 %) of which will be completely lost in ignition process. Then weighed out about 1.0 g ignited sample and accurately four times flux of anhydrous lithium tetrabolate was well mixed in an agate mortar to homogenization (about five minutes). The mixture of the sample and the flux was put in a platinum melting pot and about 10 drops of an exfoliating agent (LiI solution) was added. The platinum melting pot was then placed in an automatic high-frequency furnace. The mixture was formed into a fusion glass disc therein. Melting condition of the bead sampler was as follows: initial heating for 130 seconds at 800 C°, main heating for 120 seconds at 1200 C°, and vibration heating for 240 seconds at 1200 C°. The size of the disc thus obtained was 3 cm in diameter and about 2.5 mm in thickness. According to the above, we could make regulated clear glass beads irrespective of their rock types. The fused glass bead was kept in a plastic bag and dried in a desiccator containing silica gel to guard against contamination and humidity.

Summary

The preparation procedure of fusion glass beads of rocks samples used for the XRF analysis is described. Using fused glass beads of wide compositional rocks issued from GSJ and USGS, single set of calibration lines which correspond to wide compositional samples were determined for X-ray fluorescence spectrometer RIGAKU System3070®. Detailed analytical procedures such as X-ray measuring conditions will be described in another paper. In recent, trace elements analyses by XRF using low dilution glass beads (i.e., sample : flux ratio of 1 : 2) have been performed (e.g. Takahashi and Shuto, 1997; Goto et al., 2002). In future, we will try XRF analyses for trace elements such as Ba, Cr, Nb, Ni, Rb, Sr, V, Y and Zr using fused glass beads with sample : flux ratio of 1 : 4.

References

Nakada, S., Yanagi, T., Maeda, S., Fang, D. and Yamaguchi, M. (1985) X-Ray fluorescence analysis of major elements in silicate rocks. *Sci. Rep., Dept. Geol., Kyushu Univ.*, **14**, 103-115.

Nakada, S. (1987) X-Ray fluorescence determination of trace elements in silicate rocks (part2). *Sci. Rep., Dept. Geol., Kyushu Univ.*, **15**, 37-44.

Shibata, T., Sugimoto, T., Takahashi, T., Yoshikawa, M., Miyazaki, T., Nishimura, K. and Takemura, K. (2004) Trace element analysis of rock samples by X-Ray Fluorescence Spectrometry. *Annual Rep. FY2004, Inst. Geotherm. Sci., Kyoto Univ.*, 46-48.

Takahashi, T. and Shuto, K. (1997) Major and trace element analyses of silicate rocks using X-ray fluorescence spectrometer RIX3000. *RIGAKU Jour.*, **28**, 25-37 (in Japanese).

Timothy, E. T. (1989) Analysis of rocks using X-Ray fluorescence spectrometry. *RIGAKU Jour.*, **6**, 3-9.

Tsuchiya, N., Shibata, T., Koide, Y., Owada, M., Takazawa, E., Goto, Y., Choi, J. H., Terada, S. and Hariya, Y. (1989) Major element analysis of rock samples by X-ray fluorescence spectrometry, using scandium anode tube. *Jour. Fac. Sci., Hokkaido Univ., Ser. IV*, **22**, 489-502.

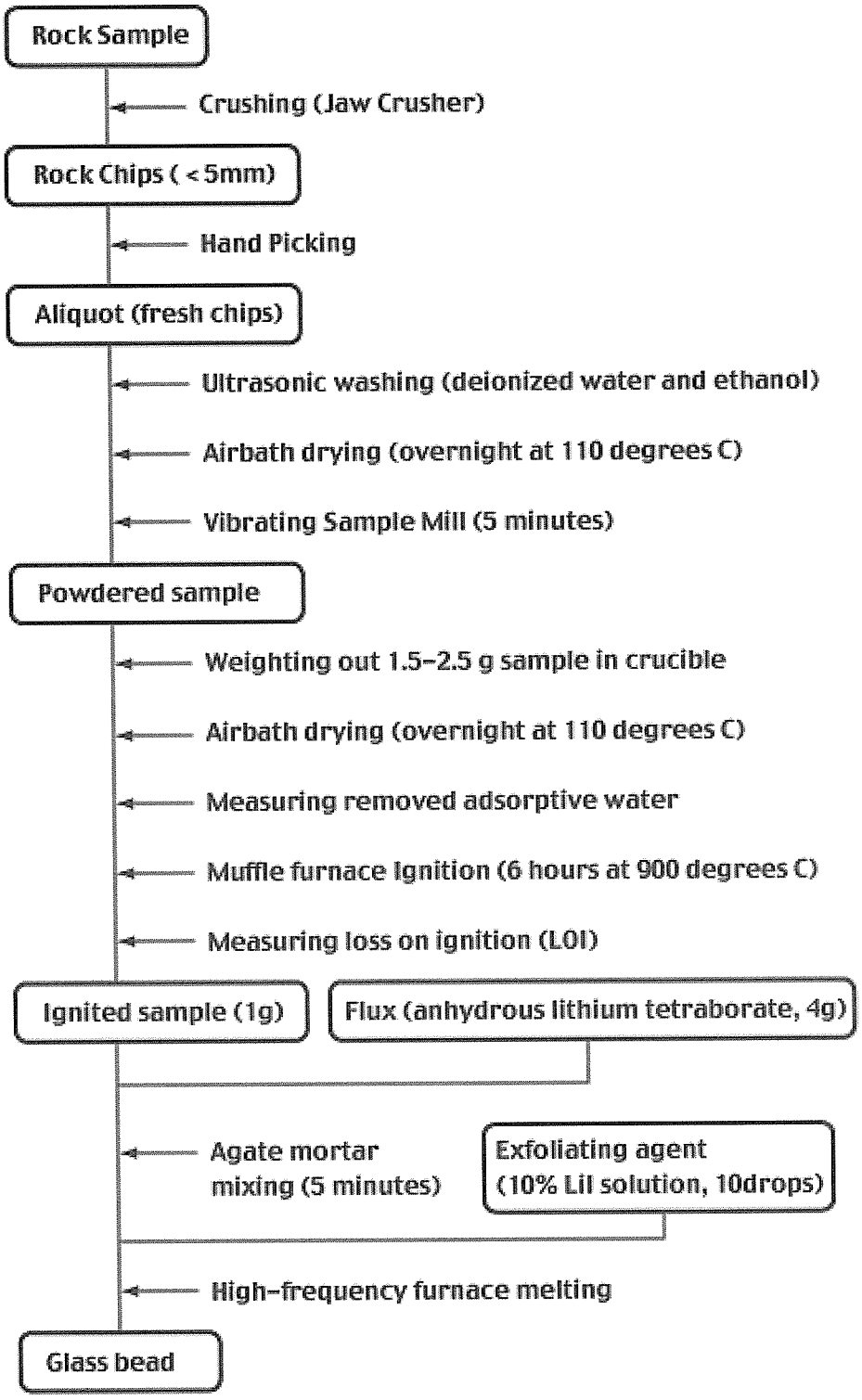

Fig. 1. Sample and glass bead preparation for XRF analyses.

Kinematic Features of Isolated Volcanic Clouds Revealed by Video-records

***A. Terada*, Y. Ida (Univ. of Hyogo)**

Analyses of observed volcanic clouds using 1D models have given some useful information on the dynamics of eruptions and some properties of the erupted mass. It should be noted that the 'entrainment hypothesis' assuming that the volume of the entraining air is proportional to the ascent velocity has played a central role in these analyses. In addition to the entrainment hypothesis, another relation that was obtained from a simple dimensional analysis by Scorer (1957) may be usefully applied to volcanic clouds. If this Scorer's relation is combined with the entrainment hypothesis and the mass conservation law, we can calculate the location, size and density of a volcanic cloud as a function of time in a simple way as far as the conversion of thermal to mechanical energy in it can be neglected.

To apply the above simple models to real volcanic clouds, we must check the kinematic feature of the cloud, i.e., the relationships among the ascent velocities, radius and height of the clouds. In this study, we examined the applicability of the entrainment hypothesis and the Scorer's relation to volcanic clouds in nature with their characteristic constants.

We analyze sequential photographs of volcanic clouds obtained at Asama and Miyakejima volcanoes. In this analysis, each segment of the volcanic cloud is treated as an isolated thermal, i.e. a spherical body ascending independently by its buoyancy. Our kinematic analysis reveals simple relationships among the ascent velocity, radius and height of volcanic clouds. The empirical dimensionless constants characterizing the entrainment hypothesis k and the Scorer's relation C are more or less scattered and their mean values are about 0.36 and 0.6, respectively. The wide dispersions of the values of k obtained here are probably caused by more irregular conditions of the fluid ejection compared with those in laboratory.

These empirical relations can be used to evaluate kinematic features of volcanic clouds approximately without thermodynamic consideration. Our results suggest, however, that C may change with the height, probably reflecting the effect the ambient density stratification in part. Furthermore, the values of C for the volcanic clouds tend to be less than those obtained by the laboratory experiments. So we have to examine the applicability of Scorer's relation more carefully.

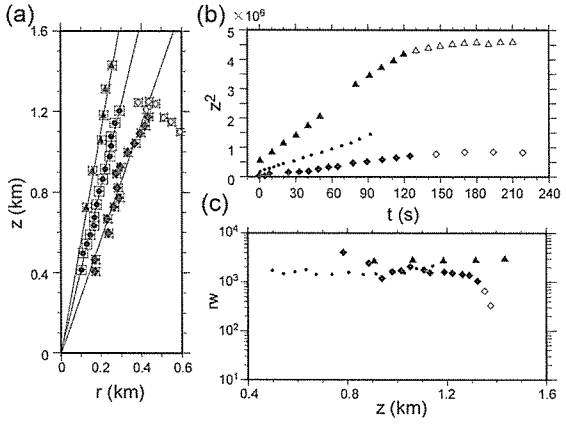

Figure. Kinematic relations that are examined for the volcanic clouds observed at 11:55 am on 15 (circles) and 8:38 am on 18 (squares) September 2004 at Asama volcano and at 6:42 am on 16 (triangles) October 2001 at Miyakejima volcano. (a) The relation between the radius *r* and the cap heights *z* that can be fitted by (1). (b) The change of z^2 with time to examine (9). (c) The variability of *rw*.

Approaches of volcanomagnetic change detection by repeated aeromagnetic survey

M. Utsugi, Y. Tanaka

To obtain the detailed information about the spatial distribution of the volcano-magnetic change, we tried to use the repeated aeromagnetic survey. The main problem is the difficulty of the observation point control. In the two flights, it will be impossible to flight exactly same position. So that, it is very difficult to separate observed field changes to temporal variation due to the volcanic activities and the spatial variation due to the difference of the observation points. If the detailed distribution of geomagnetic field is obtained on quiet period of the volcano, and the field intensity on the arbitrary point above the active area is estimated interpolating the observed data, we can correct the spatial variation caused by the difference of flight position, and it may be possible to detect the field changes associated with the volcanic activities.

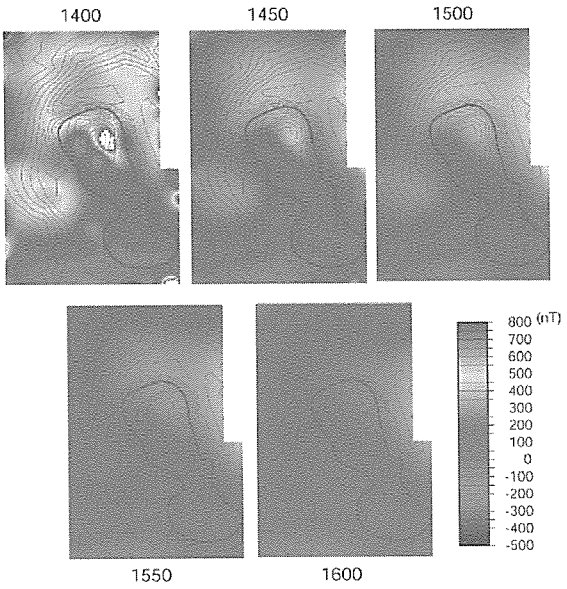

Fig. 1 Estimated geomagnetic field 3D distribution over Nakadake crater.

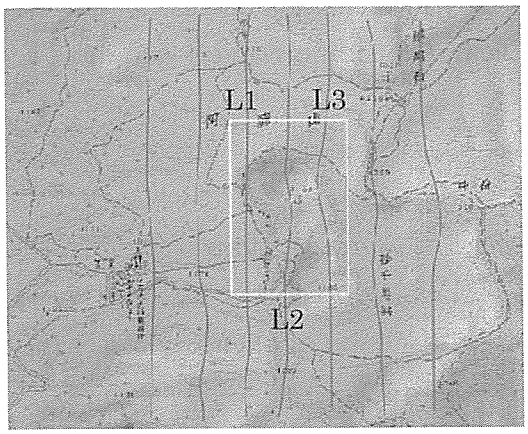

Fig.2 Flight course of 2005 aeromagnetic survey on Aso volcano.

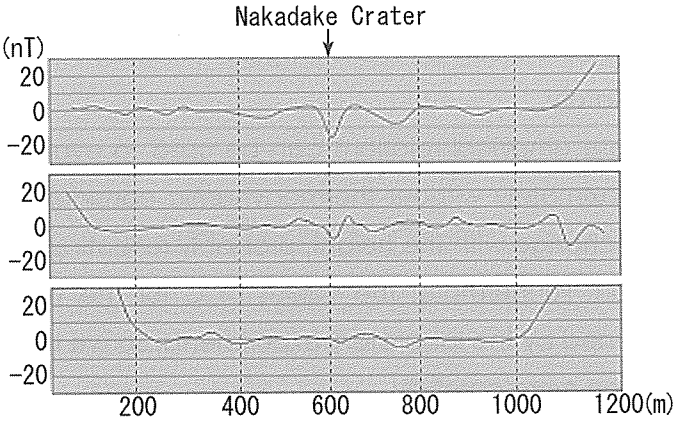

Fig. 3 Difference between observed data (2005) and calculated value (based on 2002 survey).

For this purpose, we made very high density and low altitude helicopter-borne aeromagnetic survey on Aso Volcano in July 2002. The survey area was NS1200 x EW1200 x 300m region above the Nakadake crater. Using these data, we tried to estimate the special distributions of the geomagnetic field around the Nakadake crater (Fig. 1). To estimate the

geomagnetic field intensity on the arbitrary point inside the flight area, we applied the technique of equivalent anomaly method.

To evaluate the accuracy of the obtained geomagnetic field distribution, we made other geomagnetic survey in Aug. 2005 (Fig. 2). Flight altitude is 100m. Fig.3 shows the difference between observed data and calculated value. From this figure, we can see, the accuracy of our estimated geomagnetic field distribution is less than 10 nT. According to the prevoiuse observation, the maximum amplitude of volcanomagnetic change observed on Aso volcano was 20-30 nT. So, we think it is possible to detect the volcanomagnetic change by the repeated aeromagnetic survey using Fig.2 as the reference field.

Paleo-Moho depth determined from the pressure of CO_2 fluid inclusions: Raman spectroscopic barometry of mantle- and crust-derived rocks

J. *Yamamoto*, H. Kagi (Tokyo Univ.), Y. Kawakami (Tokyo Univ.), N. Hirano (Tokyo Univ.)
M. Nakamura (Meteorological College)

The structures of the crust and upper mantle of an active island arc attract great attention for understanding island arc evolution and magma genesis. The boundary between the lower crust and upper mantle, the Moho discontinuity, is determined by seismic wave velocity structures based on the considerable density gap between these two layers. Seismological observations provide very high-precision estimates of the depth for the Moho discontinuity (Moho depth) in cases where sufficient seismic activity and seismic stations are available. In principle, it is possible to determine the Moho discontinuity from petrological observations by providing a depth scale for collected rock samples. However, the accuracy of petrological constraints on the depth origin estimated using a geothermobarometer is insufficient to discern the fine structure of the crust-mantle boundary. A precise barometer that is applicable to samples originating from the lower crust and upper mantle with various geologic ages can offer insight into the evolution of the global structure beneath the surface of the Earth.

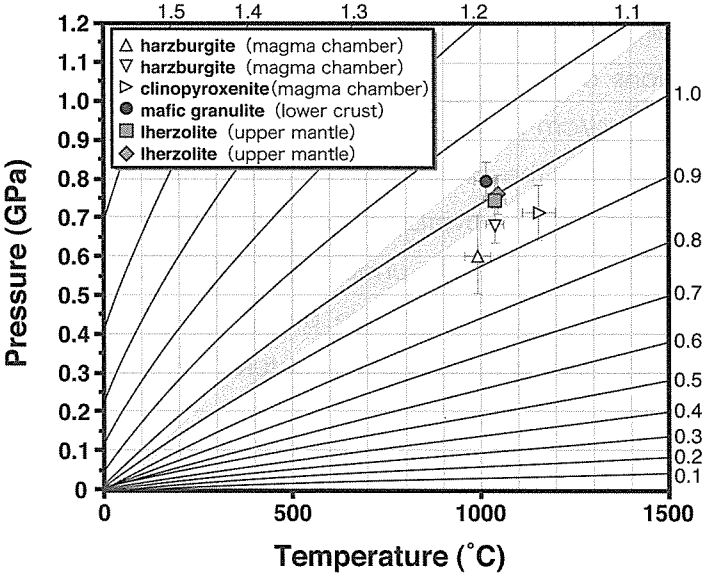

P-T diagram for the system CO_2, from Pitzer and Sterner (1994). Contours represent density in g/cm^3 (i.e. isochores). Fluid inclusion pressure can be estimated from the density of CO_2 fluid inclusions and the temperature obtained using the pyroxene thermometer.

A promising depth scale for rocks

originating from the lower crust and upper mantle is the pressure of fluid inclusions. In general, the inclusions in mantle-derived minerals retain their high internal pressure. The most prominent examples are inclusions in natural diamonds, which preserve pressures of 1–5 GPa, corresponding to the diamond stability field (> 150 km) if extended to 1000°C, a typical temperature of the upper mantle. Silicate minerals are not as strong as diamond. Nevertheless, they can preserve the pressure in inclusions, as deduced from the fact that some CO_2 fluid inclusions in minerals appear as liquid under optical microscopic observation, even at room temperature. If the pressure, and consequently the density, of CO_2 were determined, the in-situ pressure of the trapped CO_2 could be estimated based on equilibrium temperature from a mineral thermometer when the fluid inclusions were thermally equilibrated with surrounding host minerals.

The internal pressure of CO_2 fluid inclusions can be determined using microthermometry with high precision. However, various technical difficulties hinder the application of microthermometry to respective analyses of inclusions smaller than 5 μm, multiple component fluids, metastable states, and of inclusions comprising gas phase or low-density liquid. To overcome these difficulties, Yamamoto et al. (2002) applied micro-Raman spectroscopy to the estimation of residual pressures of CO_2 fluid inclusions in mantle-derived xenoliths. Micro-Raman spectroscopy has a high spatial resolution of 1 μm and the capability of rapid analysis without encountering the inherent difficulties of microthermometry. The authors have demonstrated that mantle xenoliths from Far Eastern Russia originated from a depth up to 40 km, corresponding to the uppermost mantle.

In this study, we applied spectroscopic observation of CO_2 fluid inclusions to ultramafic-mafic xenoliths from Oki-Dogo Island in the Sea of Japan and explored the depth distribution of rocks from the lower crust to the upper mantle. The density of CO_2 fluid inclusions in the mafic granulite was 1.02–1.05 g/cm^3. Those of lherzolites were 0.98–1.02 g/cm^3. In contrast, CO_2 fluid inclusions of olivine gabbro, clinopyroxenite and harzburgite exhibited lower densities of 0.86–0.99 g/cm^3. Taking into account the temperature condition estimated using a pyroxene thermometer, the mafic granulite originated from a depth of 27–30 km and the lherzolites from 25–29 km. The overlapping depth of 27–29 km can be interpreted as the depth including the Moho discontinuity under Oki-Dogo Island 3.3 Ma. This estimation is consistent with geophysical observations. The present spectroscopic method introduces the possibility of deciphering ancient tectonic structures from pieces of rock fragments containing CO_2 fluid inclusions.

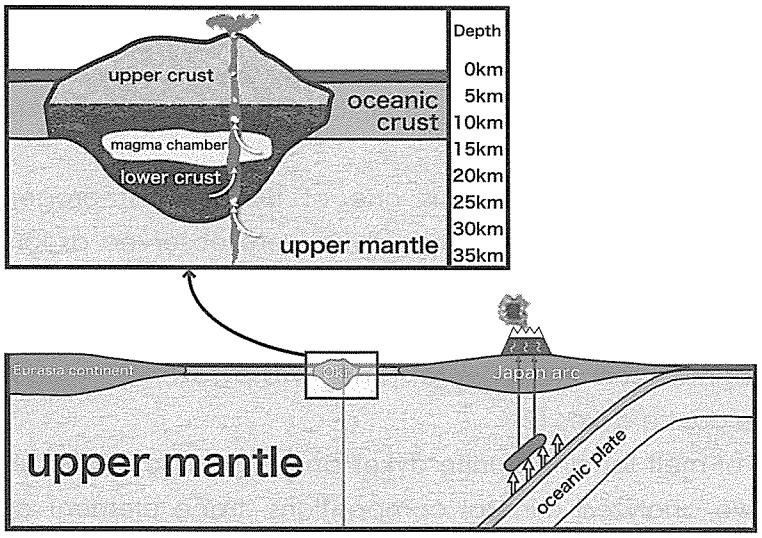

Schematic cross section around Oki-Dogo Island.

Rb-Sr mineral isochron ages of mantle peridotite xenoliths from Kurose, Southwest Japan.

***M. Yoshikawa*, S. Arai (Kanazawa Univ)**

Mantle peridotite xenoliths in Cenozoic alkaline basalts of the North Kyushu have been expected to characterize the geochemical and isotopic compositions of the upper mantle under the island arc or continental margin. On the basis of petlogical studies of these peridotite xenolits (e.g. Arai et al., 2001), it has been suggested that the Kurose peridotite xenoliths had escaped from metasomatism related to alkali basalt magmatism and asthenospheric upwelling. In order to obtain chemical and isotopic signature before asthenospheric upwelling, we propose mineral compositions, trace element compositions of clinopyroxenes and the Rb-Sr and Sm-Nd isotopic compositions of constituent minerals of the five Kurose peridotite xenoliths.

The Rb-Sr mineral isochron of sample KR375 gives an age of approximately 120 Ma with an initial Sr isotopic ratio of 0.70380. This initial Sr isotopic ratio is higher than MORB value. Abe and Yamamoto (1999) reported three mineral-whole rock Rb-Sr isochron ages (130Ma, 313Ma, 487 Ma) from the Kurose xenoliths. Our estimated age is consistent with the youngest reported age. However, there is difference of initial Sr isotopic ratios between their sample (0.70431) and our sample. This difference suggests that upper mantle of this region was isotopically heterogeneous 120 Ma ago.

(Abstract of Japan Earth and Planetray Science Joint Meeting, 2006)

Trace and isotopic (Sr and Nd) compositions of clinopyroxenes in dunite channels of the Horoman peridotite complex, Hokkaido, Japan

M. Yoshikawa, **K. Niida (Hokkaido Univ), S.M. Eggins, D. H. Green (ANU)**

The Horoman peridotite complex of Japan is one of the freshest orogenic peridotite complex in the world and two types of dunite dyke were observed as large scale (several hundred meters width) concordant layers [1] and small scale (< several meters width) discordand layers [2]. The later layer was as replacive origin by reaction between olivine saturated magma and harzburgite, and two-pyroxenes + spinel segregations are observed in the dunite dykes [2].

In order to discuss origin of melt forming dunite dykes and a genetic relationship between melt and wall rock, we analyzed mineral compositions, trace element and isotopic (Sr and Nd) compositions of clinopyroxenes (cpx) in the segregations of three discordant dunite dykes (SPR, 811-3 and 1.6Ol-III) and Rb-Sr isotopic ratios of constituent minerals of SPR and cpx of wall harzburgite (5cm separated from SPR).

Mineral compositions and trace element and isotopic compositions of the cpx are differ with each samples and there were not a simple correlation between them. These observations suggested that each dyke was formed from different melt. The isotopic and trace element compositions of cpx of the wall harzburgite are consistent with those of dunite dykes SPR. Additionally, the $^{87}Sr/^{86}Sr$ ratios of constituent minerals except orthopyroxene (opx) of dunite dyke and cpx of the wall rock show positive correlation with both $^{87}Rb/^{86}Sr$ and 1/Sr. These observations were likely supported that cpx in wall rock crystallized from migrating melt and opx in SPR was relict mineral from wall harzburgite. Similar cpx was observed in wall peridotite of replacive dunite channel in the mantle section of the Oman ophiolite [3].

References

[1] Takahashi, N. (1992) *Nature* **359,** 52-55.
[2] Niida, K. (2002) GCA **103,** 22-33.
[3] Kelemen, P.B., Shimizu, N.

(Abstract of Goldschmidt Conference, Geochim. Cosmochim. Acta, 70, 724, 2006)

公表論文　Publications

＜原著論文＞

Arakawa M., Yamamoto, J., Kagi, H. (2007) Developing Micro-Raman Mass Spectrometry for Measuring Carbon Isotopic Composition of Carbon Dioxide. Applied Spectroscopy, 61, 701-705.

Fukui, H., Huotari, S., Andrault, D., Kawamoto, T., (2007) Oxygen K-edge fine structures of water by x-ray Raman scattering spectroscopy under pressure conditions. Journal of Chemical Physics, in press.

Hanyu, T., Tatsumi, Y., Nakai, S., Shibata, T., Yoshida, T., Contribution of slab melting and slab dehydration to magmatism in the NE Japan arc for the last 25 Mar: Constraints from geochemistry, Geochemistry Geophysics Geosystems, 7, 10.1029/2005GC001220.

Hirano N., Takahashi, E., Yamamoto, J., Machida, S., Abe, N., Ingle, S., Kaneoka, I., Hirata, T., Kimura, J., Ishii, T., Ogawa, Y., Suyehiro, K. (2006) Evidence for partial melt in Earth's asthenosphere: volcanism in response to plate flexure during subduction of the Cretaceous Pacific Plate. Science, 313, 1426-1428.

岩城啓美, 伊藤浩子, 北田奈緒子, 井上直人, 香川敬生, 宮腰研, 竹村恵二, 岡田篤正 (2006) 大規模地震に伴う地表地震断層と深部起震断層に関する既存資料の整理とカタログの作成. 活断層研究, 26, 37-61.

鍵山恒臣 (2007) 富士山の地下構造, 富士火山, 山梨県環境科学研究所, 137-150.

鍵山恒臣 (2006) 火山噴火予知研究の課題と構造探査, 物理探査, 59, 539-548.

鍵山恒臣, 小山悦郎 (2006) 浅間火山 2004 年噴火に関連した噴煙の時間変動, 火山, 51, 75-89.

Kawamoto, T., Hydrous phases and water transport in the subducting slab. In Reviews in Mineralogy and Geochemistry, Vol 62, "Water in Nominally Anhydrous Minerals" edited by H. Keppler and J. R. Smyth, Geochemical Society and Mineralogical Society of America, 273-289 (2006)

Kuritani, T., Yokoyama, T., Nakamura, E. (2007) Rates of thermal and chemical evolution of magmas in a cooling magma chamber: a chronological and theoretical study on basaltic and andesitic lavas from Rishiri Volcano, Japan. Journal of Petrology, doi:10.1093/petrology/egm018 .

栗谷豪 (2007) ウラン系列短寿命核種を用いた地殻下におけるマグマ進化の時間スケールの解明－研究の現状と課題－, 火山, 52, 71-78.

栗谷豪 (2007) 水とマグマ, 地学雑誌, 116, 133-153.

牧野内猛, 森忍, 檀原徹, 竹村恵二(2006) 濃尾平野における第一礫層（BG）の層位と形成過程. 地質学論集, 59, 129-140.

Mibe, K., Kanzaki, M., Kawamoto, T., Matsukage, K. N., Fei, Y., Ono, S., Second critical endpoint in the peridotite-H_2O system, Journal of Geophysical Research, 112, B03201

Nakamura T., Sugimoto, N., Tsuda, T., Abo, M., Hashimoto, T., Terada, A. (2006) Observation of water vapor with a portable Raman Lidar - Continuous monitoring and filed experiment over the forest and at the volcano -, Reviewed and Revised Papers, 23rd International Laser Radar Conference 2006, Part II, 897-900.

Nishimura, K. (2006) Numerical modeling of trace element behavior during crystal settling and reequilibration in high-silica magma bodies. Journal of Geophysical Research, 111, B08201, doi: 10.1029/2005JB003844.

大沢信二 (2006) 流体地球化学的にみた雲仙地溝の熱水系と温泉の生成過程. 日本地熱学会誌, 28, 361-371.

大久保綾子, 田中良和, 鍵山恒臣, 宇津木充, 神田　径 (2006) ヘリボーン空中磁気探査から推定される雲仙西部地域の磁化強度分布, 火山, 51, 175-181.

Okubo, A., Nakatsuka, T., Tanaka, Y., Kagiyama T., Utsugi, M. (2006) Aeromagnetic constraints on the subsurface structure of the Unzen Graben, Kyushu, Japan. Earth Planets Space, 58, 23 – 31

Saito, T., Ishikawa, N., Magnetic petrology and its implication for magma mixing of the 1991-1995 dacite at Unzen volcano, Japan. Earth Planets Space. 2007 (in press).

Saito, T., Ishikawa, N., Kamata, H., Magnetic petrology of the 1991-1995 dacite lava of Unzen volcano, Japan: degree of oxidation and implications for the growth of lava domes. J. Volcanol. Geotherm. Res. 2007 (in press).

佐藤忠信, 竹村恵二, 吉井真, 香川敬生, 高橋嘉樹, 南部光(2006) 神戸空港建設プロジェクトにおける護岸と滑走路の耐震安全性の検討. 土木学会論文集、Vol.62, No.3.

Srigutomo, W. , Kagiyama, T., Kanda, W., Munekane, H., Hashimoto, T., Tanaka, Y., Utada, H., Utsugi, M. (2007): Resistivity structure of Unzen Volcano derived from Time Domain Electromagnetic (TDEM) survey, J. Volcanol. Geotherm. Res, （印刷待ち）

杉本健 (2006) 島原半島の地質と岩石 -近年の研究成果より-. 日本地熱学会誌, 28, 347-360.

Sugimoto, T., Shibata, T. , Yoshikawa, M., Takemura, K. (2006) Sr-Nd-Pb isotopic and major and trace element compositions of the Yufu-Tsurumi volcanic rocks: implications for the magma genesis of the Yufu-Tsurumi volcanoes, northeast Kyushu, Japan. Jour. Mineralogical and Petrological Sciences, 101, 270-275.

Terada, A., Ida, Y. (2007) Kinematic features of isolated volcanic clouds revealed by video records, Geophys. Res. Lett., 34, L01305, doi:10.1029/2006GL026827.

寺田暁彦, 日野正幸, 竹入啓司 (2006) 御蔵島火山・ヤスカジヶ森溶岩ドーム山頂で冬季に白煙を上げる温風穴, 地質学雑誌, 112, 503-509.

Tomaru, H., Ohsawa, S., Amita, K., Lu, Z., Fehn, U. (2007) Influence of subduction zone settings on the origin of forearc fluids: Halogen concentrations and $^{129}I/I$ ratios in waters from Kyushu, Japan. Applied Geochemistry, 22, 676-691.

Ujike, O., Goodwin, A. M., Shibata, T. (2006) Geochemistry and origin of Archean volcanic rocks from the Upper Keeatin assemlage (ca 2.7 Ga), Lake of the Woods Greenstone Belt, Western Wabigoon Subprovince, Superior Province, Canada. Island Arc, 16, 191-208.

山本順司 (2007) マントル鉱物の流体包有物から探る沈み込み帯の物質循環系　—マントルウェッジの四次元解析—, 地球化学, 印刷中

Yamamoto, J., Kagi, H., Kawakami, Y., Hirano, N., Nakamura, M. (2007) Paleo-Moho depth determined from the pressure of CO_2 fluid inclusions: Raman spectroscopic barometry of mantle- and crust-derived rocks. Earth and Planetary Science Letters, 253, 369-377.

Yamamoto, J., Kagi, H. (2006) Extended micro-Raman densimeter for CO_2 applicable to mantle-originated fluid inclusions. Chemistry Letters, 35, 610-611.

Yoshikawa, M., Ozawa, K. (2007) Rb-Sr and Sm-Nd isotopic systematics of the Hayachine-Miyamori ophiolitic complex: Melt generation process in the mantle wedge beneath an Ordovician island arc. Gondowana Res., 11, 234-246.

＜報告書等＞

青木陽介，鍵山恒臣 (2006) 九州地方の地殻変動と火山，月刊地球，28, 98-102.

後藤章夫，鍵山恒臣，宮本 毅，横尾亮彦，谷口宏充 (2007) 放熱率測定に基づいた有珠 2000 年噴火の活動推移長期予測，北海道大学地球物理学研究報告，70, 137-144.

橋本武志，茂木透，鈴木敦生，山谷祐介，三品正明，中塚正，小山悦郎，小山崇夫，相澤広記，平林順一，松尾元広，野上建治，小川康雄，氏原直人，鍵山恒臣，神田径，大久保綾子，田中良和，宇都智史，宇津木充，平成 17 年度浅間山電磁気構造探査の概要，CA 研究会 2006 年論文集，79-80, 2006

井口正人，平林順一，大倉敬宏 (2007) インドネシア国における火山観測の予備調査 –特に Semeru 火山と Guntur 火山について-，防災科学技術研究所研究資料，304, 77-90.

井口正人，八木原寛，為栗健，清水洋，平林順一，宮町宏樹，鈴木敦生，筒井智樹，及川純，森健彦，相沢広記，河野裕希，馬場龍太，大倉敬宏，吉川慎，齋藤武士，福嶋麻沙代，平野舟一郎，諏訪之瀬島火山における人工地震探査．京都大学防災研究所年報，No49B, 339-354, 2006.

井上和久，金子克哉，小屋口剛博，芳川雅子，柴田知之，古川邦之，鎌田浩毅 (2006) 阿蘇火山における Aso-3 大規模噴火をもたらしたマグマ溜まりの形成過程，月刊地球，28, 392-399.

伊藤久敏，海江田秀志，楠建一郎，茂木透，田中良和，藤光康宏，結城洋一 (2007)ヘリコプターを用いた総合的な空中物理探査システムの開発（その 1）—空中電磁、空中磁気、空中放射能、空中熱赤外映像の各探査手法の高度化—：電力中央研究所報告、研究報告：N06011

伊藤久敏，海江田秀志，楠建一郎，茂木透，田中良和，藤光康宏，結城洋一 (2007) ヘリコプターを用いた総合的な空中物理探査システムの開発（その 2）—阿蘇火山、磐梯火山への適用と防災への適用性の検討—：電力中央研究所報告、研究報告：N06012

鍵山恒臣，田中良和 (2006) ニュージランド・ホワイトアイランド火山の噴気活動について、平成１５～１７年度科学研究費補助金「空中磁気測量による火山性磁場変動の検出」（基盤Ｂ）研究成果報告書，69-73

鍵山恒臣，田中良和，池辺伸一郎 (2007) 阿蘇火山中岳火口における噴湯現象の画像解析，「科学研究費報告特定領域研究（領域番号 422）火山爆発のダイナミックス　領域代表者　井田喜明」，52-54.

鍵山恒臣，スリグトモ ワヒュー，橋本武志，神田 径，宗包浩志，田中良和，歌田久司，清水久芳，宇津木充，小河勉，大湊隆雄 (2006) 雲仙火山の比抵抗構造から推定されるマグマからの脱ガス，第 2 回雲仙火山集中総合観測報告書，32-44.

鍵山恒臣，森田裕一 (2006) カルデラ研究の展望，月刊地球，28, 63-66.

鍵山恒臣，宗包浩志 (2006) 九州火山地域・非火山地域の比抵抗構造，月刊地球，28, 110-114.

鍵山恒臣(2006) 九州の変動・構造と火山の分布　公開講座「火山学 Q&A　in 熊本」，火山学会公開講座テキスト 14.

鍵山恒臣，スリグトモ　ワヒュー，橋本武志，神田径，宗包浩志，田中良和，歌田久司，清水久芳，宇津木充，小河勉，大湊隆雄 (2006) 雲仙火山の比抵抗構造から推定されるマグマからの脱ガス、第 2 回雲仙火山の集中総合観測報告書、32-44.

神田径，田中良和，宇津木充，高倉伸一，橋本武志，井上寛之，岡田靖章 (2006) 阿蘇中岳周辺の

比抵抗構造, CA 研究会 2006 年論文集, 86-88.
神田径, 橋本武志, 田中良和, 宇津木充, 吉村令慧, ホワイト島火山空中磁気測量チーム (2006) ホワイトアイランドにおける全磁力連続観測, 空中磁気測量による火山性磁場変動の検出(科学研究費補助金, 基盤研究(B)研究成果報告書), 49-56.
神田径, 田中良和, 宇津木充, 岡田靖章, 井上寛之 (2007) 爆発発生場の比抵抗構造 (2) -九重と阿蘇の比較-, 火山爆発のダイナミックス平成 18 年度研究成果報告書, 41-46.
北田奈緒子, 竹村恵二 (2007) 地盤の生成と地質構造, 題名, 『実用地盤調査技術総覧』(太田秀樹監修), 35-48.
三輪学央, 寅丸敦志, 井口正人(2007)桜島ブルカノ式噴火に関する物質科学的検討, 火山爆発のダイナミックス, 科学研究費補助金, 特定領域研究 (領域代表 : 井田喜明) 平成 18 年度研究成果報告書, 5, pp. 163-167.
中西利典, 竹村恵二, 松山尚典(2006) 別府浜脇地区のボーリングコア解析—東別府駅前ボーリングコアの堆積相. 大分県温泉調査研究会報告, 57, 1-5
西村光史, 柴田知之, 小林哲夫, 竹村恵二 (2006) 大規模珪長質マグマ溜まりにおける結晶沈降と再平衡化-ビショップタフと姶良火砕噴出物の例-. 月刊地球, 28, No. 2, 81-87.
大久保綾子, 田中良和, 神田径, 石原和弘, 宇津木充 (2007) Magnetic structure of Sakurajima volcano determined from high-resolution aeromagnetic survey, 空中磁気探査から推定された桜島火山の磁化強度分布, 火山爆発のダイナミックス平成 18 年度研究成果報告書, 31-33.
大沢信二 (2006) 阿蘇火山の温泉・地熱現象 公開講座「火山学 Q&A in 熊本」, 火山学会公開講座テキスト 32-34.
齋藤武士, 鎌田浩毅, 石川尚人 (2006) 雲仙火山歴史溶岩の示す磁気岩石学的特徴. 月刊地球, 28, 379-385.
齋藤武士 (2006) 京都からハルカ遠くの京都大学 - 別府地球熱学研究施設より. 人環フォーラム, 19, 52.
須藤靖明 (2006) 阿蘇火山の火山活動と火口表面活動 公開講座「火山学 Q&A in 熊本」, 火山学会公開講座テキスト 23-25.
須藤靖明 (2006) 火山性微動 公開講座「火山学 Q&A in 熊本」, 火山学会公開講座テキスト 26-28.
須藤靖明 (2006) マグマ溜まりと開放型火山 公開講座「火山学 Q&A in 熊本」, 火山学会公開講座テキスト 29-31.

杉本健, 柴田知之, 芳川雅子, 竹村恵二 (2006) 全岩微量元素組成を用いた由布岳・鶴見岳におけるマグマ生成の解明. 大分県温泉調査研究会報告, 57, 33-39.
竹村恵二(2006) 活断層活動性評価の基礎としての高精度堆積物分析. 月刊地球, 号外 54, 223-226.
竹村恵二(2006) 陸水学辞典 (分担執筆).
竹村恵二(2006) 分担執筆 日本の地形 中部地方.
竹村恵二(2006) サイスモすこーぷ「ふるさと地盤診断ウオーク」, SEISMO, 117 号, 12-12.
竹村恵二(2006) 九州はどのように変形しているか? 公開講座「火山学 Q&A in 熊本」, 火山学会公開講座テキスト 11-13.
竹村恵二(2007) 隔地施設紹介「理学研究科附属地球熱学研究施設」, 京大広報 No.620, 2321-2322.

竹村恵二(2007) サイスモすこーぷ「市町村合併と地球科学的防災基礎情報の多様化」, SEISMO, 123 号, 12-12.

田中良和, 宇津木充 (2006) 吉野における空中磁気測量の予備実験、平成１５～１７年度科学研究費補助金「空中磁気測量による火山性磁場変動の検出」（基盤Ｂ）研究成果報告書, 85-93.

田中良和, 宇津木充 (2006) 電磁気観測で火山を知る　公開講座「火山学 Q&A　in 熊本」, 火山学会公開講座テキスト 35-37.

寺田暁彦 (2006) 地勢, 御蔵島島史自然編, （株）ぎょういせい, 東京, 6-22（分担執筆）.

宇津木充, 田中良和(2006) 阿蘇中岳における高密度空中磁気観測～繰り返し空中磁気観測からの磁場時間変化検出の試み～, 特定領域研究「火山爆発のダイナミクス」H18 年度報告書, 203-207.

宇津木充, 田中良和, 橋本武志, Hurst Anthony White, 神田径, 松島健, 吉村令慧 (2006) NZ ホワイトアイランド火山における高密度空中磁気観測, 空中磁気測量による火山性磁場変動の検出(科学研究費補助金, 基盤研究(B)研究成果報告書), 150-162.

宇津木充, 田中良和, 神田径, 松島健 (2007) 口永良部島火山における空中磁気測量, 薩摩硫黄島火山・口永良部島火山の集中総合観測, 121-127.

宇津木充, 田中良和 (2006) 空中磁気測量を用いた火山爆発場解明についての試み～空中磁気測量からの磁場時間変化検出の試み～、平成 15～17 年度科学研究費補助金「空中磁気測量による火山性磁場変動の検出」（基盤Ｂ）研究成果報告書, 28-34.

宇津木充, 田中良和, 平林順一, 小川康夫, 浜野洋三 (2006) 草津白根山における空中磁気測量、平成１５～１７年度科学研究費補助金「空中磁気測量による火山性磁場変動の検出」（基盤Ｂ）研究成果報告書, 94-100.

山本順司, 竹村恵二 (2006) 別府地域の熱源となっているマグマの供給機構を探る. 大分県温泉調査研究会報告, 57, 41-43.

＜学会発表　Conference Presentations＞

Abe N., Yamamoto, J., Hirano, N., Arai, S. (2006) Petrology and geochemistry of mantle xenoliths from petit-spot volcano, NW Pacific Plate. Goldschmidt conference（2006 年 8 月, Melbourne, Australia）, Geochimica Cosmochimica Acta, 70, A1.

Ahmed, A., Helmy, H., Arai, S., Yoshikawa, M, Magmatic Exsolution and Unmixing in Spinel from Late Precambrian Concentrically-Zoned Mafic-Ultramafic Intrusions, Eastern Desert, Egypt, KAGI 21 International Symposium, 2006, December, Japan

畑真紀, 大志万直人, 吉村令慧, 田中良和, 上嶋誠, 九州地域 Network-MT 研究グループ：九州 Network-MT 法観測データの再解析―別府・島原地溝帯周辺の大規模比抵抗構造の推定―, 2006 年度ＣＡ研究会, 京都大学木質ホール, 2007 年 3 月 9 日, ポスター

池田さや香, 大倉敬宏, 山本希, 金嶋聰, 高木憲朗, 川勝均　阿蘇火山における長周期微動の時間変化-2002ー2004 年- 地球惑星科学関連学会 2006 年合同大会予稿集, J241-P007（幕張メッセ国際会議場, 千葉, 2006 年 5 月 14 日–18 日）.

Inoue, N., Kitda, N., Takemura, K. Relationship between Gravity Anomaly and Subjacent Source Fault in Japan. AGU, Fall Meet.（2006 年 12 月サンフランシスコ　U. S. A.）

井上直人, 楠本成寿, 竹村恵二, SA インバージョンによる由布院盆地の 2 次元地下構造. 日本火山学会 2006 年大会, 阿蘇いこいの村、熊本, 2006 年 10 月.

鍵山恒臣, マグマからの脱ガスと電磁気観測－休止期の長い噴火を考える－, CA 研究会 2006 年度研究会, 宇治市, 2007 年 3 月.

鍵山恒臣，休止期の長い火山噴火の準備過程研究への私案，東京大学地震研究所特定共同研究 B 第 3 回カルデラ研究会，東京都，2007 年 2 月．

鍵山恒臣，田中良和，池辺伸一郎，阿蘇火山中岳火口における噴湯現象の画像解析，日本火山学会 2006 年度秋季大会，阿蘇市，2006 年 10 月．

鍵山恒臣，田中良和，池辺伸一郎，ビデオ解析で明らかになった阿蘇火山中岳火口における噴湯現象の短周期変動，平成 18 年度京都大学防災研究所研究発表講演会，京都市，2007 年 3 月．

鍵山恒臣，火山噴火予知研究の課題と構造探査，地球惑星科学関連学会 2006 年合同大会予稿集，U051-037（幕張メッセ国際会議場，千葉，2006 年 5 月 14 日–18 日）．

鍵山恒臣，火山噴煙の可視画像の解析，地球惑星科学関連学会 2006 年合同大会予稿集，V101-P022（幕張メッセ国際会議場，千葉，2006 年 5 月 14 日–18 日）．

鍵山恒臣，田中良和，池辺伸一郎：ビデオ解析で明らかになった阿蘇火山中岳火口における噴湯現象の短周期変動、平成１８年度京都大学防災研究所研究発表講演会、京都テルサ、３月 6 日、ポスター

鍵山恒臣，田中良和，池辺伸一郎：阿蘇火山中岳火口における噴湯現象の画像解析、特定領域年度末シンポジウム、東京大学地震研究所２／１９－２１

Kagiyama, T., Tanaka, Y., Ikebe, S., Short term variation of bubbling in the Naka-Dake Crater, Aso Volcano inferred from video analysis, The 4th KAGI21 Symposium, Kyoto, December, 2006.

神田径，田中良和，宇津木充，岡田靖章，井上寛之：爆発発生場の比抵抗構造(2) —九重と阿蘇の比較—、特定領域年度末シンポジウム、東京大学地震研究所２／１９－２１

神田径，田中良和，宇津木充，高倉伸一，橋本武志，井上寛之：阿蘇火山中岳周辺の浅部比抵抗構造（２）、平成１８年度京都大学防災研究所研究発表講演会、京都テルサ、３月５日

川本竜彦，神崎正美，三部賢治，松影香子，澤井啓伍，古川善紹，小野重明　高温高圧 X 線ラジオグラフィー法を用いた高 Mg 安山岩マグマと水の間の第２臨界点．地球惑星科学関連学会 2006 年合同大会予稿集（幕張メッセ国際会議場，千葉，2006 年 5 月 14 日—18 日）

川本竜彦　スラブから放出される水の性質：高温度高圧力実験からの制約条件．地球惑星科学関連学会 2006 年合同大会予稿集（幕張メッセ国際会議場，千葉，2006 年 5 月 14 日—18 日）

Kawamoto, T., Kanzaki, M., Mibe, K., Matsukage, K. N., Ono, S. Second critical endpoint between aqueous fluids and a high-magnesian andesite by high-pressure and high-temperature X-ray radiography International Mineralogical Association Meeting, Kobe, July 2006.

Kawamoto, T., Kumagai, Y. Raman Spectroscopy of LiCl Solution: Implications for Chemical and Physical Features of Aqueous Fluids in the Mantle Wedge Beneath the Volcanic Arcs International Mineralogical Association Meeting, Kobe, July 2006.

川本竜彦，熊谷仁孝　高圧下におけるアルカリ塩化物水溶液のその場観察　日本地球化学会年会（日本大学文理学部、2006 年９月）

川本竜彦，神崎正美，三部賢治，松影香子，澤井啓伍，古川善紹，小野重明　高温高圧条件でのマグマと水のその場観察実験：火山弧の下のスラブ由来物質は超臨界流体である　日本火山学会秋季大会　阿蘇　２００６年１０月

川本竜彦，熊谷仁孝　アルカリ塩化物(LiCl, NaCl, KCl, CsCl)水溶液の高圧下におけるラマン散乱　高圧討論会（熊本市、２００６年１１月）

Kawamoto, T., Hydrous phases and water transport in the subducting slab. Short course in

Mineralogy and Geochemistry, "Water in Nominally Anhydrous Minerals" Geochemical Society and Mineralogical Society of America, Verbania, Italy, September 2006.

Kitada, N., Inoue, N., Takemura, K., Kagawa, T., Okada, A. Relationship between subjacent source faults and surface ruptures - For the purpose of estimate of source fault using active fault -. AGU, Fall Meet.（2006年12月サンフランシスコ U. S. A.）

北田奈緒子，竹村恵二，三田村宗樹，大島昭彦，関西圏における表層地質の分布状況 -ボーリングデータベースを用いた地層の分布-．日本地質学会 2006 年大会，高知大学理学部、高知，2006年9月

小森省吾，鍵山恒臣，宇津木充，星住英夫，田中良和，井上寛之，雲仙火山北東部における熱水の移動，地球惑星科学関連学会2006年合同大会予稿集，V101-P021（幕張メッセ国際会議場，千葉，2006年5月14日–18日）．

小森省吾，鍵山恒臣，宇津木充，星住英夫，田中良和，井上寛之，寺田暁彦，スリグトモ ワヒュー 雲仙火山北東部における浅部比抵抗構造と熱水の流れ，99（リゾートホテル阿蘇いこいの村，阿蘇市，2006年11月23－25日）

小森省吾，鍵山恒臣，宇津木充，寺田暁彦，井上寛之，スリグトモワヒュー，田中良和，星住英夫：火山体浅部における比抵抗構造と熱水、2006年度ＣＡ研究会、京都大学木質ホール、2007年3月9日

小山崇夫，宗包浩志，鍵山恒臣，歌田久司，半無限地球中の 3 次元電気伝導度構造インバージョンコードの開発，地球惑星科学関連学会 2006 年合同大会予稿集，E134-P003（幕張メッセ国際会議場，千葉，2006年5月14日–18日）．

栗谷豪，横山哲也，中村栄三，Ｕ－Ｔｈ放射非平衡を用いたマグマ進化の時間スケールの決定：利尻火山，沓形・種富溶岩流，日本地球惑星科学連合 2006 年大会（幕張メッセ国際会議場，千葉，2006年5月14日–18日）．

栗谷豪，横山哲也，中村栄三，マグマ溜まりにおけるマグマの熱・物質進化の速度：利尻火山，沓形・種富溶岩流からの制約，日本火山学会（リゾートホテル阿蘇いこいの村，阿蘇，2006年10月23日–25日）．

Kuritani, T., Yokoyama, T., Nakamura, E. Time scales of magmatic evolution from a parental alkali basalt to trachytic andesite beneath Rishiri Volcano, Japan, AGU, Fall Meet.（2006年12月サンフランシスコ U. S. A.）

楠本成寿，竹村恵二，粒状体個別要素法によるマグマ溜りの重力崩壊シミュレーション，地球惑星科学関連学会2006年合同大会（幕張メッセ国際会議場，千葉，2006年5月14日–18日）

Matsuoka, H., Watanabe, Y., Ueda, J., Tagami, T., Takemura, K., Brahmantyo, B., Maryunak.A., Ni, Ohsawa, S., Yamada, M., Kitaoka, K., Yoden, S. Cave survey trips to the limestone caves of Java, Indonesia: 1, Buniayu, West Java and 2, Karangbolong, Central Java. The 4th KAGI21 International Symposium Kyoto, 2006, (2006年12月，京都)

松島健，齊藤政城，杉本健（2006）伊豆鳥島火山の火山活動と 2002 年噴出物の分析．地球惑星科学関連学会2006年連合大会

松山尚典，千田昇，竹村恵二，首藤次男，大分平野の沖積層：堆積相と伏在断層の活動による堆積相の変化，地球惑星科学関連学会2006年合同大会（幕張メッセ国際会議場，千葉，2006年5月14日–18日）

村瀬雅之，伊藤武男，宮島力雄，森済，青山裕，大島弘光，吉田友香，寺田暁彦，小山悦郎，武田豊太郎，渡辺秀文，木股文昭，藤井直之　水準測量から推定する 1902-2005 浅間山圧力源体積時間依存モデル 2，日本火山学会秋季大会 70（リゾートホテル阿蘇いこいの村，阿蘇市，2006 年 11 月 23－25 日）

中村卓司，杉本尚悠，津田敏隆，橋本武士，寺田暁彦　小型水蒸気ラマンライダーによる境界層内水蒸気の空間構造観測，E139-P001（幕張メッセ国際会議場，千葉，2006 年 5 月 14 日–18 日）

中塚正，宇津木充，大熊茂雄，田中良和，浅間山電磁気構造探査グループ：浅間火山 2005 年空中磁気異常の 1992 年データとの比較、2006 年度ＣＡ研究会、京都大学木質ホール、2007 年 3 月 9 日

Niida, K., Green, D.H., Yoshikawa, M., Eggins, S.M., Dunite channels in the Horoman peridotites, Japan: Textural and geochemical constraints on melt/fluid transport through the lithosphere, Geochim. Cosmochim. Acta, 70, 445, 2006. Goldschimdt Conference, Geochim. Cosmochim. Acta, 70, 724, 2006 (2006 年 8 月メルボルン Australia)

新井田清信，Green, D. H.，芳川雅子，Eggins, S. M.，幌満かんらん岩体のダナイトチャネル：上部マントルにおける高温メルト/フルイド移動の考察，P-138（高知大学，高知，2006 年 9 月 16－18 日）

Nishimura, K., Amita, K., Ohsawa, S., Kobayashi, T., Hirajima, Microthermometry and chemical composition of fluid inclusion in quartz veins from the Sanbagawa metamorphic belt, Japan: direct analysis of the fluids released by metamorphic dehydration of the subducting plate, The 4th KAGI21 International Symposium, Kyoto（2006 年 12 月，Kyoto, Japan）

西村光史，柴田知之，小林哲夫，竹村恵二，姶良火砕噴出物にみられる鉛直組成変化，日本火山学会，（2006 年 10 月，阿蘇）

西村光史，珪長質マグマ溜まりの同化分別結晶作用による微量元素・同位体組成変化の熱物質輸送モデル，日本地球惑星科学連合 2006 年大会（2006 年 5 月，幕張）

大久保綾子，田中良和，神田径，石原和弘，宇津木充：空中磁気探査から推定された桜島火山の磁化強度分布、特定領域年度末シンポジウム、東京大学地震研究所２／１９－２１

大久保綾子，田中良和，神田径，石原和弘，味喜大介，宇津木充：桜島火山における空中磁気探査と岩石磁気測定、2006 年度ＣＡ研究会、京都大学木質ホール、2007 年３月９日、ポスター

大倉敬宏，Glenda BESANA，安藤雅孝　フィリピン・マコロード回廊周辺の地殻変動 地球惑星科学関連学会 2006 年合同大会予稿集，T225-P004（幕張メッセ国際会議場，千葉，2006 年 5 月 14 日–18 日）．

大倉敬宏，及川純　阿蘇火山におけるGPS観測　地球惑星科学関連学会2006年合同大会予稿集，V101-P016（幕張メッセ国際会議場，千葉，2006 年 5 月 14 日–18 日）．

大倉敬宏，岡本響，Raul Armand SALGUERO GIRON，小野博尉 阿蘇火山における地震活動 -HypoDD による震源再決定-　日本火山学会 2006 年秋季大会予稿集，P90（阿蘇いこいの村，阿蘇，2006 年 10 月 23 日–25 日）．

大倉敬宏，池田さや香，山本希，金嶋聰，高木憲朗，川勝均　阿蘇火山で発生する長周期微動について　日本地震学会 2006 年秋季大会予稿集，P131（名古屋国際会議場，名古屋，2006 年 10 月 31 日–11 月 2 日）．

岡田靖章，神田径，宇津木充，田中良和，井上寛之，小森省吾，小豆畑逸郎，山崎健一，吉村令慧，大志万直人、2006 年度ＣＡ研究会、京都大学木質ホール、2007 年３月９日

奥田昌明，三好教夫，竹村恵二，花粉層序によるステージ 11，5e，1 の比較，日本第四紀学会 2006 年大会，首都大学東京、東京，2006 年 8 月

Ohsawa, S. Geochemical features of the dehydrated fluid from the subducting hydrous

oceanic plate inferred from chemical and isotopic signatures of strongly mineralized waters emerging in fore-arc regions of convergent plate boundaries, 4th KAGI21 International Symposium. (December 4-5, 2006, Kyoto University Clock Tower, International Conference Room, Kyoto)

大沢信二, 網田和宏, 山田誠, 風早康平　宮崎県の大深度掘削温泉から流出する続成流体, 第 59 回日本温泉科学会大会講演要旨集, 34 (秋田県総合保健センター, 秋田, 2006 年 9 月 5 日–8 日)

Saito, S., Ohsawa, S., Hashimoto, T., Terada, A., Yoshikawa, S., Ohkura, T., Water, heat and chloride budgets of the crater lake at Naka-dake, Aso volcano, Japan, The 4th KAGI21 International symposium (2006 年 12 月 3 日-4 日, 京都市)

斎藤武士, 大沢信二, 橋本武志, 寺田暁彦, 吉川　慎, 大倉敬宏　阿蘇火山中岳火口湯溜まりの水・熱・塩化物イオン収支, 日本火山学会秋季大会 54 (リゾートホテル阿蘇いこいの村, 阿蘇市, 2006 年 11 月 23－25 日)

Saito, T. Different eruptive conditions among the last three eruptions at Unzen volcano, Japan, identified by magnetic petrological analyses. 日本地球惑星科学連合 2006 年大会, 千葉, 2006 年 5 月.

齋藤武士, 大沢信二, 橋本武志, 寺田暁彦, 吉川慎, 大倉敬宏, 阿蘇火山中岳火口湯溜まりの水・熱・塩化物イオン収支. 火山学会, 阿蘇, 2006 年 10 月.

齋藤武士, 井口正人, 石川尚人, 鳥居雅之, 大倉敬宏, 諏訪之瀬島火山 1884 年溶岩の示す磁気岩石学的特徴. 京都大学防災研究所研究発表講演会, 京都, 2007 年 3 月.

柴田知之, 氏家治, 伊藤順一, 杉本健, 竹村恵二 日本列島第四紀アダカイト質マグマの分布と地球物理学的特徴の関係, 地球惑星科学関連学会 2006 年合同大会予稿集, (幕張メッセ国際会議場, 千葉, 2006 年 5 月 14 日–18 日).

柴田知之, 小林哲夫, 西村光史, 杉本健, 竹村恵二 九州-琉球弧第四紀マグマの島弧縦断方向化学変化傾向, 日本火山学会講演予稿集 2006 年度秋季大会、(阿蘇憩いこいの国、阿蘇、2006 年 10 月 23 日 - 25 日)

柴田知之, 小林哲夫, 杉本健, 氏家治, 伊藤順, 西村光史, 竹村恵二, 九州弧火山フロント第四紀マグマの化学的特徴の島弧縦断方向変化, 2006 年日本質量分析学会同位体比部会 (鬼怒川温泉, 2006 年１１月８日－１０日)

柴田知之, 芳川雅子, 表面電離型質量分析計を用いた食品 (ワイン) のストロンチウム・ネオジム・鉛同位体測定法, 日本分析化学会第 55 年回講演要旨集, (大阪大学、豊中、2006 年 9 月 20 日–22 日)

Srigutomo, W., Kagiyama, T., Kanda, W., Munekane, H., Hashimoto, T., Tanaka, Y., Utada, H., Utsugi, M., 3-D modeling of resistivity structure of Unzen Volcano, Japan, using TDEM data, The 4th KAGI21 Symposium, Kyoto, December, 2006.

Srigutomo, W., Kagiyama, T., Kanda, W., Munekane, H., Hashimoto, T., Tanaka, Y., Utada, H., Utsugi, M., Resistivity structure of Unzen Volcano from Time Domain Electromagnetic (TDEM), 地球惑星科学関連学会 2006 年合同大会予稿集, V101-024 (幕張メッセ国際会議場, 千葉, 2006 年 5 月 14 日–18 日).

杉本健, 柴田知之, 芳川雅子, 竹村恵二 (2006) 由布・鶴見火山群の微量元素および Sr, Nd, Pb 同位体組成. 地球惑星科学関連学会 2006 年連合大会

杉本健, 黒川将, 中田節也, 吉本充宏, 嶋野岳人, 小栗和清, 星住英夫 (2006) USDP-4 カッティングス試料の岩相記載と全岩化学分析. 地球惑星科学関連学会 2006 年連合大会

杉本健, 柴田知之, 芳川雅子, 竹村恵二 (2006) Sr, Nd, Pb 同位体および微量元素組成からみた由布・鶴見火山のマグマ起源. 2006 年度日本地球化学会年会

杉本健, 星住英夫, 清水洋 (2006) 雲仙眉山火山の形成史 -ボーリングコア試料の岩相記載および全岩化学分析-. 日本火山学会 2006 年度秋季大会. P15.

杉本健, 柴田知之, 芳川雅子, 竹村恵二 (2006) 由布・鶴見火山群のマグマ起源（その２）-微量元素および Sr, Nd, Pb 同位体組成による制約. 日本火山学会 2006 年度秋季大会. A38.

Tagami, T., Takemura, K. An overview of the new KAGI-J3b project on the paleoclimate study using Indonesian speleothems. The 4th KAGI21 International Symposium Kyoto, 2006, (2006 年 12 月, 京都)

竹村恵二, 中部九州地域の密度構造, 東京大学地震研究所特定共同研究 B 第 3 回カルデラ研究会, 東京都, 2007 年 2 月.

竹村恵二, 北田奈緒子, 三田村宗樹, 大島昭彦, 関西圏における表層地質の研究状況 ボーリングデータベースによる理学・工学分野の相互研究. 日本地質学会 2006 年大会, 高知大学理学部、高知, 2006 年 9 月

竹村恵二, 林田明, 檀原徹, 山下透, 岩野英樹, 現琵琶湖堆積盆地の年代層序の再検討と堆積環境変遷, 地球惑星科学関連学会 2006 年合同大会（幕張メッセ国際会議場, 千葉, 2006 年 5 月 14 日–18 日）

田中良和, 火山活動に伴う地磁気変化、2006 年度ＣＡ研究会、京都大学木質ホール、2007 年 3 月 9 日

寺田暁彦, 橋本武志, 佐々木寿, 鍵山恒臣, 田中良和, 阿蘇火山・火口湖における水温・水深の変動解析, 平成 18 年度京都大学防災研究所研究発表講演会, 京都市, 2007 年 3 月.

寺田暁彦, 橋本武志, 佐々木寿, 鍵山恒臣, 田中良和：阿蘇火山・火口湖における水温・水深の変動解析、平成１８年度京都大学防災研究所研究発表講演会、京都テルサ、３月５日

豊田和弘, 篠塚良嗣, 竹村恵二, 北川浩之, 安田喜憲, 琵琶湖と水月湖の堆積物コア中から放射化分析で検出した複数の鬱陵島テフラとその噴出年代, 地球惑星科学関連学会 2006 年合同大会(幕張メッセ国際会議場, 千葉, 2006 年 5 月 14 日–18 日)

筒井智樹, 及川 純, 鍵山恒臣, 人工地震で見た富士火山の内部構造, 地球惑星科学関連学会 2006 年合同大会予稿集, U051-033 (幕張メッセ国際会議場, 千葉, 2006 年 5 月 14 日–18 日).

寺田暁彦, 橋本武志, 佐々木 寿, 鍵山恒臣, 田中良和 阿蘇火山・火口湖における水温・水深の変動解析, 2006 年度京都大学防災研究所研究発表講演会 (京都テルサ, 2007 年 3 月 5 日-6 日)

寺田暁彦, 佐々木寿, 橋本武志, 鍵山恒臣, 齋藤武士, 吉川慎 阿蘇火山中岳第一火口・火口湖水変動量の定量化, 日本火山学会 2006 年秋季大会予稿集, 206(リゾートホテル阿蘇いこいの村, 阿蘇市, 2006 年 11 月 23－25 日)

寺田暁彦 有珠火山 KA 火口から発生した渦輪噴煙. 地球惑星科学関連学会 2006 年合同大会予稿集, J240-002 (幕張メッセ国際会議場, 千葉, 2006 年 5 月 14 日–18 日)

宇津木充, 阿蘇カルデラの電磁気構造, 東京大学地震研究所特定共同研究 B 第 3 回カルデラ研究会, 東京都, 2007 年 2 月.

宇津木充, 田中良和, 九重火山における繰り返し空中磁気観測～1995 年噴火に伴う磁場時間変化検出～, 火山学会 2006 年秋季大会予稿集, P204 (阿蘇いこいの村, 熊本, 2006 年 10 月 23 日–25 日).

Terada, A., Ida, Y. Kinematic Features of Isolated Volcanic Clouds Revealed by Video-records, The 4th KAGI21 International symposium(京都市, 2006 年 12 月 3 日-4 日)

Utsugi, M., Tanaka, Y., Approaches of volcanomagnetic change detection by repeated aeromagnetic survey - aeromagnetic survey on Aso volcano, central Kyushu Japan -, AGU, Fall Meet.（2006年12月サンフランシスコ　U. S. A.）

宇津木充，田中良和，阿蘇火山における空中磁気観測，地球惑星科学関連学会2006年合同大会予稿集，E134-P005 (幕張メッセ国際会議場，千葉，2006年5月14日–18日).

宇津木充，田中良和，阿蘇火山における空中磁気観測～これまでの研究成果と今後の展望～，火山学会2006年秋季大会予稿集，P203 (阿蘇いこいの村，熊本，2006年10月23日–25日).

宇津木充，田中良和，鍵山恒臣，神田径 繰り返し空中磁気測量による火山性磁場変化検出の試み、平成１８年度京都大学防災研究所研究発表講演会、京都テルサ、３月５日

宇津木充，田中良和，鍵山恒臣，神田径，繰り返し空中磁気測量による火山性磁場変化検出の試み，平成18年度京都大学防災研究所研究発表講演会，京都市，2007年3月.

宇津木充，田中良和，中塚正，鍵山恒臣，橋本武志，神田径，浅間火山における空中磁気観測，地球惑星科学関連学会2006年合同大会予稿集，E134-P005（幕張メッセ国際会議場，千葉，2006年5月14日–18日）.

宇津木充，田中良和 阿蘇火山における高密度空中磁気観測～繰り返し空中磁気観測による火山地磁気効果の検出の試み～、2006年度ＣＡ研究会、京都大学木質ホール、2007年３月９日、ポスター

宇津木充 阿蘇火山における高密度空中磁気観測～繰り返し空中磁気観測からの時間変化検出の試み～、特定領域年度末シンポジウム、東京大学地震研究所 2/19-21

渡邉康平，高松信樹，大沢信二，加藤尚之 温泉排水が河口・沿岸海洋環境に及ぼす影響について，第59回日本温泉科学会大会講演要旨集，9（秋田県総合保健センター，秋田，2006年9月5日–8日）

Watanabe, Y., Matsuoka, H., Ohsawa, S., Yamada, M., Kitaoka, K., Kiguchi, M., Ueda, J., Yoshimura, K., Kurisaki, K., Nakai, S., Brahmantyo, B., Maryunani, K. A., Tagami, T., Takemura, K., Yoden, S. Paleoclimatological study using stalagmites from Java island, Indonesia. AGU, Fall Meet.（2006年12月サンフランシスコ　U. S. A.）

Watanabe, Y., Matsuoka, H., Ohsawa, S., Yamada, M., Kitaoka, K., Kiguchi, M., Satomura, T., Ueda, J., Kurisaki, K., Yoshimura, K., Nakai, S., Brahmantyo, B., Maryunani, K.A., Tagami, T., Takemura, K., Yoden, S. , An overview of the KAGI21-J3b project on the paleoclimate study using Indonesian speleothems. The 4th KAGI21 International Symposium Kyoto, 2006, (2006年12月，京都)

Watanabe, Y., Matsuoka, H., Ueda, J., Kurisaki, K., Yoshimura, K., Nakai, S., Tagami, T., Takemura, K., Preliminary report on speleothem characteristics from West and Central Java, Indnesia. The 4th KAGI21 International Symposium Kyoto, 2006, (2006年12月，京都)

Yamada, M., Ohsawa, S., Kitaoka, K., Watanabe, Y., Matsuoka, H., Brahmantyo, B., Maryunani, K.A., Tagami, T., Takemura, K., Yoden, S. Preliminary report on isotopic and geochemical analyses of drip water samples from Buniayu limestone caves, in Sukabumi, west Java, Indonesia. The 4th KAGI21 International Symposium Kyoto, 2006, (2006年12月，京都)

Yamamoto J., Nakai S., Nishimura K., Kaneoka I., Kagi H., Sato K., Prikhod'ko V. S., Arai S. Occurrence of subduction-related fluid in mantle wedge-derived xenoliths, KAGI International Symposium Kyoto（2006 年 12 月, Kyoto, Japan）

山本順司、荒川雅、平野直人、羽生毅、三浦弥生、鍵裕之 マントルを駆け巡る炭酸流体の起源, 質量分析学会同位体比部会（2006 年 11 月, 栃木県日光市）

山本 順司 マントル起源鉱物中の流体包有物から探る沈み込み帯の物質循環系の研究, 日本地球化学会年会（2006 年 9 月, 東京都世田谷区）

Yamamoto J., Nakai S., Kaneoka I., Kagi H., Sato K., Prikhod'ko V. S., Arai S. Trace elements in grain-boundary component in mantle xenoliths from Far Eastern Russia. Goldschmidt conference（2006 年 8 月, Melbourne, Australia）, Geochimica Cosmochimica Acta, 70, A718.

山本 順司、平野直人、後藤秀作、鍵 裕之 日本へ沈み込む直前の海洋リソスフェア—その地温勾配—, 日本地球惑星科学連合 2006 年大会（2006 年 5 月, 千葉県千葉市）

芳川雅子, 荒井章司, 黒瀬マントルかんらん岩捕獲岩のRb-Sr 鉱物アイソクロン年代, 日本地球惑星科学連合2006年大会予稿集, K104-008 （幕張メッセ国際会議場, 千葉, 2006年5月14日–18日）.

Yoshikawa, M., Arai, S. Geochemical and Sr-Nd isotopic characteristics of the lithospheric mantle beneath the Southwest Japan arc, The 4th KAGI21 International Symposium, J2b-23 (2006年12月京都, Japan)

Yoshikawa, M., Niida, K., Eggins, S.M., Green, D.H., Trace element and isotopic (Sr and Nd) compositions of clinopyroxenes in dunite channels of the Horoman peridotite complex, Hokkaido, Japan, Goldschimdt Conference, Geochim. Cosmochim. Acta, 70, 724, 2006 (2006年8月メルボルンAustralia)

芳川雅子, 小澤一仁, 南部北上帯早池峰-宮守オフィオライト的岩体のSr-Nd同位体組成：オルドビス紀島弧下マントルウェッジ中でのメルト形成過程, 日本地質学会第113年学術大会予稿集, P-4（高知大学, 高知, 2006年9月16－18日）

Yoshikawa, M., Kawamoto, T., Yamamoto, J., Equilibrium temperature and pressure conditions of the peridotite xenoliths in the French Massif Central, presented in a seminar at Laboratoire Magma et Volcan, Universite Blaise Pascal, Clermont Ferrand, France October 2006.

共同研究一覧 List of Collaborations

国内

鍵山恒臣，竹村恵二，大倉敬宏，大沢信二，柴田知之，西村光史，宇津木充，東京大学地震研究所　特定共同研究（B）カルデラの構造と活動そして現在− Out of range への挑戦

川本竜彦，愛媛大学地球深部ダイナミクス研究センター　客員研究員

川本竜彦，岡山大学固体地球研究センター　共同利用研究員

栗谷豪，岡山大学地球物質科学研究センター　嘱託研究員（研究課題：マグマ溜まり内の組成対流についての研究）

大倉敬宏，東京大学地震研究所一般共同研究　阿蘇火山における 1HzGPS 観測

大倉敬宏，東京大学地震研究所特定共同研究(B) 新世代無線通信データ伝送システムの開発

大沢信二，河川及び河口域に及ぼす温泉排水の影響評価に関する環境化学的研究　参加機関：東邦大学理学部化学科

大沢信二，岡山県下の鍾乳洞の水文調査　参加機関：岡山理科大学理学部基礎理学科

杉本健，中田節也，東京大学地震研究所，平成１８年度一般共同研究（研究課題：USDP-3 コアを用いた雲仙火山の噴火史の解明）

杉本健，星住英夫，清水　洋，研究課題：雲仙火山眉山の火山活動史の解明

竹村恵二，京都大学防災研究所一般共同研究 17G-03　代表：大塚悟（長岡技術科学大学助教授）（分担）：地盤情報を活用した大規模斜面崩壊危険箇所の同定に関する研究

竹村恵二，国際日本文化研究センター共同研究員

寺田暁彦，鍵山恒臣，吉川　慎，2006 年度集中総合観測 熱観測（有珠火山）

山本順司，中井俊一，東京大学地震研究所一般共同利用　海洋プレートの屈曲部で生じるマグマの活動源を探る

国際

川本竜彦，日本学術振興会とフランス外務省の間での日仏交流促進事業 SAKURA：沈み込み帯における鉱物・フルイド・マグマによる水と二酸化炭素の循環

大沢信二，国際協力銀行（JBIC）円借款による中国「内陸部・人材育成事業」　相手機関：雲南大学（中華人民共和国）

竹村恵二，ICDP Project Lake Biwa and Lake Suigetsu: Recorders of Global Paleoenvironments and Island arc Tectonics

研究費　Funding

科学研究費補助金

鍵山恒臣，特定領域研究 赤外・可視映像解析による噴煙の時間変動と噴火発生場の構造に関する研究　1200　千円

川本竜彦（代表），基盤研究(c)　沈み込み帯における水の構造と物性の変化　800 千円

栗谷豪（代表），若手研究(B)　マグマ分化プロセスの時間スケールの定量的解明　1700　千円

大倉敬宏，　基盤研究(A)　火山流体のモニタリングと深部マグマ上昇メカニズムの解明（代表：川勝均）3800　千円

齋藤武士（代表），特別研究員奨励費　「火山体の磁気と火山噴出物の磁性の研究-磁気岩石学からのアプローチ」1200 千円

柴田知之（代表），基盤研究(c)　沈み込むスラブが部分溶融する物理条件の推定　900　千円

竹村恵二，21 世紀 COE　プログラム　（代表：余田成男）　活地球圏の変動解明

竹村恵二，基盤研究(B)（代表：岡田篤正）　要注意の長大活断層を対象とした活動域区分・活動履歴の高精度化．5,700 千円

竹村恵二，基盤研究(B)（海外）（代表：北川浩之）炭素１４年代キャリブレーション年代域の拡大にむけた中国東北部火口年縞堆積物の採集

竹村恵二，基盤研究(S)（代表：安田喜憲）年縞の分析による年単位の環境史復元と稲作漁労文明の興亡

田中良和，　特定領域研究（２）、火山爆発の発生場と発生過程、12800 千円

寺田暁彦，　萌芽研究　火山噴煙のリモートセンシングに関する新手法の開発，3，300 千円（代表：橋本武志）

山本順司（代表），若手研究(B) 超高精度地質圧力計の開発とマントル流体の四次元精査　2 000 千円

受託研究、奨学寄付金

鍵山恒臣，大分県温泉調査研究会，平成 18 年度調査研究事業（研究課題：塚原噴気地帯における噴気活動の短周期時間変動特性，70 千円

川本竜彦（日本側代表），　日本学術振興会とフランス外務省の間での日仏交流促進事 SAKURA：沈み込み帯における鉱物・フルイド・マグマによる水と二酸化炭素の循環 850 千円

大沢信二　産業総合技術研究所深部地質環境研究センター研究費　1000 千円

杉本健，京都大学，平成 18 年度「21 世紀ＣＯＥプログラム」若手研究者研究活動経費（研究課題：九州弧第四紀マグマの島弧横断方向での微量元素・放射起源同位体組成変化–フィリピン海プレート由来物質寄与の有無の解明，350 千円）

杉本健，中田節也，東京大学地震研究所，平成 18 年度一般共同研究（研究課題：USDP-3 コアを用いた雲仙火山の噴火史の解明，課題番号 2006-G-05，248 千円）

杉本健，大分県温泉調査研究会，平成 18 年度調査研究事業（研究課題：Sr，Nd，Pb 同位体組成を用いた由布岳・鶴見岳におけるマグマ生成の解明，70 千円）

寺田暁彦，京都大学 21 世紀 COE プログラム・若手研究者研究活動経費，阿蘇火山地下浅部～地表への物質・熱移送モデルの構築，500 千円

芳川雅子，九電産業株式会社　熱水ストロンチウム同位体組成の測定に対する研究助成，150千円

教育活動 Education

学位，授業 Academics

学位審査

鍵山恒臣：（審査員）Sukir Maryanto（博士　京都大学大学院理学研究科）
（審査員）Sri Hidayati（博士　京都大学大学院理学研究科）
（主査）　小森省吾（修士　京都大学大学院理学研究科）
（審査員）三根崇彦（修士　京都大学大学院理学研究科）
（審査員）長野雄大（修士　京都大学大学院理学研究科）
（審査員）岡田靖章（修士　京都大学大学院理学研究科）
（審査員）畑真紀　（修士　京都大学大学院理学研究科）

大倉敬宏：（副査）　Raul Armando SALGUERO GIRON（修士　政策研究大学院大学政策研究科）
（主査）　岡本響（修士　京都大学大学院理学研究科）
（審査員）Sri HYDAYATI（博士　京都大学大学院理学研究科）
（審査員）Sukir MARYANTO（博士　京都大学大学院理学研究科）

大沢信二：（審査員）渡邊康平（修士　東邦大学大学院理学研究科）
（審査員）三根崇彦（修士　京都大学大学院理学研究科）

竹村恵二：（主査）　三根崇彦（修士　京都大学大学院理学研究科）
（審査員）小森省吾（修士　京都大学大学院理学研究科）
（審査員）垣内裕哉（修士　京都大学大学院理学研究科）
（審査員）末岡茂　（修士　京都大学大学院理学研究科）
（審査員）山本晋也（修士　京都大学大学院理学研究科）
（審査員）畑真紀　（修士　京都大学大学院理学研究科）
（審査員）林辰也　（修士　九州大学大学院比較文化研究院）

田中良和：（審査員）岡田靖章（修士　京都大学大学院理学研究科）
（審査員）畑真紀　（修士　京都大学大学院理学研究科）
（審査員）長野雄大（修士　京都大学大学院理学研究科）
（審査員）小森省吾（修士　京都大学大学院理学研究科）
（審査員）小野友督（修士　京都大学大学院理学研究科）
（審査員）九里崇博（修士　京都大学大学院理学研究科）
（審査員）橘亮匡　（修士　京都大学大学院理学研究科）
（審査員）寺本万里子（修士　京都大学大学院理学研究科）
（審査員）酒巻厚志（修士　京都大学大学院理学研究科）

講義，ゼミナール

（学部）

ポケットゼミ：地球の熱を測ってみよう　Introductory Seminar on Observation in Volcanoes
鍵山恒臣，田中良和，大倉敬宏

地球惑星科学 I　　平原和朗，福田洋一，竹村恵二
観測地球物理学演習 A　田中良和，鍵山恒臣，須藤靖明，大倉敬宏，宇津木充，里村雄彦，藤森邦夫，西憲敬，古川善紹
観測地球物理学演習 B　竹村恵二，大沢信二，堤浩之，柴田知之，川本竜彦，山本順司，杉本健，西村光史，斎藤武士，栗谷豪
グローバルテクトニクス　田上高広，古川善紹
地球熱学　　竹村恵二，鍵山恒臣，大沢信二，古川善紹
火山物理学 I　　古川善紹
火山物理学 II　　田中良和，鍵山恒臣，須藤靖明，大倉敬宏，石原和弘，井口正人，古川善紹
陸水物理学　　大沢信二，諏訪浩
課題演習 DA　固体地球系　　古川善紹ほか
課題演習 D3：地下構造と活構造，地表変動　竹村恵二，堤浩之，赤松純平，福岡浩，岩田知孝
課題研究 D4：地球熱学古川善紹，柴田知之，川本竜彦，宇津木充，山本順司
課題研究 D6：気象学総合演習　余田成男，石岡圭一，内藤陽子，大沢信二，林泰一，石川裕彦
課題研究 D7：地球磁気圏の構造と波動現象　町田忍，家森俊彦，田中良和，亀井豊永，竹田雅彦，齋藤昭則，能勢正仁
課題研究 T8：地表変動，固体地球物理，火山物理　　竹村恵二，須藤靖明，堤浩之

（大学院，修士課程）
第四紀地質学　　竹村恵二
活地球変動，結合論 B　田上高広，福田洋一，竹村恵二，堤浩之
活地球固体圏 B　　平島崇男，小畑正明，中西一郎，大沢信二，古川善紹，竹村恵二
水圏地球物理学 IIA　　大沢信二，Sidle, Roy C.，諏訪浩
水圏地球物理学 IIB　　大沢信二，Sidle, Roy C.，諏訪浩
地球熱学，地熱流体学 IA　田中良和，大沢信二，鍵山恒臣
地球熱学，地熱流体学 IB　田中良和，大沢信二，鍵山恒臣
地球熱学，地熱流体学 IIA　　竹村恵二，須藤靖明，古川善紹，大倉敬宏
地球熱学，地熱流体学 IIB竹村恵二，須藤靖明，古川善紹，大倉敬宏
応用地球電磁気学 A　大志万直人，田中良和，鍵山恒臣
応用地球電磁気学 B　大志万直人，田中良和，鍵山恒臣
地球惑星科学特殊研究（修士論文）　全教員

（大学院修士課程および博士後期課程）
地球物質科学セミナーI　小畑正明，平島崇男，柴田知之，山本順司
地球生物圏史セミナー　増田富士雄，前田晴良，竹村恵二，大野照文
固体地球物理学ゼミナール IV　　中西一郎，久家慶子，大倉敬宏
水圏地球物理学ゼミナール III　　大沢信二，Sidle, Roy C.，諏訪浩，斉藤隆志
活構造論ゼミナール I　　竹村恵二，堤浩之
活構造論ゼミナール II　　竹村恵二，堤浩之
地球熱学，地熱流体学ゼミナール I　竹村恵二，大沢信二，川本竜彦，柴田知之，山本順司
地球熱学，地熱流体学ゼミナール II　　田中良和，鍵山恒臣，須藤靖明，古川善紹，大倉敬宏，宇津木充

応用地球電磁気学ゼミナール　　大志万直人，田中良和，鍵山恒臣，神田径，吉村令慧

野外実習

観測地球物理学演習 A　（別府，7 月 30 日～8 月 1 日）教員・研究員多数
観測地球物理学演習 B　（阿蘇，8 月 1 日～4 日）教員多数
地質鉱物学野外実習　（3 月 5 日～7 日）竹村恵二ほか
課題演習 D2 阿蘇実習　（阿蘇，9 月 25 日～28 日）大倉敬宏ほか
課題演習 D3 別府実習　（別府，8 月 1 日～3 日）竹村恵二
課題演習 D5 別府実習　（別府，11 月 25 日～27 日）大沢信二
観測地球物理学演習 B　（別府，7 月 30 日～8 月 1 日）教員多数
課題演習 D5 別府実習　（別府，11 月 25 日～27 日）大沢信二
活地球圏科学実習（大学院）　余田成男，他（随時の実習で，大沢は活地球圏科学実習結合系を実施した．11 月 25 日～27 日）

その他

京都大学ジュニアキャンパスセミナー「火山の噴火を見てみよう」鍵山恒臣，大倉敬宏
大沢信二　日本文理大学「大分学」（集中講義）5 月 23 日

セミナー　Seminars

＜地熱セミナー＞　別府　(テレビ会議システムを用い阿蘇セミナー室で放送)

平成 18 年（2006 年）

4 月 12 日　A-01 竹村，山本，斎藤，馬渡：　第四紀堆積物・ローム層セクションの測色に基づく環境変遷と火山活動史
A-03　柴田，芳川，西村，杉本，竹村：　九州弧火成岩類の地球化学的特徴の時空変化
A-06　大倉，馬渡，古川，竹村：　九州中部地域の地震活動

4 月 19 日　A-02 大沢，網田，西村，頼，山本，平島：　ICP-MS を用いた地球深部流体活動解明に関する研究
A-04　山本，頼：　ウェッジマントルに浸入した流体の起源

4 月 26 日　A-05 川本，山本，芳川：　マントルゼノリスの岩石学
A-07　頼，芳川，柴田，山本：　東アジア，マントル由来ゼノリスの微量元素・同位体組成挙動の研究

5 月 9 日　栗谷：　Ｕ－Ｔｈ放射非平衡を用いたマグマ進化の時間スケールの決定～利尻火山、アルカリ玄武岩・安山岩質溶岩流

6 月 7 日　杉本：　ガラスビード法による広い組成範囲にわたる岩石試料中の主成分元素の蛍光 X 線分析

6 月 14 日　斎藤：　ビデオカメラによる阿蘇火山の赤熱観測

6 月 28 日　西村：　メルト包有物に記録されたマグマ溜まりの進化：　姶良火砕噴出物の例

7 月 5 日　山田：　(U-Th)/He 年代法とそれによる熱年代学的研究の紹介

7 月 12 日　山本：　沈み込む海洋プレートの地球化学的特徴と温度構造　－流体包有物の残留圧力と希ガス同位体比－

7 月 18 日　大沢：　温泉の起源水としての続成流体」

10 月 4 日　杉本：　微量元素および同位体組成からみた先雲仙・雲仙火山のマグマ起源

10月18日　山本：　深部起源鉱物の深さ指標としての流体包有物の残留圧力
11月1日　Hassan Mohamed Helmey：　Examination of the deep levels of Precambrian island arcs: evidence from Alaskan-type complexes from Egypt
11月14日　浜田：　島弧玄武岩マグマの結晶分化作用に及ぼす水と圧力の効果
11月29日　柴田：　The along arc variations of Sr, Nd and Pb isotopic and trace element compositions for Quaternary volcanics from Kyushu, Japan
12月19日　芳川雅子：　西南日本弧下のリソスフェリックマントルの地球化学的特徴
平成19年（2007年）
1月10日　竹村：　関西国際空港地盤
1月16日　西村：　三波川変成帯の石英脈に保存されたプレート脱水流体
1月31日　齋藤：　雲仙火山歴史3噴火溶岩の示す磁気岩石学的特徴

＜特別セミナー＞
平成18年（2006年）
6月16日　新井田清信（北海道大学）
上部マントルにおけるマグマの通路（ダナイト-クロミタイトチャネルの起源）
（1）ダナイト-クロミタイトチャネルの形態・組織と結晶作用
（2）幌満かんらん岩体の層状構造とダナイトチャネルの観察
7月11日　藤井俊行（京大原子炉）
Nuclearfield vs. nucleosynthetic effects as cause of isotopic anomalies in the early Solar System
12月14日 大出茂　（琉球大学）
サンゴ礁のながい旅：ストロンチウム同位体を使った環礁 ボーリングコアの年代測定－海面変動と海洋プレートの沈降・隆起の歴史－
平成19年（2007年）
1月11日　佐野有司教授（東大海洋研）
ヘリウム同位体比とテクトニクス
1月15日　Marie Python　（金沢大学）
海洋底上部マントルでの火成活動と熱水作用：　オマーンオフィオライトの例
(Magmatism and hydrothermalism in the oceanic upper mantle: Example of the Oman Ophiolite)
1月31日　山崎徹　（北海道大学）
海洋地殻の構成と地殻内プロセスの岩石学的・地球化学的実態

＜京都ゼミ＞　北白川4号館1階会議室
(テレビ会議システムを用い別府・阿蘇セミナー室で放送)
平成18年（2006年）
4月28日 岡田靖章：　合同大会ポスターセッション発表練習
4月28日 小森省吾：　合同大会ポスターセッション発表練習
5月12日　三根崇彦：　土壌CO_2ガス探査を主軸とした，火山・地熱地域における地質構造－流体相互作用についての研究――別府地域を例として――
5月26日　岡本響：　九州地方中南部のスラブ内地震について

6月2日　田中良和：　空中磁気測量による火山性磁場変動の検出
6月9日　鍵山恒臣：　マグマの貫入／噴出比と火山活動の多様性
6月16日　岡田靖章：　九重火山の見かけ比抵抗と位相の特徴
6月23日　小森省吾：　雲仙火山北東部における熱水の移動
6月30日　大倉敬宏：　阿蘇火山における長周期微動
7月7日　竹村恵二：　九州の第四紀テクトニクス
10月6日　小森省吾：　雲仙火山北東部における浅部比抵抗構造と熱水の流れ
10月13日　岡田靖章：　九重硫黄山周辺の浅部比抵抗構造について～進捗状況～
10月13日　小森省吾：　雲仙火山北東部における浅部比抵抗構造と熱水の流れ
10月20日　小森省吾：　雲仙火山北東部における浅部比抵抗構造と熱水の流れ
10月20日　岡本響：　九州地方中南部のスラブ内地震について～進捗状況～
10月27日　岡田靖章：　九重火山における浅部比抵抗構造（2）
11月10日　岡田靖章：　九重火山における浅部比抵抗構造（2）
11月17日　三根崇彦：　CO_2ガスフラックスによる，地熱活動の評価について－別府地域を例に－
12月15日　鍵山恒臣：　浅間火山の2004年噴火に学ぶ

平成19年（2007年）
1月26日　熊谷仁孝：　分子動力学計算を用いたNaCl水溶液の観察
2月9日　岡本響：　九州地方中南部におけるフィリピン海スラブ内地震
2月9日　岡田靖章：　九重火山における浅部比抵抗構造の推定
2月9日　小森省吾：　火山体浅部における比抵抗構造と熱水

＜火山研究センターゼミ＞　(テレビ会議システムを用い別府セミナー室で放送)
阿蘇　火山研究センター講義室
4月18日(火)13時30分-15時00分　寺田暁彦，火山噴煙現象の観測的研究
5月30日(火)13時30分-15時00分　宇津木　充，磁化構造３Ｄインバージョンに関連する話題
6月13日(火)15時00分-16時00分　Raul Armando, Guatemala land of mountains of fire
7月25日(火)13時30分-15時00分　Asep Harja, Bandung Basin
10月31日(火)13時30分-15時00分　須藤靖明，阿蘇火山のマグマだまりについて
11月7日(火) 13時30分-15時00分　宮縁育夫（森林総合研究所），吉岡噴気地帯を含む阿蘇火山中央火口丘群西部地域の発達史
11月21日(火) 13時30分-15時00分　寺田暁彦　活動的火口湖における水温・水深の時間変動モデル
12月26(火) 13時30分-15時00分　鍵山恒臣　三宅島２０００年噴火に伴う全磁力変化
1月23日(火) 13時30分-15時00分　宇津木　充　阿蘇火山に於ける高密度空中磁気観測～繰り返し空中磁気観測による時間変化検出の試み～
2月27日(火) 13時30分-15時00分　大倉敬宏　阿蘇火山周辺の地殻変動
3月30日(火) 11時00分-12時00分　坂口弘訓（島根大学）　微動観測と地質調査による1928年以降の阿蘇火山の噴火活動

＜21 世紀 COE 関連＞

大沢信二：沈み込み帯下の流体活動に関する分野横断的研究の背景にある熱水流体研究．21 世紀 COE「活地球圏の変動解明」KAGI J2b 成果報告会　2007 年 3 月 16 日～17 日　地球熱学研究施設（別府）

Ohsawa, S. : Preliminary report on isotopic and geochemical analyses of drip water samples from Buniayu limestone caves in Sukabumi, West Jave, Indonesia. Seminar on the active geosphere「Paleoclimate study using Indonesian speleothems」 2006 年 9 月 14 日 バンドン工科大学（ITB），インドネシア

Ohsawa, S. : Hydrogeology of limestone caves using dripwater samples. Seminar on the active geosphere「Limestone cave and paleoclimatic studies」 2006 年 6 月 5 日 バンドン工科大学（ITB），インドネシア

学会活動 Activities in Scientific Societies

鍵山恒臣

日本火山学会事業委員

川本竜彦

Geochemical Journal 誌　Associate Editor

栗谷豪

Island Arc 誌　Associate Editor

大倉敬宏

日本火山学会大会委員

大沢信二

日本温泉科学会理事（広報・交流委員長）

日本水文科学会評議員

地球惑星科学委員会国際対応分科会 IAHS（国際水文科学協会）委員

杉本健

日本火山学会 2006 年秋期大会プログラム編集委員

竹村恵二

日本第四紀学会評議員

日本地質学会地方地質誌九州地方編集委員会委員

日本地質学会地方地質誌近畿地方編集委員会委員

社会活動　Public Relations

鍵山恒臣

火山噴火予知連絡会，委員
火山活動評価検討委員会，委員
東京都三宅島活動検討委員会，委員
霧島火山防災検討委員会および霧島火山災害予測図検討分科会，霧島火山災害警戒避難検討分科会，委員
地震予知・火山噴火予知研究協議会，委員
火山噴火予知研究委員会，委員
JICA 研修「火山学，総合土砂災害対策コース」，カリキュラム委員および講師

大沢信二

大分県温泉調査研究会理事
大分県温泉監視調査委員会委員
別府市緑の基本計画策定委員
大分市廻栖野地区地下水調査検討委員
別府八湯語り部の会講師
別府市中央公民館別府再発見講座講師
大分舞鶴高校スーパーサイエンスハイスクール指導教官

竹村恵二

大分県地震被害想定委員会副委員長
関西国際空港深部地盤掘削委員会委員
地震調査研究推進本部ニュース　サイスモ　サイスモスコープ執筆委員
独立行政法人産業技術総合研究所研究ユニット評価委員会委員
大阪府大規模地震ハザード評価部会
日本学術振興会科学研究費委員会専門委員
独立行政法人産業技術総合研究所　「地層処分にかかる地質情報データの整備」評価委員会委員
『三重県地域活断層調査委員会』委員
『京都府地震被害想定委員会』委員
『京都府地域活断層調査委員会』委員
『大分県温泉監視調査委員会』委員
文部科学省　科学技術政策研究所　科学技術動向研究センター　専門調査員
『関西国際空港（二期地区）地盤挙動調査委員会』委員
『石川県能登町真脇遺跡調査指導委員会』委員
大分地質学会　特別講演：大分の火山活動史と最近の話題，大分大学，2007 年 1 月．
地震に関するセミナー　－京都府防災講演会－　講演：京都府南部で想定される地震被害について　（京田辺市，京都）
地球熱学研究施設（別府）施設公開　「夏休み地獄ハイキング」講師

田中良和

科学技術・学術審議会専門委員(測地学分科会)　平成１７年３月―平成１９年１月
防災研究所研究担当
火山噴火予知運営協議会委員
火山噴火予知研究協議会委員
科学研究費委員会専門委員
熊本大学非常勤講師

一般公開報告　Openhouse

一般公開報告「別府」

京都大学大学院理学研究科附属地球熱学研究施設では，平成18年7月22日（土）午前9時ー午後4時まで研究施設の一般公開を行った．7月27日（木）午後2時ー午後5時半に別府市朝見川断層沿いを対象とした夏休み地獄ハイキングを行った．また，同日夜間（19時ー22時）及び翌夜同時刻に研究施設のライトアップを行い，一般市民とより親密に触れ合う場を設けた．一般公開には昨年度を大幅に上回る268名（前年度は196名）にお越し戴いた．ハイキングには非常に暑い中34名の市民に参加して戴き，ライトアップにも30名の来場者を数えた．

平成18年度研究施設一般公開担当　山本順司

夏休みハイキングの内容

今年度も，温泉や火山，地震を肌で感じられる企画を設けることにした．温泉や火山，地震を全て網羅するにはやはりある程度移動しなければならないが，竹村教授によって昨年度のルートが更に改訂され，それらを短時間で見聞できる理想的なルートが策定された．

ハイキング内容

7月27日（木）13時半ー14時，スギノイパレス前に集合し，受付を済ませた後，杉の井地熱発電所の見学から始まった．案内者は6名（竹村教授・山本助手・馬渡技術員・齋藤博士・杉本博士・山田博士・宮崎事務補佐員）．参加者は34名．その他2つの新聞社と地元ケーブルテレビ局の記者兼カメラマンが同行した．

タイトルは「夏休み地獄ハイキング」．参加者全員に，竹村教授監修のパンフレットが配布され，ハイキング中は随時，竹村教授による解説が行われた．杉の井地熱発電所では，発電所所員による発電所についての説明を受けた．移動距離は約7km，標高差は約150mほどもあったが，全参加者が有事に備えて随行していた研究施設の公用車に頼ることもなく歩き切った．ハイキング中は天候に恵まれ，事故もなく無事にラクテンチで解散することができた．

以下にハイキングで参加者に配布したパンフレットの一部と，オープンハウスの概要を示す．詳細な報告書は本施設のホームページで公開してある．

ハイキングの見所と目的

私たちの住んでいる別府は、世界でも有数の湯の町です。そして断層と火山の町でもあります。皆さんは、これらが密接に関係していることを知っていますか？別府は、地下の地熱活動と、地表の火山からの堆積物の上に立っており、それらをたくさんの断層が切っています。そのおかげでお湯が湧いたり、水が湧いたりしているのです。今日は、別府の南を走る朝見川断層に沿って歩きながら、温泉湧水地帯を観察して、別府の成り立ちを考え、さらには私たちの住んでいる地球の息吹を感じてみましょう。

案内　竹村恵二 教授

名前：　　学年：

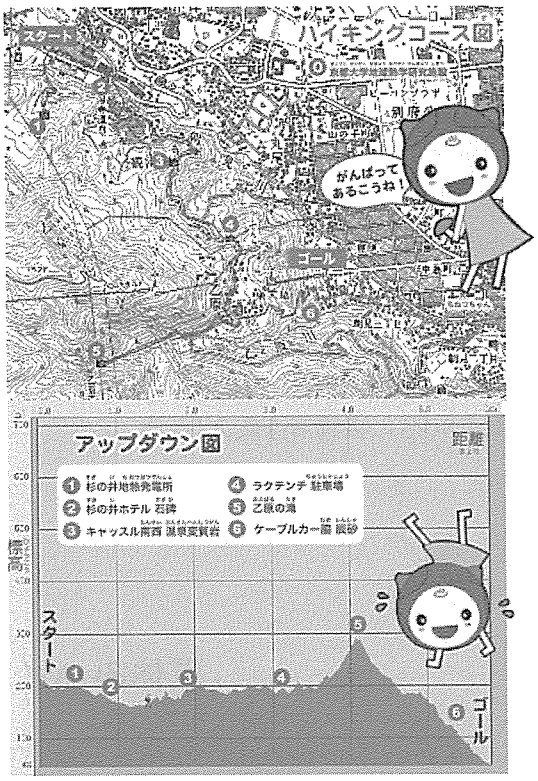

0 京都大学 地球熱学研究施設

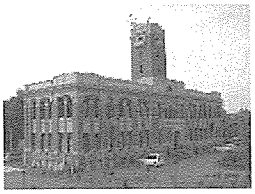

1924年につくられました

右の写真は、京都大学地球熱学研究施設です。大正13年に完成した赤レンガ造りの建物は平成9年に国の文化財にも指定されました。現在も14人のスタッフが研究や教育を行っています。最初にハイキングの説明と注意がありますので、よく聞きましょう。

ここから車で第1地点の杉乃井地熱発電所に向かいます。研究所を富士見通りに出ると、左手由すそに高層があがる風景が目に入ります。観海寺の温泉街です。その中で、ひときわ目立つ高い建物群が見えます。杉乃井ホテル群です。車はこのホテル群の下の急な坂を登って行きます。30mを超えるこの崖が朝見川断層です。崖には大きな岩や砂からなる層が露出しています。昔の扇状地の堆積物で、別府の町の土台になっています。それが、断層運動で高いところと低いところに分かれているのです。この崖をあがりきるとゆるやかな上りの平坦面に出ます。昔の扇状地が作った面です。ホテル群を抜け、朝見川を渡ると地熱発電所につきます。

急な坂をのぼります

崖の下に別府の町が見えます

がけが断層なんだよ！

MEMO

1 杉乃井地熱発電所

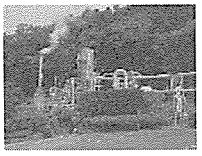

杉乃井ホテルの地熱発電所を見学します。杉乃井地熱発電所は昭和55年11月にホテル業界としては初めての本格的な地熱発電所として運転をはじめました。

地熱発電は、地下から取り出した蒸気を使ってタービンを回して電気を作ります。地熱発電は地面の下の蒸気を使うので、火力発電や原子力発電とは違って、石油やウランといった燃料を外国から輸入する必要がありません。二酸化炭素や放射性廃棄物といった地球に有害とされる物を出さないのも大きな特徴です。

地熱発電の現状

しかし、地熱活動の盛んな場所でしか行えないので、日本では九州や東北などの地熱地帯で発電が行われています。杉乃井地熱発電所は3000KWの発電量を有し、杉乃井ホテルの約1/2の電力をまかなっています。

ここでは、地熱発電のしくみについて説明を受け、発電所内を見学しましょう。見学が終わったら、いよいよハイキング出発です。トイレなどを済ませて、元気よく出発しましょう！

MEMO

② 杉乃井ホテル 石碑

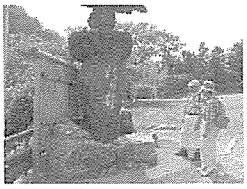

発電所から急な山麓扇状地を下り，朝見川を渡り，杉乃井ホテルの中を抜けます。ホテル正面前の道路わきに石碑があります。この石碑の岩石は，大分県の堆積岩や別府地域の火山岩から出来ています。別府の代表的な石を一度に観察できます。よく観察してみましょう。

③ キャッスル南西 温泉変質岩

杉乃井ホテル前をあとにして，朝見川にかかる橋をわたり，南側の山麓沿いの道を東へと歩きます。観海荘を過ぎ，ゆるやかな坂を上ろると，ホテルキャッスルのあたりまで左手に別府市街地が見えます。別府市街の広がる火山性扇状地を遠望しましょう。ホテルキャッスルをすぎると石碑の壁に岩石が露出しています。この岩石は「プロピライト」といい，別府地域でもっとも古い岩石です。プロピライトは，もとは「安山岩」という鶴見火山や鶴見火山で良く見られる火山岩でしたが，温泉や熱水で変質してできました。

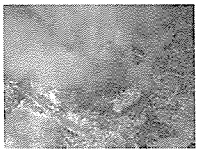

色々な所に温泉があります

MEMO

④ ラクテンチ 駐車場

さらに道路に沿って歩いて行きます。ラクテンチ駐車場の手前で急に大きく開けて，別府市街地が広く見渡せるようになります。この付近では地すべりの地形や断層地形が見られ，また鶴見岳山麓からの扇状地地形を観察することができます。ラクテンチ付近の岩石もプロピライトからなり，この付近も古い溶岩流であったことがわかります。

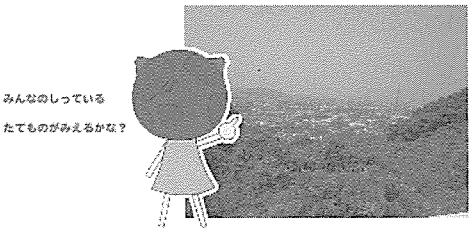

MEMO

研究施設一般公開の内容

施設公開マップ

この色で塗っている場所は
今回公開しています

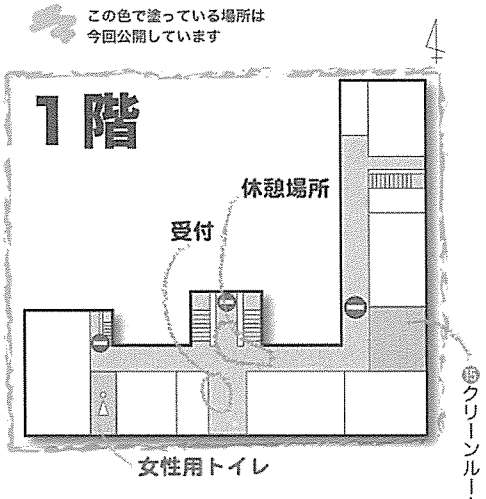

注意：
- 休憩場所以外での飲食はご遠慮下さい
- 施設内は禁煙です（玄関外側に灰皿を設置しています）
- トイレは２ヶ所あります（男性用は２階，女性用は１階）
- 職員は名札を付けています．なんでもご遠慮なくお訊き下さい

❶地震特集	地震計であなたの足音をキャッチ！波状化実験も．
❷火山噴煙を体験しよう	魅せます！噴煙
❸空から見た別府	別府を立体的に見てみよう！
❹別府を測ろう	ここから鶴見岳まで何ｋｍ？
❺研究室公開！	ふだんの研究室を大公開
❻1/130万地球断面図	地底まで6400kmのはるかな旅
❼地球史カレンダー	地球の歴史４６億年をカレンダーにしました
❽石の世界	別府石をはじめ，さまざまな石を観察しましょう！
❾別府温泉の科学	これだけ知っていればあなたも温泉博士！
❿水飴で作るマントルプルーム	地球内部のマントル対流を水あめで再現
⓫マグマのはやさ	マグマはどんな速さで上がってくるのだろう
⓬ダイヤを割ろう！	もっともかたい物質であるダイヤを割ります
⓭別府の自然	別府の地形に秘められた地球の息吹に迫る
⓮ハザードマップ	火山噴火に備えよう
⓯クリーンルームのぞき窓	ほこり１/10万の部屋

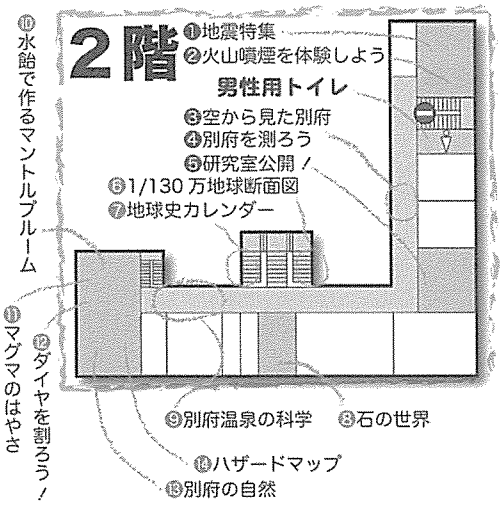

来年度の一般公開において改善すべき点や提案

今年度の一般公開の反省会において交わされた議論の中心は，来場者の世代構成についてであった．第1回会合から特に重視する世代を中学生及び高校生にしぼって開催時期や曜日，企画等を検討してきたが，昨年度，一昨年度同様その世代からの来場者は全く増えていない．その原因の一つとして考えられるのは広報活動の偏りが挙げられるかもしれない．例えば教育委員会を通して配布をお願いしている市立小中学校対象のポスターを県庁を通して県立高校まで届ける努力をすべきであるかもしれない．しかし，他の世代の来場者数はこの3年間で着実に伸びてきており，我々の広報活動がそれほど的外れなものであるとは考えられない．だからと言って単純に昨今の理科離れが原因であるとサジを投げるにはまだデータが不足しているであろう．来場していない市民になぜ来られないのかその理由を訊ねるのは困難であるが，中高生特有の来られない事情（部活動や模試など）があるのか，来場された親の世代から情報を得るなど，掘り起こしに向けた努力の余地は残っているかもしれない．

その他に交わされた意見として多かったものは企画の内容に関するものであった．アンケート結果から明らかであるが，好評な企画は実際に体験できる実験的なものであった．専門的で且つポスター中心の展示は評価が低い．しかし，次年度の企画内容が今年度の評価の高低だけに左右されるのは間違っているだろう．別府の地質や防災情報，研究施設の紹介など基本的な情報の紹介はたとえ評価が低くとも潜在的な要望は絶えることがないであろう．そのような展示は常設展示として単年度の企画物とは異なる次元で評価すべきであるかもしれない．

今年度は開催時期を休日に変更した．来場者から戴いた感想にもあるように，休日開催は多くの市民を呼び込む基本的な要素なのであろう．今回，一旦決定した平日開催を臨時会合を開いてまで休日開催に変更した甲斐はあったと思われる．しかし，このような活動は非常勤職員の名目上の業務ではないかもしれず，開催日の日当の支給の可否だけでなく，万が一事故が起こった際の補償問題など制度上の問題をはらんでいる．今回は構成員のアウトリーチに対する理解によって休日開催が実現できたが，大学自体が時折行う社会貢献活動が大学の本分として推奨されるものであるならば，非常勤職員の休日出勤や振替え休日を認めるなど制度の整備を先に行うべきであろう．

来年度は施設の一般公開が始まって7年目となり，企画や運営上のコツはかなり蓄積されたと思われる．そろそろ一度じっくり振り返ってデータを整理し，もっとも効率的な運営方法を確立できる時期であるかもしれない．

オープンハウス報告（阿蘇）

1．目的

一般市民，特に地域住民・関係機関に，当センターの活動内容を広く知ってもらうことで，センターに対する関心・理解を得る．また，社会への学術的知識の還元・啓蒙をはかる．

2．開催日時

平成１８年　８月　６日（日）　９：３０～１６：００

3．内容

○ ポスター展示（約３０点）による研究内容の紹介・火山学の一般向け解説
○ 公開実験・工作
- 「地震計のデモンストレーション」
- 「立体震源模型をつくろう」
- 「渦輪の実験」
- 「阿蘇の溶岩を磨こう」
- 「空気中のマイナスイオンを測る」

○ 施設備品展示（新旧地震計等各種観測装置の展示・解説）
○ 火山に関するビデオの上映
○ 火山に関する書籍の閲覧供与
○ 視覚的展示物
- 「九州の地震活動リアルタイムモニター」
- 「阿蘇火山の微動振幅レベルモニター」
- 「サーモトレーサーを使った体温モニター」
- 「石の世界（別府―島原地溝帯の石の展示）」
- 「空から見る阿蘇」

○ 特別講演（午前：須藤「超ふしぎな阿蘇火山」，午後：田中「阿蘇火山のお医者さん」各３０分）
○ 見学者パンフレット（大人用，子供用）を配布
○ お年寄りの来場者を考慮し休憩室を設置

4．社会告知の方法

○ Ａ４・Ａ３版ポスター・チラシを配布・掲示

赤水郵便局・アゼリア・阿蘇駅・阿蘇火山防災協議会・阿蘇火山博物館・阿蘇北中学校・阿蘇山測候所・阿蘇市体育館・阿蘇市役所・阿蘇中学校・阿蘇図書館・阿蘇西小学校・一の宮中学校・一の宮図書館・内牧小学校・尾ヶ石小学校・乙姫小学校・温泉センターウィナス・温泉センター瑠璃・株式会社キンキ・河陽郵便局・九州東海大学・久木野小学校・久木野中学校・熊本大学・古城小学校・坂梨小学校・立野小学校・たわら屋・地球熱学研究施設・地球物理学教室・長陽小学校・長陽西部小学校・長陽中学校・長陽パークゴルフ場・テレワークセンター・田園空間博物館・中通小学校・農村環境改善センター・白水小学校・白水中学校・碧水小学校・中松小学校・波野小学

校・波野中学校・南阿蘇村観光協会・南阿蘇村教育委員会・南阿蘇村役場・宮地小学校・山田小学校・夢の湯・両併小学校（50 音順）

○ 阿蘇テレワークセンターメールマガジン

○ 校外学習通信（メールマガジン）

○ 火山研究センターホームページによる公示

5．見学者に関する集計

来場者数：６３名（大人４９，小人１４）

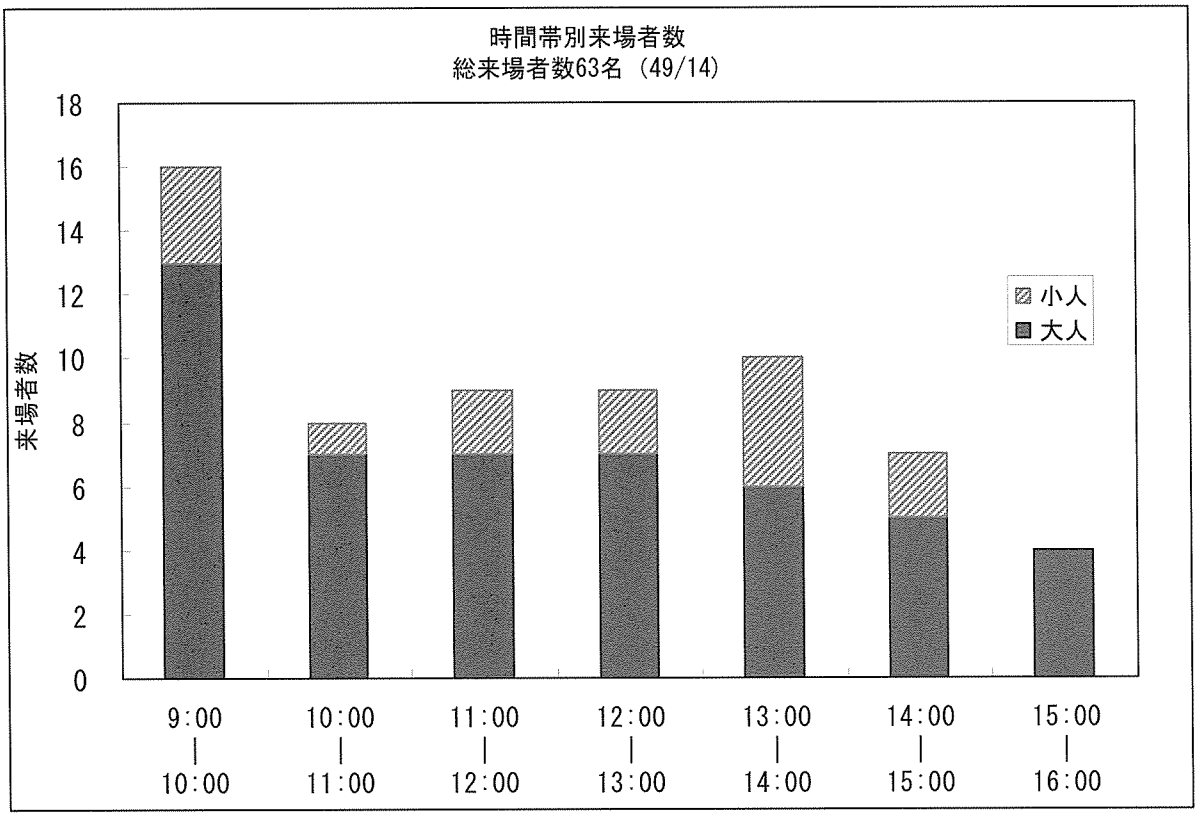

Ｑ１．どちらからお越しになりましたか？

	阿蘇郡市内	熊本県内阿蘇郡市以外	熊本県外	合計
回答数	12	20	8	40
百分率	30.00%	50.00%	20.00%	100%

Ｑ２．年代を教えてください

	１０代	２０代	３０代	４０代	５０代	６０代以上	合計
回答数	4	8	5	6	4	12	39
百分率	10.26%	20.51%	12.82%	15.38%	10.26%	30.77	100%

Q３．どのようにして今回の一般公開を知りましたか？

	友人・知人	インターネット	新聞・雑誌	ポスター	その他	合計
回答数	14	2	7	11	6	40
百分率	35.00%	5.00%	17.50%	27.50%	15.00%	100%

Q４．特別講演は面白かったですか？

	面白かった	つまらなかった	難しかった	いずれでもない	聞かなかった	合計
回答数	25	4	0	0	0	29
百分率	86.21%	13.79%	0%	0%	0%	100%

Q５．一般見学会に参加して，火山研究センターに興味を持ちましたか？

	持った	持たなかった	合計
回答数	34	0	34
百分率	100%	0%	100%

Q６．一般見学会に参加して，阿蘇火山への興味を持ちましたか？

	持った	持たなかった	合計
回答数	38	0	38
百分率	100%	0%	100%

Q７．夏休み期間中の開催は良かったですか？

	良かった	良くなかった	合計
回答数	38	2	40
百分率	95.00%	5.00%	100%

６．まとめ

今年度は１０月に日本火山学会秋季大会が阿蘇で開催されたため，一般見学会の開催を８月へと変更した．その結果，昨年度を上回る数の小学生や親子連れの参加があった．また，アンケートでは９０％以上の方が夏休みの開催を良かったと回答している．さらに，前回までは一般公開の情報を人伝いに知ったという方が圧倒的に多かったのだが，今回は新聞・ポスターで知ったという方が約半数を占めた．これらは開催時期および前年度からの課題でもあった告知方法が正しかったことを意味している．

来年度は，８月５日に開催される南阿蘇村のイベントに合わせて開催することを計画している．したがって，より多くの来場者があることが予想されるが，これは同時に多くの方に阿蘇火山の魅力や火山研究センターを知っていただける良い機会でもあると考えている．

最後にアンケートに回答していただいた方々の感想をいくつか紹介する．

- 説明がわかりやすく楽しい時間をすごせました
- これまでのご研究に，ただただ頭が下がる思いでした．
- 色々な機械があって興味が持てた．学校にはこういうものはあまり無いので楽しかった．
- とても面白かったです．火山性地震の観測は，普段学校ではあまり触れ合うことがない話題なので新鮮でした．
- ここに来ただけでテンションが上がりました．

小学生の感想

- 毎年来ているけど，毎回違う内容なので楽しく学べます．授業で習う前だったので，予習が出来たと思います．ありがとうございました．
- 火山や磁石の働きなどを学べました．もっと火山いついて知りたいです．
- 火山の石，また煙の輪っかの事や火山の石の中で，鉄が強い磁石だっていうこともわかり，面白かったです．ツルツルの石も作ることが出来ました．あと地震の震源地を知ることが出来ました．
- 火山のことや地震のことをたくさん知りました．もっと火山のことを知りたいです．

火山研究センター　吉川　慎

来訪者 Visitors

【別府】

平成 18 年（2006 年）

4 月 10 日～11 日　足立守，田中功夫　計 3 名（名古屋大学）

4 月 14 日　清崎聖一（明治コンサルタント）

4 月 17 日 藤原留美　（大分合同新聞）

4 月 21 日～23 日 下山（九大）大木（鹿児島大）ほか 37 名

4 月 24 日　森山晃，他 1 名（杵築市役所）

4 月 24 日～28 日　渡邉康平（東邦大学）

4 月 25 日～26 日 高畑武志，片桐統　（京大理情報担当）

4 月 27 日～5 月 2 日　山田誠，他 2 名（岡山理科大学）

5 月 13 日　玉手義朗　（TBS）

5 月 25 日　Agola 編集部

6 月 15 日～17 日 新井田清信　（北海道大学理学部）

6 月 16 日　和氣敏治（松尾機器産業）

6 月 19 日～20 日　鍵裕之　（東京大学理学部）

6 月 19 日～28 日　渡邉康平（東邦大学）

6 月 20 日　本山友彦（西日本新聞社）

7 月 2 日　船田工ほか約３０名　（大分に青少年科学館を作る会）

7 月 5 日 藤原留美　（大分合同新聞）

7 月 10 日 永楽悦子　（別府教育事務所）

7 月 10 日～18 日 山田誠，三島　（岡山理科大）

7 月 11 日～12 日 藤井　（京大，熊取）

7 月 22 日　施設一般公開　一般 268 名

7 月 21 日～22 日 大倉，寺田　（火山センター）

7 月 25 日　野田雅之ほか 2 名　（大分地質学会）

7 月 27 日　施設一般公開　ハイキング　一般 34 名

7 月 27 日　施設一般公開　ライトアップ

7 月 28 日　施設一般公開 ライトアップ

7 月 30 日～8 月 1 日　堤浩之ほか学生　１０名　観測地球物理学演習 B　（京都大学）

8 月 1 日～8 月 3 日　堤浩之ほか学生 3 名　課題演習 D3 現地実習　（京都大学）

8 月 2 日　橋本尚英，他 4 名（大分舞鶴高校）

8 月 2 日　大分舞鶴高校　高校生 13 名，教員　2 名

8 月 11 日　永楽悦子，黒木　（別府教育事務所）

8 月 11 日～12 日 田上高広ほか 2 名　（京大地質学鉱物学）

8 月 16～19 日　石田義人　（金沢大学理学部）

8 月 18 日　立石ほか 2 名　（大分大附属中 2 年）

8 月 18 日　大上　（明豊高校）

8 月 23 日　大上和敏，他多数（明豊高校）

8 月 22 日　吉見　（産総研）

8 月 22 日　江竜，志村　（京都大学理学研究科事務部）

8月22日　大倉　（火山センター）
8月23日　明豊高校　高校生55名，教員 3名
8月24日～9月12日　三根崇彦　（京都大学　　）
8月24日　渡辺，坂本，山本，大槻　（本部，財務，理，企画）
8月25日～8月26日　沖村　孝ほか7名　（神戸地盤研究会）
8月28日　永川（基礎地盤コンサルタント）
8月28日～9月2日　網田和宏（秋田大学）
9月4日龍敏晃　　（内藤建築事務所）
9月14日　永楽　（別府教育事務所）
9月27～9月28日　片桐　（京大理学研究科）
10月2日～8日　網田和宏（秋田大学）
10月7～10月8日　野田雅之ほか23名　（大分地質学会）
10月9～2007年1月2日 高博　（中国，雲南大学）
10月14日　大井信夫　（ONP研究所）
10月18日～31日　渡邉康平（東邦大学）
10月22日　石川孝弘　（西日本インテリアプランナー協会）
10月22日　風早康平，他4名（産総研）
10月24日　江平義雄，他2名（九州建設コンサルタント）
10月25日　塩地（大分市教育委員会）
10月27日　財前，本山　（大分県防災危機管理課）
11月7日　山田守ほか2名　（名古屋大学博物館）
11月9日　Ayu　ITB　（インドネシア）
11月10日　井内美郎　（愛媛大学）
11月11～11月22日　Audrey Martin　（クレルモンフェラン大学院生）
11月14日　梶原ほか1名　　（地熱エンジニアリング）
11月24～11月28日　余田，田上，石岡，松岡，Budi (ITB)ほか19名
12月8～12月11日　鈴木勝彦　（JAMSTEC）
12月14日　波多野健志，他1名（九州建設コンサルタント）
12月15～12月16日 大出，Sirirattanachai（琉球大学，Burapha Univ.）

平成19年（2007年）
1月9日～2月7日　Marie Python（金沢大学）
1月10～12日　佐野有司　（東京大学海洋研究所）
1月15日　進藤，本山　（大分県防災危機管理課）
1月16日　小田圭之介　（大分合同新聞）
1月17日　早川，濱田，川原，松山　（応用地質）
1月22日　大塚祐司，他2名（大分舞鶴高校）
2月10～2月12日　木村，中西　（産業技術総合研究所）
2月27～3月1日　　氏家治，柴田慎二郎　（富山大学）
3月5日～7日　嶋本，松岡ほか　（京大・理・地質学鉱物学）
3月9日～11日　宮縁育夫　（森林総研）
3月9日～11日　星住英夫　（産総研）

3月13日　川原ほか２名　（応用地質）
3月13日　黒川陽一郎，金子浩二，他２名（環境省自然環境局）
3月16日～18日 平島崇男，三宅，河上，大見ほか７名　（京大理・防災研）
3月17日～18日 石橋秀巳　（神戸大）
3月18日　ウイヘルト地震計公開・市民講演会　一般市民60名
3月18日　ウイヘルト地震計公開・市民講演会　足立守　（名古屋大）
3月18日～19日　ウイヘルト地震計公開・市民講演会　平原和朗　　（京大）
3月19日～22日 山田功，山田守ほか２名　（名古屋大）
3月23日　大塚祐司，他多数（大分舞鶴高校）
3月24日～31日　網田和宏（秋田大学）
3月25日～31日　山田誠（岡山理科大学）
3月30日　飯沼賢司　（別府大学）

【阿蘇】
平成18年（2006年）
5月30日　気象庁阿蘇山測候所　２名
7月4-6日　及川氏（東大）
7月25-26日　金嶋氏（九大）
7月26日　九州大学大野正夫火山ガス調査
8月18日　　長谷中氏（熊本大）、松島氏（九大）、柴田氏（火山学会）
9月12-14日　山本氏（東北大）
10月5日　石原氏（JAMSTEC）
10月21日　石黒耀夫妻
11月2日　気象庁阿蘇山測候所　２名
11月24日　地磁気センター家森教授ほか１名、微気圧計設置
12月9-10日　特定領域研究Ａ０１班研究報告会、平林順一、井口正人ほか１０名
12月9-10日　　地球科学実験B受講者４名
12月13日　本田　健　他2名　（砂防・地すべり技術センター）

平成19年（2007年）
1月24日　気象庁阿蘇山測候所　2名
3月13-15日　川勝氏（東大）
3月13-16日　山本氏（東北大）
3月14-16日　金嶋氏（九大）、高木氏（東工大）

定常観測　Routine Observations

Geophysical Monitoring Under Operation at AVL

Aso Volcanological Laboratory

Permanent Stations

Nakadake monitoring network

Seismic Stations: HNT, PEL, KSM, SUN, KAE, KAE, KAN, UMA, TAK (microwave telemetry)
Tiltmeters: HNT (water tilt 3-comp.), SUN, KAE, NAR, UMA, KAK (on-site logging)
Extensometers: HNT (invar 3-comp.)
Microphone: HND (microwave telemetry)
Geomagnetic Stations: C1, C3, S0, W1, CS, NGD, FF1 (proton; on-site logging)
C223 (fluxgate 3-comp.; on-site), newC223 (fluxgate 3-comp.; online)
FF2 (proton; online)
Ground Temperature: KAK (boreholes of 70 and 150 m deep; microwave telemetry)

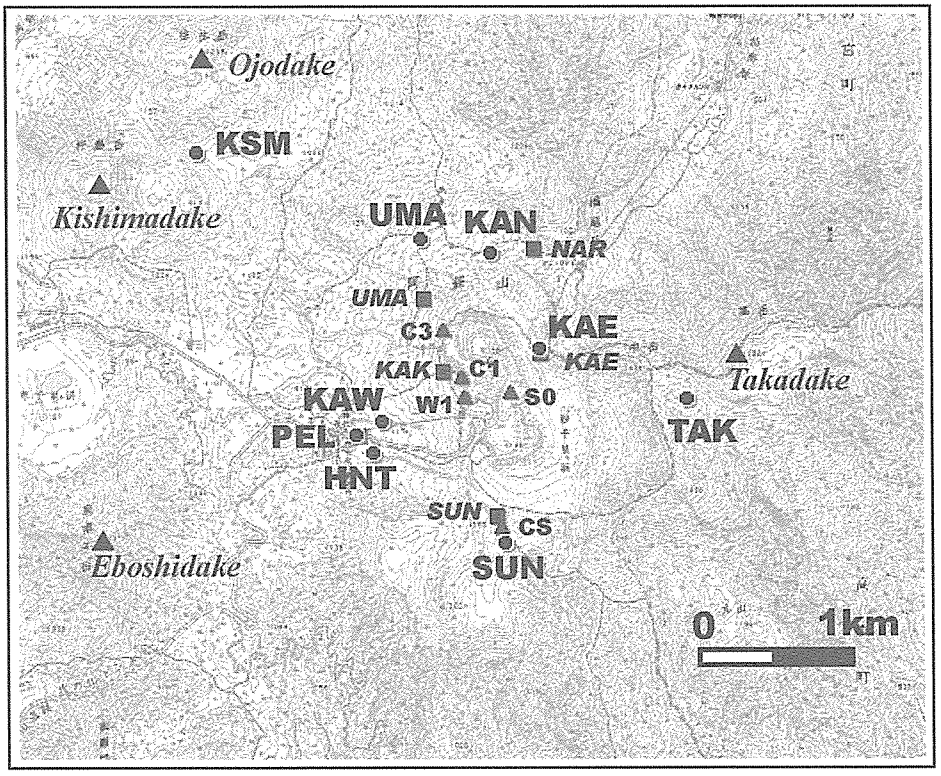

Seismic, geodetic and geomagnetic stations in the central part of Aso.

Kuju monitoring network

Seismic Stations: HNG (radio-telemetry), AKG, CJB, IOY (on-site logging)
Tiltmeters: H283, KSR (on-site logging)
Geomagnetic Stations: N2, E1, S0, SE (proton; on-site logging)

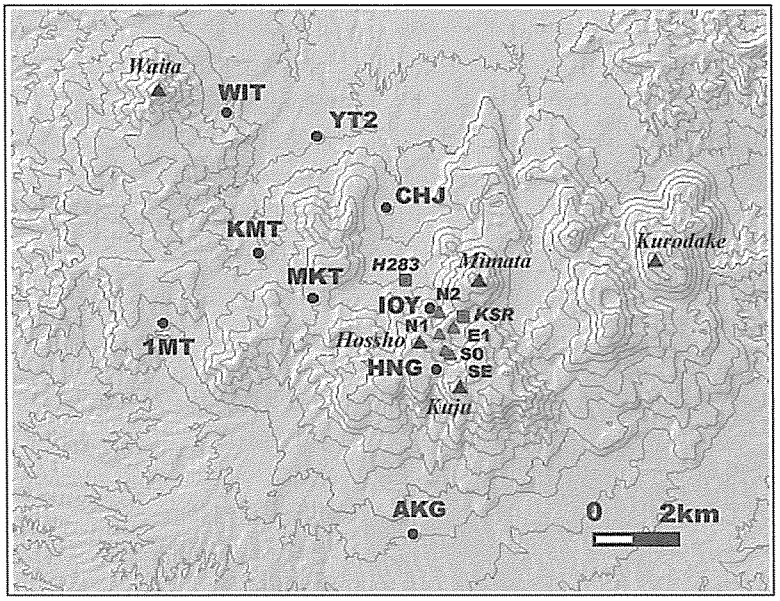

Seismic, geodetic and geomagnetic stations in Kuju area.

Central Kyushu regional network

Seismic Stations: AVL(6), MAK, NBR, MKN, HDK, TAT, MGR (online telemetry)
ASJ, HNY, SKM, KBM, TRM (dial-up)

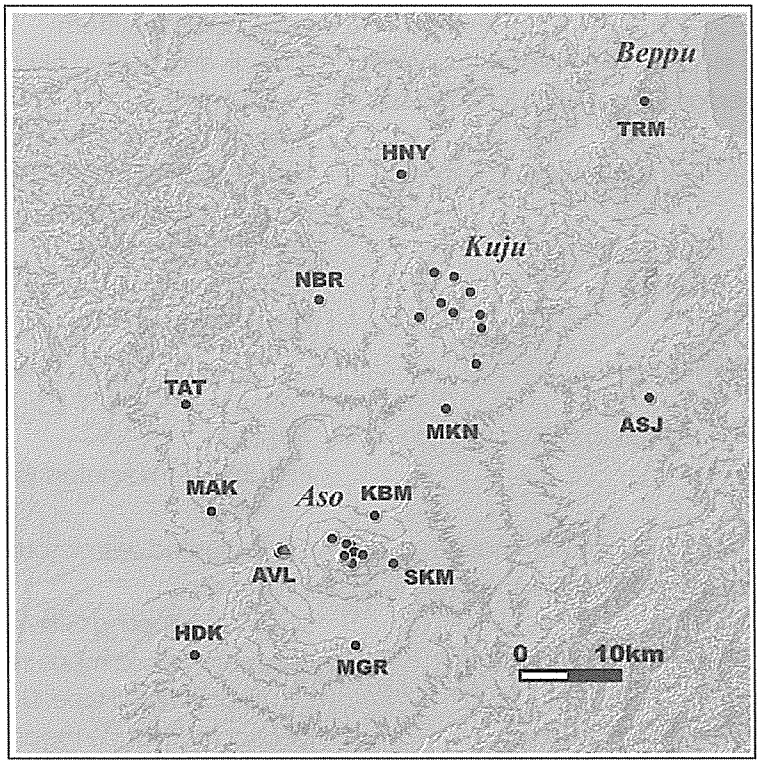

Seismic network in the central Kyushu.

装置，設備　Instruments and Facilities

装置　Instruments

【別府】

ICP 発光分光分析装置
波長分散型電子プローブマイクロアナライザー（海洋科学技術センターに貸し出し中）
エネルギー分散型電子プローブマイクロアナライザ
波長分散型蛍光 X 線分析装置
エネルギー分散型蛍光 X 線分析装置
粉末 X 線回折装置
液体シンチレーションシステム
イオンクロマトグラフ
ガスクロマトグラフ
自動滴定装置
ピストンシリンダー型高圧発生装置
ICP-MS 用レーザーアブレーション装置
四重極型 ICP-MS 装置
表面電離型質量分析装置
外熱式ダイアモンドアンビル
ラマン顕微鏡
フーリエ変換型近赤外分光光度計
赤外顕微鏡
加熱ステージ

【阿蘇】

阿蘇，九重火山連続地震観測システム
地殻変動観測坑道
孔中温度観測システム
ビデオ映像監視システム
プロトン磁力計
フラックスゲート磁力計
地磁気絶対測定システム
傾斜計
可搬型地震計（広帯域，短周期）
人工震源車
重力計
超伝導重力計
地磁気地電流測定装置（広帯域型 ULF, ELF, VLF 型）
光波測距儀
水準測量システム（自動読み）

【Beppu】

ICP emission Spectrometer
Wavelength dispersive electron microprobe (lent to JAMSTEC)
Energy dispersive electron microprobe analyzer
Wavelength dispersion type X-ray Fluorescence analyzer
Energy dispersionty type X-ray Fluorescence analyzer
Powder X-ray diffractometer
Liquids scintillation system
Ion chromatography
Gas chromatography
Automatic titration system
Piston cylinder type high pressure apparatus
Laser ablation system
Inductively coupled plasma mass spectrometer (ICP-MS)
Thermal ionization mass spectrometer (TIMS)
Externally heated diamond anvil cell
Raman microscope
FT-NIR spectrometer
IR microscope
Heatings stage

【Aso】

Continuous seismic monitoring system for Aso and Kuju Volcanoes
Observation tunnel for ground deformation
Borehole temperature monitoring system for Aso
Video monitoring system of Aso and Kuju Volcanoes
Proton and fluxgate magnetometers
Geomagnetic absolute measurement system
Tiltmeters
Portable seismometers (broadband short period)
Car-mounted seismicsource
Gravimeters
Super-Conducting Gravimeter
Magneto-Telluric measurement system (broad-band type, ULF, ELF, VLF-band)
Electronic distance measurement system
Leveling survey system (automatic reading)

設備 Facilities

岩石粉砕, 鉱物分離室

パックミル, ディスクミルによる岩石粉砕やアイソダイナミックセパレータによる鉱物分離を行う.

器具洗浄室

実験に用いる器具の洗浄を行う. クリーンドラフト1台, ドラフト1台, イオン交換筒, Milli-Q が設置されている.

クリーンルーム

ニューロファインフィルターを設置し極力金属使用を控えた設計で, クラス100のクリーン度を達成している. Sr, Nd, Pb 同位体比分析のための化学処理 (試料の分解, イオン交換クロマトグラフィーによる目的元素の抽出) を行っている.

地下観測坑道 (阿蘇火山地殻変動観測坑道)

阿蘇中岳第一火口から南西1kmの, 地下30mに設けられた, 直角三角形の水平坑道で, 1987年度に竣工した. 現在は, 水管傾斜計 (25m), 伸縮計 (20, 25m), 短周期地震計, 長周期地震計, 広帯域、地震計、強震計、超伝導重力計が設置されている.

火山研究センター構内地震観測システム

火山研究センター構内では, 従来からトリパタイトによる地震観測を行ってきたが, 平成13年度に, ノイズ低減の為, 約200mのボーリング孔を4本掘削し, 孔底に地震計を導入した. これにより, S/N 比は大幅に改善され, 従来識別できなかった中岳の長周期微動が検出されるようになった. また, ボーリングコアを採取したことにより, 研究センターの丘, 高野尾羽根 (たかのおばね) 火山について地質学的に新たな知見が得られつつある. これは, 阿蘇中央火口丘の噴火史を研究する上でも貴重な資料である.

An analysing system of trace element and isotopic compositions

Radiogenic isotope and trace element compositions of natural samples (e.g. rock and water, etc.) provide us important information about source materials of a sample, generating processes from the sources and age of the sample formation. Therefore isotope and trace element compositions of natural samples are important for investigating the phenomena accompanied with material transfer, such as magma genesis and mantle-crust recycling. Hence, we established an analytical method for determining trace elements by using an inductively coupled plasma mass spectrometer (Fig. 1) and for isotopic ratios of Sr, Nd and Pb: employing a thermal ionization mass spectrometer (Fig. 2) at Beppu Geothermal Research Laboratory (BGRL). The system presented here is made from collaboration with Institute for Frontier Research on Earth Evolution. The methods of chemical preparation for the each analysis were also established. All our chemical procedures are performed under a clean environment, which is basically handmade with our original design (eg. Fig. 3). The analytical methods established at BGRL realize the precise analyses of trace and isotopic compositions of ultra trace amounts of the samples (Fig. 4). Furthermore, we are developing methods to realize the mass production of the assay tests. By employing the described analytical methods, we are progressing with the study of magma genesis and material transfer in the mantle, etc.

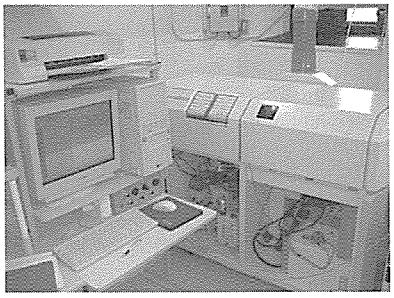

Fig. 1. Inductively coupled plasma mass spectrometer

Fig. 2. Thermal ionization mass spectrometer

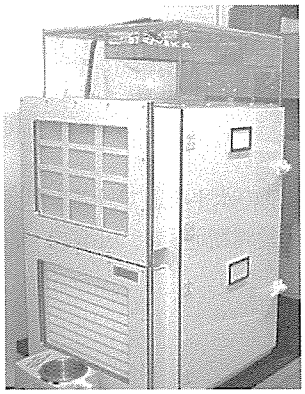

Fig. 3. Sample evaporation system under the ultra clean environment

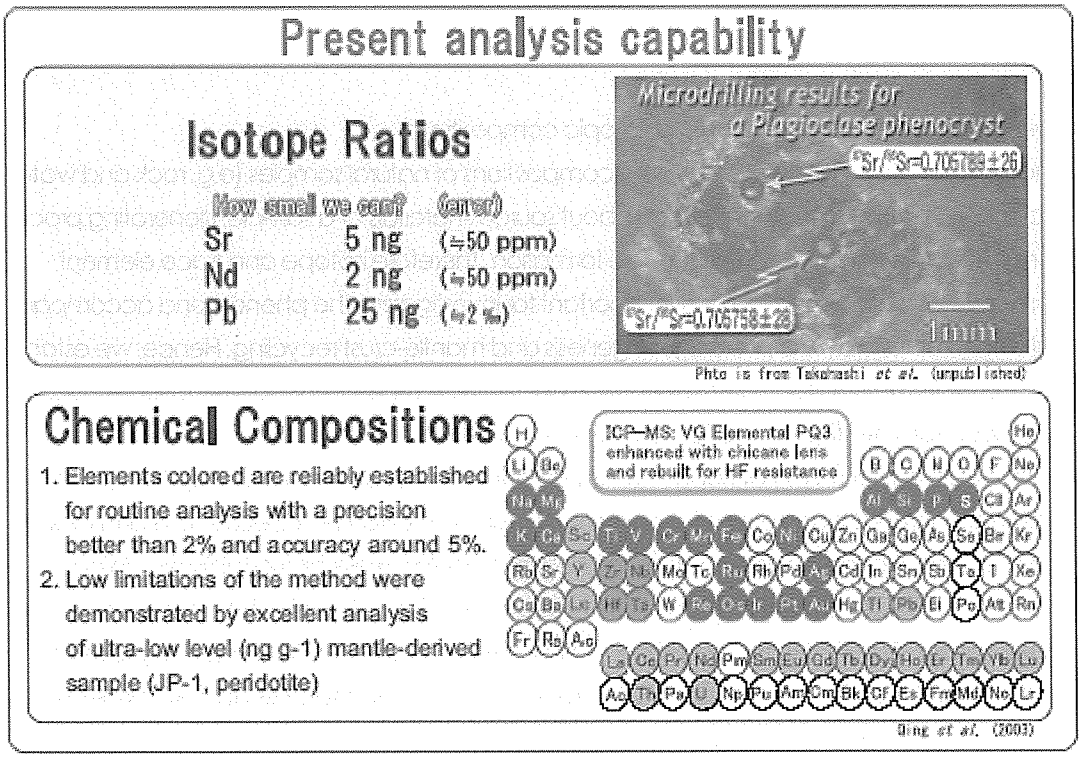

Fig. 4. Analytical method for isotopic and trace element compositions established at BGRL